

N
P

**JOURNAL
OF
FOOD
PROCESS
ENGINEERING**

**D.R. HELDMAN
and
R.P. SINGH
COEDITORS**

**FOOD & NUTRITION
PRESS, INC.**

VOLUME 20, NUMBER 2

MAY 1997

JOURNAL OF FOOD PROCESS ENGINEERING

Editor: **D.R. HELDMAN**, 214 Agricultural/Engineering Building,
University of Missouri, Columbia, Missouri
R.P. SINGH, Agricultural Engineering Department, University of
California, Davis, California

Editorial

Board: **J.M. AGUILERA**, Santiago, Chile
G. BARBOSA-CANOVAS, Pullman, Washington
S. BRUIN, Vlaardingen, The Netherlands
M. CHERYAN, Urbana, Illinois
P. CHINACHOTI, Amherst, Massachusetts
J.P. CLARK, Chicago, Illinois
A. CLELAND, Palmerston North, New Zealand
M. ETZEL, Madison, Wisconsin
R. HARTEL, Madison, Wisconsin
F.-H. HSIEH, Columbia, Missouri
K.H. HSU, E. Hanover, New Jersey
M.V. KARWE, New Brunswick, New Jersey
E.R. KOLBE, Corvallis, Oregon
J. KROCHTA, Davis, California
L. LEVINE, Plymouth, Minnesota
M. McCARTHY, Davis, California
S. MULVANEY, Ithaca, New York
H. RAMASWAMY, St. Anne Bellevue PQ, Canada
M.A. RAO, Geneva, New York
T. RUMSEY, Davis, California
Y. SAGARA, Tokyo, Japan
S.K. SASTRY, Columbus, Ohio
E. SCOTT, Blacksburg, Virginia
K.R. SWARTZEL, Raleigh, North Carolina
A.A. TEIXEIRA, Gainesville, Florida
G.R. THORPE, Melbourne, Victoria, Australia
H. WEISSER, Freising-Weihenstephan, Germany

All articles for publication and inquiries regarding publication should be sent to DR. D.R. HELDMAN, COEDITOR, *Journal of Food Process Engineering*, University of Missouri-Columbia, 214 Agricultural Engineering Bldg., Columbia, MO 65211 USA; or DR. R.P. SINGH, COEDITOR, *Journal of Food Process Engineering*, University of California, Davis, Department of Agricultural Engineering, Davis, CA 95616 USA.

All subscriptions and inquiries regarding subscriptions should be sent to Food & Nutrition Press, Inc., 6527 Main Street, P.O. Box 374, Trumbull, CT 06611 USA.

One volume of six issues will be published annually. The price for Volume 20 is \$164.00, which includes postage to U.S., Canada, and Mexico. Subscriptions to other countries are \$187.00 per year via surface mail, and \$198.00 per year via airmail.

Subscriptions for individuals for their own personal use are \$134.00 for Volume 20, which includes postage to U.S., Canada and Mexico. Personal subscriptions to other countries are \$157.00 per year via surface mail, and \$168.00 per year via airmail. Subscriptions for individuals should be sent directly to the publisher and marked for personal use.

The *Journal of Food Process Engineering* is listed in *Current Contents/Agriculture, Biology & Environmental Sciences (CC/AB)*, and SciSearch, and Research Alert.

The *Journal of Food Process Engineering* (ISSN:0145-8876) is published (February, April, June, August, October and December) by Food & Nutrition Press, Inc.—Office of Publication is 6527 Main Street, P.O. Box 374, Trumbull, Connecticut 06611 USA.

Second class postage paid at Bridgeport, CT 06602.

POSTMASTER: Send address changes to Food & Nutrition Press, Inc., 6527 Main Street, P.O. Box 374, Trumbull, Connecticut 06611 USA.

JOURNAL OF FOOD PROCESS ENGINEERING

JOURNAL OF FOOD PROCESS ENGINEERING

Editor: **D.R. HELDMAN**, 214 Agricultural/Engineering Building, University of Missouri, Columbia, Missouri
R.P. SINGH, Agricultural Engineering Department, University of California, Davis, California

Editorial

Board:

J.M. AGULERA, Univ. Catolica, Department of Chemical Engineering, P.O. Box 6177, Santiago, Chile

G. BARBOSA-CANOVAS, Washington State University, Department of Biosystems Engineering, 207 Smith Ag Building, Pullman, Washington 99164

S. BRUIN, Unilever Research Laboratory, Vlaardingen, The Netherlands

M. CHERYAN, 110 Agricultural Bioprocess Laboratory, University of Illinois, 1302 West Pennsylvania Ave., Urbana, Illinois 61801

P. CHINACHOTI, University of Massachusetts, Department of Food Science, Chenoweth Lab, Amherst, Massachusetts 01003

J.P. CLARK, Fluor Daniel, 200 West Monroe St., Chicago, Illinois 60606

A. CLELAND, Department of Food Technology, Massey University, Palmerston North, New Zealand

M. ETZEL, University of Wisconsin, Department of Food Science, Babcock Hall, Madison, Wisconsin 53706

R. HARTEL, University of Wisconsin, Department of Food Science, Babcock Hall, Madison, Wisconsin 53706

F.-H. HSIEH, Departments of Biological & Agricultural Engineering and Food Science & Human Nutrition, University of Missouri, Columbia, Missouri 65211

K.H. HSU, RJR Nabisco, Inc., P.O. Box 1944, E. Hanover, New Jersey 07936

M.V. KARWE, Rutgers, The State University of New Jersey, P.O. Box 231, Center for Advanced Food Technology, New Brunswick, New Jersey 08903

E.R. KOLBE, Oregon State University, Dept. of Bioresource Engineering and Food Science & Technology, Gilmore Hall 200, Corvallis, Oregon 97331-3906

J. KROCHTA, Department of Food Science & Technology, University of California, Davis, California 95616

L. LEVINE, Leon Levine & Associates, 2665 Jewel Lane, Plymouth, MN 55447

M. McCARTHY, Biological and Agricultural Engineering Department, University of California, Davis, California 95616

S. MULVANEY, Cornell University, Department of Food Science, Stocking Hall, Ithaca, New York 14853-7201

H. RAMASWAMY, Macdonald Campus of McGill, Dept. of Food Science & Agricultural Chemistry, 21111 Lakeshore Rd., St. Anne Bellevue PQ, H9X 3V9, Canada

M.A. RAO, Department of Food Science and Technology, Institute for Food Science, New York State Agricultural Experiment Station, Geneva, New York 14456

T. RUMSEY, Biological and Agricultural Engineering Department, University of California, Davis, California 95616

Y. SAGARA, Department of Agricultural Engineering, Faculty of Agriculture, The University of Tokyo, 1-1-1 Yayoi, Bunkyo-ku, Tokyo 113, Japan

S.K. SASTRY, Agricultural Engineering Department, Ohio State University, 590 Woody Hayes Dr., Columbus, Ohio 43210

E. SCOTT, Department of Mechanical Engineering, Virginia Polytechnic Institute and State University, Blacksburg, Virginia 24061

K.R. SWARTZEL, Department of Food Science, North Carolina State University, Box 7624, Raleigh, North Carolina 27695-7624

A.A. TEIXEIRA, Agricultural Engineering Department, University of Florida, Frazier Rogers Hall, Gainesville, Florida 32611-0570

G.R. THORPE, Department of Civil and Building Engineering, Victoria University of Technology, P.O. Box 14428 MCMC, Melbourne, Victoria, Australia 8000

H. WEISSER, University of Munich, Inst. of Brewery Plant and Food Packaging, D 85350 Freising-Weihenstephan, Germany

**Journal of
FOOD PROCESS
ENGINEERING**

**VOLUME 20
NUMBER 2**

**Coeditors: D.R. HELDMAN
R.P. SINGH**

**FOOD & NUTRITION PRESS, INC.
TRUMBULL, CONNECTICUT 06611 USA**

© Copyright 1997 by
Food & Nutrition Press, Inc.
Trumbull, Connecticut 06611 USA

All rights reserved. No part of this publication may be reproduced, stored in a retrieval system or transmitted in any form or by any means: electronic, electrostatic, magnetic tape, mechanical, photocopying, recording or otherwise, without permission in writing from the publisher.

ISSN 0145-8876

Printed in the United States of America

CONTENTS

Simulation of Dynamic Properties of Batch Sterilizer with External Heating M. LOUČKA	91
Yield and Quality of Onion Flavor Oil Obtained by Supercritical Fluid Extraction and Other Methods A. DRON, D.E. GUYER, D.A. GAGE and C.T. LIRA	107
Concentration of Onion Juice Volatiles by Reverse Osmosis and Its Effects on Supercritical CO ₂ Extraction J.S. NUSS, D.E. GUYER and D.A. GAGE	125
Flow Modeling of a Power-Law Fluid in a Fully-Wiped, Co-Rotating Twin-Screw Extruder Y. LI, H.E. HUFF and F. HSIEH	141
Velocity Profiles of Fluid/Particulate Mixtures in Pipe Flow Using MRI K.L. McCARTHY, W.L. KERR, R.J. KAUTEN and J.H. WALTON	165

SIMULATION OF DYNAMIC PROPERTIES OF BATCH STERILIZER WITH EXTERNAL HEATING

MILOSLAV LOUČKA

*Department of Applied Mathematics
Institute of Chemical Technology, Prague
Technika-5, 166 28 Prague 6
Czech Republic*

Accepted for Publication February 22, 1996

ABSTRACT

A computer program for simulation of a sterilizer with an external recirculation heating system was developed on the basis of a requirement formulated in our previous work (Loučka and Vinklárková 1990) containing the analysis and comparison of sterilization equipment with respect to technological aspects. The originally derived mathematical model provides the characteristic curves in the dimensionless form which solves many technical problems under the condition that bath temperature is reached in the required time period. From this calculation it follows that plate arrangement of the heat exchanger is significantly better than a tubular one.

INTRODUCTION

Among all food processing equipments, sterilizers (or retorts or autoclaves) are perhaps the most important both from the point of view of technological significance of operation, and energy consumption. Many works dealt with this problem from different points of view: for optimal nutrient retention (Teixeira *et al.* 1975; Saguy and Karel 1979; Ohlson 1980), correction for process deviations (Giannoni-Succar and Hayakawa 1982; Datta *et al.* 1986). All these works need the derivation of dynamic model and its solution to obtain the time-temperature profiles (Singh 1977; Barreiro 1984; Bhowmik *et al.* 1985). The experimental verification of their conclusion is recently performed by (Mulvaney *et al.* 1990). This work concentrated on technological requirements, involving the development and subsequent solution of a system of two ordinary differential equations describing the simulation problem.

Author's e-mail: louckam@vscht.cz

At first a special study was worked out (Loučka and Vinklárková 1990) which was presented to answer the question whether import or self manufacture of batch sterilization equipment was more suitable for the Czech Republic food industry. The conclusions of this work included, among others, the recommendation for construction of a horizontal autoclave by the firm Barriquand 1300 with external heating recirculation system. In our work we used some parameters of this device as a technical model. This situation is illustrated in Fig. 1.

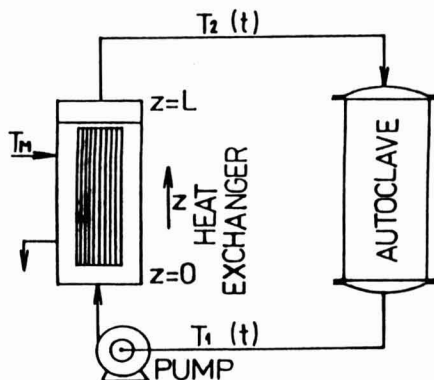


FIG. 1. SCHEMATIC OF RECIRCULATION SYSTEM IN EXTERNALLY HEATED RETORT OR AUTOCLAVE

The main technological concern is the rate of temperature increase in the retort or autoclave. For the same size autoclave, it depends on two parameters: flow rate of heating medium in the recirculation system, and efficiency of the heat exchanger. These parameters govern the response time required for achieving the desired constant process temperature.

The purpose of this work was to develop and present graphical relationships between various dimensionless parameters showing the effects of volumetric flow rate and heat exchanger efficiency on the response time for both plate and tubular-type heat exchangers when used for heating the recirculating water in an externally-heated retort or autoclave in canned food sterilization.

MATERIAL AND METHODS

Theoretical Background for Formulation of the Problem

Sterilizers with external heating are produced by all prestigious firms for their low energy and water consumption. Heating can be arranged either by

direct injection of steam or indirectly with a heat exchanger (Fig. 1). The second alternative has the advantage, that there are less strict sanitary requirements on the quality of the cooling media, because it is not in contact with the sterilized food.

Plug flow is assumed in the heat exchanger, meaning that flow velocity is uniform over the cross-sectional area, (Levenspiel and Bischoff 1963). The differential balance can be written:

$$c_w \dot{m}_w dT_2 = U(T_M - T_2) dA \quad (1)$$

for tubular exchanger

$$\begin{aligned} dA &= N\pi d dz \\ x &= z/L \end{aligned} \quad (2)$$

after substitution to (1) we get

$$\frac{dT_2}{dx} = \frac{U\pi dLN}{c_w \dot{m}_w} (T_M - T_2) \quad (3)$$

Now we put

$$q = \frac{U\pi dLN}{c_w \dot{m}_w} \quad (4)$$

where for the plate exchanger instead of relationship $\pi \cdot d \cdot L$ is special A_p . For both cases we get now

$$\frac{dT_2}{dx} + qT_2 = qT_M \quad (5)$$

with boundary condition on the inlet of exchanger

$$x=0 \quad T_2 = T_1(t) \quad (6)$$

the solution has for $x = 1$ a form

$$T_2(1) = T_1(t)e^{-q} + T_M(1 - e^{-q}) \quad (7)$$

For $t=0$ the relation $T_2 = T_1$ is held.

Tubular Exchanger

It is supposed, that resistance of overall heat transfer on the side of steam is negligible. Tubes of exchanger are made of steel and on the side of medium (water) the turbulence or transient condition are present. The correlation for this case was found (Hansen 1943).

$$\text{Nu} = 0.116(\text{Re}^{2/3} - 125)\text{Pr}^{1/3} \left[1 + \left(\frac{d}{L} \right)^{2/3} \right] (\mu/\mu_s)^{0.14} \quad (8)$$

where the value of $(\mu/\mu_s)^{0.14}$ is closely equal to one. The circumstances mentioned correspond with intervals of variables

$$\begin{aligned} 2.3 \times 10^3 < \text{Re} < 2 \times 10^6 \\ 0.5 < \text{Pr} < 5 \times 10^2 \\ d/L \leq 1 \end{aligned} \quad (9)$$

in which the correlation (8) is valid. The expression for overall heat transfer coefficient

$$\frac{\pi}{U} = \frac{1}{h_i d_i} + \frac{1}{2\lambda} \ln \frac{d_v}{d_i} \quad (10)$$

does not contain the term $1/(h_v \cdot d_v)$ on the side of steam, which was neglected as explained earlier. The amount of heat per unit time is now

$$dQ/dt = U \Delta T_{LS} A_p \quad (11)$$

Plate Heat Exchanger

This equipment has wide application for pasteurization of fluid foods and recently for sterilization under pressure. Analogically to (8) the correlation

$$\text{Nu} = a \text{Re}^b \text{Pr}^c (\mu/\mu_s)^d \quad (12)$$

is valid and it is supposed that $(\mu/\mu_s)^d$ is again nearly one. The constants can be found from the range (Jackson and Lamb 1981)

$$\begin{aligned} 0.15 < a < 0.4 \\ 0.65 < b < 0.85 \\ 0.30 < c < 0.45 \\ 0.05 < d < 0.2 \end{aligned} \quad (13)$$

and overall heat transfer coefficient is determined by the formula

$$\frac{1}{U} = \frac{1}{h_i} + \frac{l}{\lambda} \quad (14)$$

where the term $1/h_v$ was neglected and l means thickness of the wall. The equivalent diameter d_e is computed from a well-known equation

$$d_e = \frac{4S}{\omega} \quad (15)$$

and substituted in Re criterion in (12).

Derivation of Equation of Nonstationary Process

Differential balance of autoclave (a) with a can (k) and water as medium (w) is under condition of ideal mixing (Urban 1990), (Fig. 1.)

$$\dot{m}_w c_w (T_2 - T_1) dt = m_a c_a dT_a + m_w c_w dT_1 + m_k c_k dT_k \quad (16)$$

The quantity m_k means total mass amount of all cans loaded in the retort, c_k is average value of specific heat with respect to package and content of cans, and from the source (Loučka and Klein 1983) we know that

$$\frac{dT_k}{dt} = \alpha T_1 - \alpha T_k \quad (17)$$

The rate of heating is given by the reciprocal value of the dynamic time constant determined experimentally, for each case of package, food and geometry. For the purpose of the heat exchanger analysis in this study, the heating of food containers may be treated as lumped parameters system although that is not always the case. This assumption mathematically expressed by Eq. (17) was experimentally confirmed by (Loučka *et al.* 1991).

Equation (16) can be arranged with supposition that $dT_2 = dT_a$. This assumption is used by (Mulvaney *et al.* 1990) for similar purpose. It is based on the fact, that thermal diffusivity of steel is much greater than the one for most foods.

$$T_2 - T_1 = \beta \frac{dT_1}{dt} + \delta \frac{dT_k}{dt} \quad (18)$$

where we put

$$\beta = \frac{m_a c_a + m_w c_w}{60 m_w c_w} \quad (19)$$

and

$$\delta = \frac{m_k c_k}{60 m_w c_w} \quad (20)$$

By connection of Eq. (17) and (18) the member dT_k/dt from (18) can be eliminated. We get then the system of two ordinary differential equations in the canonical form:

$$\frac{dT_1}{dt} = \frac{1}{\beta} T_2 - \frac{(1+\delta\alpha)}{\beta} T_1 + \frac{(\delta\alpha)}{\beta} T_k \quad (21)$$

$$\frac{dT_k}{dt} = \alpha T_1 - \alpha T_k \quad (22)$$

with conditions

$$t=0; T_1=T_{10}; T_k=T_{k0} \quad (23)$$

Substitution of Eq. (7) to (21) gives

$$\frac{dT_1}{dt} = \frac{1-f}{\beta} T_M + \frac{f-(1+\alpha\delta)}{\beta} T_1 + \frac{\delta\alpha}{\beta} T_k \quad (24)$$

The derivation of the previous relationship becomes

$$\frac{d^2T_1}{dt^2} = \frac{f-(1+\alpha\delta)}{\beta} \frac{dT_1}{dt} + \frac{\delta\alpha}{\beta} \frac{dT_k}{dt} \quad (25)$$

The term where T_k occurs can be eliminated by combination with (22), obtained by multiplying both sides by α

$$\alpha \frac{dT_1}{dt} + \frac{\alpha\delta}{\beta} \frac{dT_k}{dt} = \alpha \frac{1-f}{\beta} T_M + \frac{\alpha(1-f)}{\beta} T_1 \quad (26)$$

Addition of Eq. (25) and (26) gives the canonical form

$$\frac{d^2T_1}{dt^2} + \left[\frac{1+\delta\alpha-f}{\beta} + \alpha \right] \frac{dT_1}{dt} + \frac{\alpha}{\beta} (1-f) T_1 = \frac{\alpha}{\beta} (1-f) T_M \quad (27)$$

which is non-homogeneous and where $f=e^{-\alpha}$ is assigned. It can be solved by well-known analytical methods. When initial conditions (23) are kept and supplied to Eq. (24), Eq. (24) becomes

$$t=0; T_1=T_{10}; \frac{dT_1}{dt} = \frac{\delta\alpha}{\beta} T_{k0} + \frac{1-f}{\beta} T_M + \frac{f-(1+\alpha\delta)}{\beta} T_{10} \quad (28)$$

At first the dimensionless temperatures were introduced:

$$\theta_1 = \frac{T_1 - T_{k0}}{T_M - T_{k0}} \quad (29)$$

and

$$\theta_k = \frac{T_k - T_{k0}}{T_M - T_{k0}} \quad (30)$$

Then B_1, B_2 were assigned as roots of the characteristic equation corresponding to (27) and then the solution in the dimensionless form is:

$$\theta_1 = \frac{(\alpha\theta_{10} + B_2)(\alpha + B_1)}{\alpha(B_1 - B_2)} e^{B_1 t} - \frac{(\alpha\theta_{10} + B_1)(\alpha + B_2)}{\alpha(B_1 - B_2)} e^{B_2 t} + 1 \quad (31)$$

and

$$\theta_k = \frac{\alpha\theta_{10} + B_2}{B_1 - B_2} e^{B_1 t} - \frac{\alpha\theta_{10} + B_1}{B_1 - B_2} e^{B_2 t} + 1 \quad (32)$$

To obtain the solution θ_k we can use Eq. (21) arranged in the dimensionless form. Consequently θ_k and its first derivative from (31) is substituted in Eq. (21) which then becomes Eq. (32) in which it can be simply confirmed that initial conditions (33) are kept in the dimensionless form

$$\begin{aligned} t=0; \theta_1 &= \theta_{10} \\ t=0; \theta_k &= 0 \end{aligned} \quad (35)$$

The limit relations which must be satisfied

$$\lim_{t \rightarrow \infty} \theta_1 = 1 \quad \text{and} \quad \lim_{t \rightarrow \infty} \theta_k = 1 \quad (36)$$

are valid just as

$$B_1 < 0 \quad \text{and} \quad B_2 < 0 \quad (37)$$

and these are also Ljapunov's conditions of stability.

RESULTS

The basic parameters of the equipment were chosen on the basis of the design concepts given by horizontal pressure sterilizers similar to a Barriquand 1300 Steriflow.

The values which were used as input for the computational procedure were summarized as follows (Šesták 1981):

- (1) The heating medium: steam $p=0.6$ MPa, $T=165$ C on equilibria condition. The temperature $T_M=125$ C is taken into account with regard to possible resource of energy.
- (2) Initial temperatures: bath $T_{LO}=50$ C, can $T_{KO}=20$ C
- (3) Between temperatures T_{LO} and T_M there is a mean middle value $T=85$ C. The thermophysical data for heating of recycled water are:

$$\rho = 968.5 \text{ (kg/m}^3\text{)}$$

$$\mu = 0.348 \times 10^{-6} \text{ (m}^2\text{/s)}$$

$$\text{Pr} = 2.09$$

$$c_w = 4.2 \times 10^3 \text{ (J/kg/K)}$$

- (4) The batch of autoclave is 3500 cans, each 0.5 kg of weight, diameter 0.08m, height 0.12m, total amount 1750kg, total volume 2.1 m³.
- (5) The dynamic heating characteristic of a can was chosen equal to 0.834 min⁻¹.
- (6) Specific heat of the can c_K is assumed as $c_K = y_b c_b + y_p c_p$ where subscripts b and p assigns batch and package respectively. Package is made of steel $m_p = 0.06$ kg and $y_p = 0.12$; $y_b = 0.88$ and by substitution to the above given formula we get $c_K = 2599.6$ (J/kg/K).
- (7) Arrangement of autoclave is supposed to be horizontal with a shower-bath characterized by following parameters: total weight 2300 kg; recirculation of water filling 500 kg; total volume 9.3 m³; volume of a built-in armature 0.93 m³ and remainder of air volume 5.73 m³. Thermal capacity of air $c_A m_A = 0.164 \times 10^{-3}$ J/K is neglected.
- (8) The heat exchanger is of a tubular or plate type with steel exchange walls with capacity for heating of the bath to 124C in a time interval of 12 min at 95% efficiency.

The data summarized above create the input for the algorithm performed on the basis of the equations derived in the previous paragraph (Furich 1991).

Results of the simulation are presented graphically in Fig. 2 to 5 in the dimensionless form as relationships t_1 , V_T and q criteria. These characteristics of the speed of heating (t_1), flow rate of media (V_T) and overall heat transfer (q) are compared for tubular and plate heat exchangers. Definition of variables is

$$V_T = \dot{V} t_1 / (60V) \quad (36)$$

$$q = UA_p / (c_w \rho \dot{V}) \quad (37)$$

$$\vartheta = \alpha t_1 \quad (38)$$

Where t_1 is the time required for the bath temperature to reach $T = 124C$.

In Fig. 2 and 3 the quantity ϑ is related to V_T , to illustrate the changes of heating time period for $T_1(t)$, $T_2(t)$ and $T_K(t)$ with increasing flow rate. A direct comparison between tubular and plate heat exchanger performance is shown in Fig. 4, where the relationships between quantities V_T and q is plotted. The differences between q value for plate and tube arrangement are more significant for lower values of V_T criterion. The heat transfer coefficient is higher for plate heat exchangers, and that is the reason why plate arrangements are preferable to tubular when used for heating water. The simulation of dependencies ϑ on V_T and ϑ on q precedes the construction of the graphs in Fig. 3 and 4 under conditions of constant geometric relations and variable flow rate. There are two

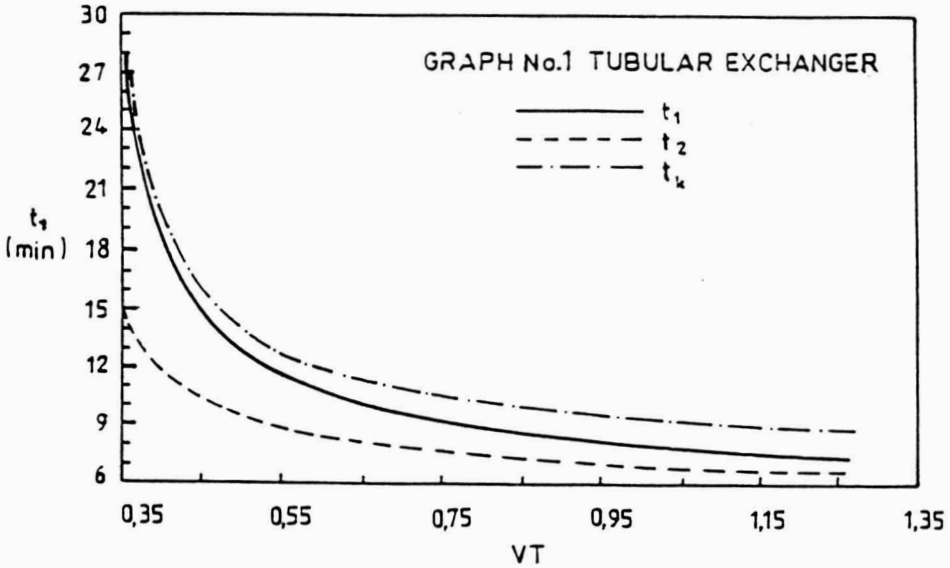


FIG. 2. DEPENDENCIES OF t_1, t_2 AND t_k ON THE V_T FOR TUBULAR EXCHANGER, WHERE V_T IS DEFINED BY EQ. (36), t_1 - TIME OF REACHING $T=123.9C$ ON AUTOCLAVE OUTLET, t_2 - TIME OF REACHING $T=123.9C$ ON AUTOCLAVE INLET, t_k - TIME OF REACHING $T = 123.9C$ IN CAN

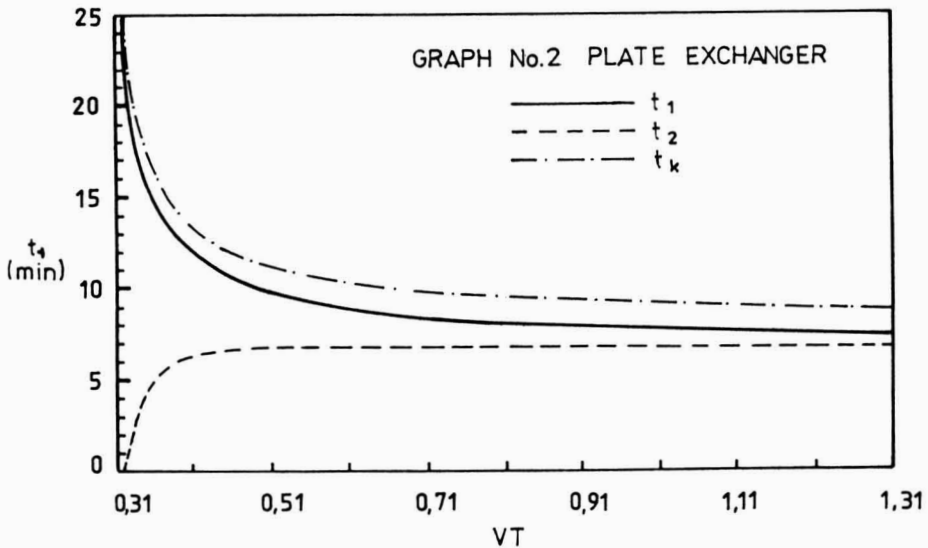


FIG. 3. GRAPH NO. 2

Dependencies of t_1, t_2 and t_k on the V_T for plate exchanger, where V_T is defined by Eq. (36), t_1 - time of reaching $T = 123.9C$ on autoclave outlet, t_2 - time of reaching $T = 123.9C$ on autoclave inlet, t_k - time of reaching $T = 123.9C$ in can.

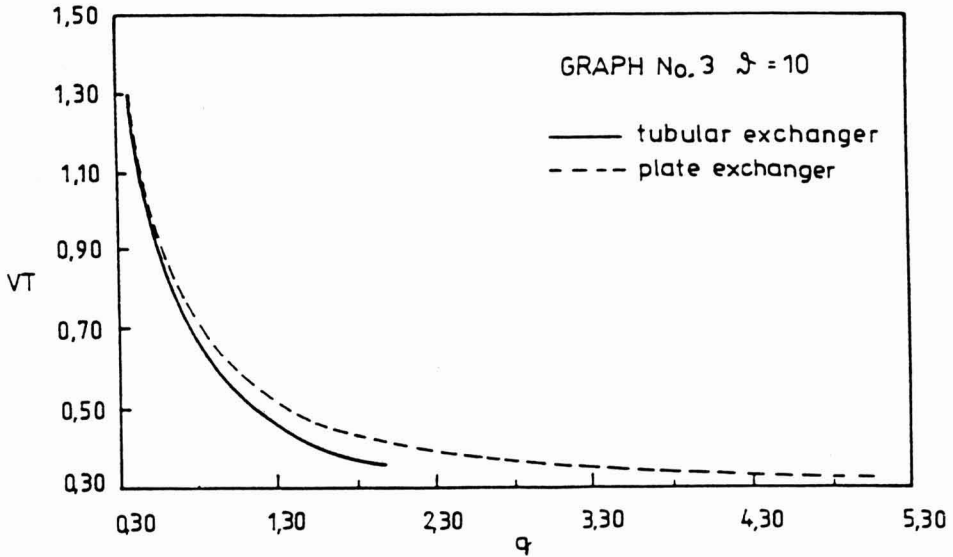


FIG. 4. GRAPH NO. 3

The comparison of the tubular and plate heat exchangers, dependence of V_T and q values, where V_T is defined by Eq. (36), q is defined by Eq. (37).

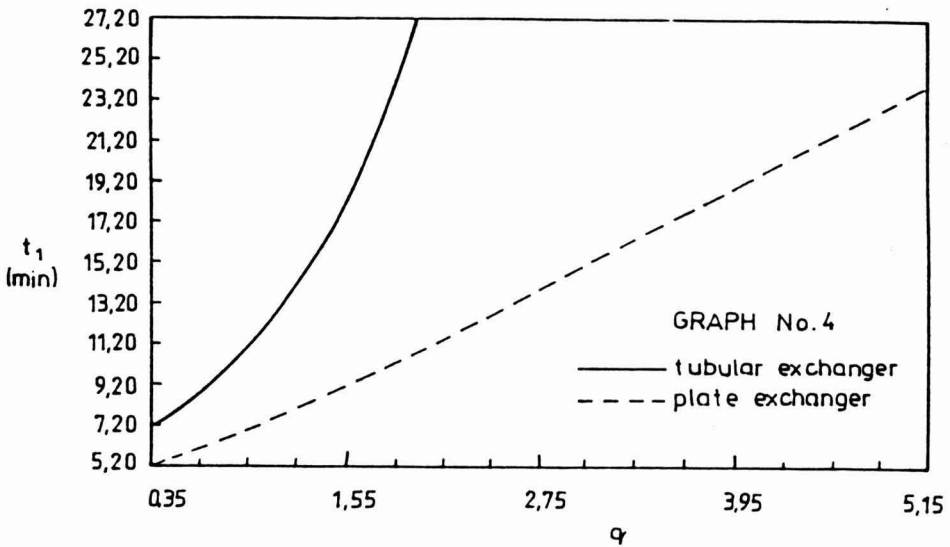


FIG. 5. GRAPH NO. 4

The comparison of the tubular and plate heat exchangers, dependence of t_1 and q values, where q is defined by Eq. (37), t_1 - time of reaching $T = 123.9^\circ\text{C}$ on autoclave outlet.

curves plotted in these graphs: for tubular heat exchanger with parameters $N=9$, $l=0.001$ and $d=0.212$, and for the plate heat exchanger with $N = 20$, $l = 0.002$ and $MEZ = 0.05\text{m}$. The same heat transfer area $AP = 6 \text{ m}^2$ was taken for both types of exchangers.

On the graphs in Fig. 2 and 3, $\vartheta=10$ was chosen and $V_T=0.68$ and $V_T=0.48$ were found for tubular and plate heat exchangers, respectively. By a similar procedure the values q were found (tubular $q = 0.85$ and plate $q = 1.6$) for constant chosen $\vartheta=10$. The graph in Fig. 4 was obtained from the pairs $[q, V_T]$ which were determined by the above described procedure. The curves characterize different geometric arrangements for both types of exchangers and fitting pump output to ensure the condition $\vartheta=10$.

Examples of solution of typical problems from graphs:

- (1) A plate heat exchanger is to be sized in which the surface area of each individual plate is $A_p=0.44 \text{ m}^2$. The geometrical dimensions of plate are length 0.7m and width 0.428m . The pump from which $\dot{V} = 0.01667\text{m}^3/\text{s}$ was determined on the basis of the hydrodynamic resistance of flow through the narrow gap between plates ($d_p=0.05 \text{ m}$). The quantity $U = 18 \text{ kWm}^{-2}\text{K}^{-1}$ was calculated from Eq. (12) and (14). The problem is to determine the number of plates that will be required (N). Now we have the relations for the area of plate

$$A_o = 0.428 \times 0.7 = 0.3 \text{ m}^2$$

for total hold-up volume

$$V = (N-1) \cdot A_o \cdot d_p$$

and for total heating surface area

$$A = N \cdot A_p$$

from which we get the dimensionless criteria defined above

$$q = 0.1168 \cdot N$$

$$V_T = \frac{13.336}{N-1}$$

The requested heating time is $t_1 = 12 \text{ min}$, dynamic heating constant of can $\alpha = 0.834 \text{ min}^{-1}$ from which follows $\vartheta = 10$.

The result of simple iteration procedure, using these formulas and the graph in Fig. 4. are given in Table 1. The procedure is successfully finished, when two subsequent iterations give satisfactory agreement of values V_T . For the first

approximation of $N = 12$ we get the number of plates $N = 40$ in the fourth step of iteration.

TABLE 1.
RESULTS OF ITERATION STEPS

Step	N	V_T	q
0	12	0.50	1.40
1	27	0.38	3.15
2	36	0.35	4.20
3	39	0.34	4.55
4	40	0.34	4.67

- (2) Decreasing the flow volume rate from the previous problem to $\dot{V} = 0.0133 \text{ m}^3/\text{s}$ causes a change in the overall heat transfer coefficient U , but allows narrowing of the distance between plates from 0.05m to 0.03m and consequently total volume reduction of exchanger with the same number of plates. We can calculate the hold-up volume of exchanger $V = 39 \times 0.03 \times 0.3 = 0.351 \text{ m}^3$. To keep the requested value of heating time $t_1 = 12 \text{ min}$ for the new value of V_T from graph in Fig. 4 we find $q = 2.5$. The heat transfer coefficient may be determined from

$$\frac{q_1}{q_2} = \frac{U_1 \dot{V}_2}{U_2 \dot{V}_1}$$

After arrangement and substitution it follows that $U = 7.69 \text{ kWm}^{-2}\text{K}^{-1}$. This is the minimum value required for reaching the specified operations performance. From Eqs. (12) and (14) it follows

$$\frac{h_2}{h_1} = \frac{\frac{1}{U_1} - \frac{l_1}{\lambda_1}}{\frac{1}{U_2} - \frac{l_2}{\lambda_2}} = \left(\frac{\dot{V}_2}{\dot{V}_1} \right)^{0.75}$$

when the mean of the range of values for exponent $b = 0.75$ was used.

After substitution of known values we get $U = 17.26 \times 10^3 \text{ Wm}^{-2}\text{K}^{-1}$. It can be seen, that the coefficient is two times greater than minimally required. This fact enables a reduction of almost 30% of the initial total volume of heat exchanger.

Other technical problems related to the thickness of plate wall use of different plate material or shape of heat transfer surface have analogous solutions. The advantages of a plate heat exchanger are evident from the course

of the curves plotted on the graph in Fig. 3. The same problem, in principle, can be solved for tubular exchangers and evaluated under particular circumstances. For illustration, Table 2 contains some particular conclusions of computer simulation.

TABLE 2.
SELECTED RESULTS OF SIMULATION

Conditions	V(l/min) Flow Rate	t ₁ (min) Time of Reaching T ₁ = 124C
Tubular exchanger	250	31
A _p = 6 m ² L = 1	600	15
d = 0.212 l = 0.002 m	1000	12
	1500	10
	2000	9
Plate exchanger	600	12
A _p = 6 m ² N = 20	1000	8
I = 0.002 MEZ = 0.05 m	1500	6
Tubular exchanger	250	28
A _p = 6 m ² L = 1	600	14
d = 0.212 l = 0.001 m	1000	10
	1500	8
Plate exchanger	600	11
A _p = 6 m ² N = 20	1000	7
I = 0.002 MEZ = 0.01 m	1500	5
Tubular exchanger	250	28
A _p = 4 m ² L = 1	600	15
d = 0.212 l = 0.001 m	1000	11
	1500	8

MEZ- distance between plates

CONCLUSION

In this article computer simulation of nonsteady state heating (or cooling) in an overpressure sterilizer with an external heating system is presented. This system contains the retort, pump and heat exchanger. Both tubular and plate steam heat exchangers were assumed.

A computer program was developed on the basis of an originally derived mathematical model of the heat exchange recirculation process. For both types

of heat exchangers, characteristic curves describing the simulation results of the process with following input data: volume flow rate, coefficient of heat transfer, exchange surface area and geometric relation, chosen in the interval of usable values. The output quantity was the response time for reaching the temperature level $T = 124\text{C}$ in the sterilization bath of the retort. In the discussion of the results, it was shown, that it is possible to solve technical problems, such as choice of geometric arrangement, material of tube or plate, determination of exchange area or flow rate for reaching the required time-temperature relationships.

From those results it followed immediately, that differences in performance of tubular and plate heat exchanger are very significant in this type of application, and it is probably the reason why tubular heat exchangers are rarely used in externally-heated retorts or autoclaves.

NOMENCLATURE

- A heat transfer area [m^2]
- B_1 first root of the characteristic eq. [min^{-1}]
- B_2 second root of the characteristic eq. [min^{-1}]
- c specific heat [J/kg/K]
- d diameter of tube [m]
- f constant
- h heat transfer coefficient [$\text{W/m}^2/\text{K}$]
- U overall heat transfer coefficient [$\text{W/m}^2/\text{K}$]
- L total length [m]
- l thickness of wall [m]
- m mass [kg]
- \dot{m} mass flow [kg/s]
- N number of elements (desks or tubes)
- Q heat [J]
- q dimensionless quantity defined by (4)
- S cross-sectional flow area [m^2]
- T temperature [$^{\circ}\text{C}$]
- t time [s]
- t_1 time of reaching $T_1 = 123.9\text{C}$ [min]
- t_2 time of reaching $T_2 = 123.9\text{C}$ [min]
- t_k time of reaching $T_k = 123.9\text{C}$ [min]
- V volume [m^3]
- \dot{V} volumetric flow rate [m^3/s]
- x dimensionless length
- y mass concentration
- z distance from exchanger inlet [m]

Dimensionless Criteria

$$\text{Re} = \frac{4\dot{V}}{\pi d \mu}$$

$$\text{Nu} = \frac{dh}{\lambda}$$

$$\text{Pr} = \frac{cd}{\rho \lambda}$$

Greek Symbols

- α reciprocal value of time constant of can [min^{-1}]
 μ kinematic viscosity [m^2/s]
 β variable def. by Eq. (19) [min^{-1}]
 δ variable def. by Eq. (20) [min^{-1}]
 λ heat conduction coefficient [$\text{W}/\text{m}/\text{K}$]
 ρ density [kg/m^3]
 Θ dimensionless temperature
 ω wetted perimeter [m]
 ϑ dimensionless time

Subscripts

- | | | | |
|---|-----------------------|----|-----------------------------|
| e | equivalent diameter | o | initial value |
| a | autoclave | M | heating medium |
| k | can | LS | logarithmic mean value |
| w | water | v | outer |
| 1 | autoclave outlet | i | inner |
| 2 | heat exchanger outlet | P | one plate of heat exchanger |

REFERENCES

- BHOWMIK, S.R., VICHNEVETSKY, R. and HAYAKAWA, K. 1985. Mathematical model to estimate the steam consumption in vertical still retort for thermal processing of canned foods. *Lebensm.-Wiss. u. Technol.* 18, 15-23.
- DATTA, A.K., TEIXEIRA, A.A. and MANSON, J.E. 1986. Computer-based control logic for on-line correction of process deviations. *J. Food Sci.* 51, 480-507.
- FÜRICH, R. 1991. Dynamic properties of batch sterilizer. M.Sc. Thesis. Prague, VŠCHT, FPBT.

- GIANNONI-SUCCAR, E.B. and HAYAKAWA, K. 1982. Correction factor of deviant thermal process applied to packaged heat conduction food. *J. Food Sci.* **47**, 642-646.
- HANSEN, H. 1943. Darstellung des Wärmeüberganges in Röhren durch verlagemeinerte. Potenzbeziehungen, *Z. VDI, Beihefte Verfahrenstechnik*, **4**, 91.
- JACKSON, A.T. and LAMB, J. 1981. *Calculations in Food and Chemical Engineering*, 1st Ed. The MacMillan Press Ltd., London.
- LEVENSPIEL, O. and BISCHOFF, K.B. 1963. Patterns of flow in chemical process vessels. *Advances in Chem. Eng.* **3**, 95.
- LOUČKA, M. and KLEIN, S. 1983. Mathematical model of heating and cooling dynamics of food in the preservation process. *Sborník UVTIZ. Potravinářské vědy 1*, 43-51.
- LOUČKA, M. and VINKLÁRKOVÁ, M. 1990. Summarization of technological demands for formulation of mechanical design problem of batch sterilizer. Prague, VŠCHT, FPBT, Research Report.
- LOUČKA, M., VINKLÁRKOVÁ, M. and KYSELA, J. 1991. Determination of parameters of heat transfer process dynamics in sterilization of packed food. *Sborník UVTIZ. Potravinářské vědy 9*, 259-267.
- MULVANEY, S.J., RIZVI, S.S.H. and JOHNSON, C.R. 1990. Dynamic modeling and computer control of retort for thermal processing *J. Food Eng.* **11**, 273-289.
- OHLSON, T. 1980. Optimal sterilization temperatures for cylindrical containers *J. Food Sci.* **45**, 1517-1521.
- OHLSON, T. 1980. Optimal sterilization temperatures for flat containers *J. Food Sci.* **45**, 848-852.
- SAGUY, I. and KAREL, M. 1979. Optimal retort temperature profile in maximizing thiamine retention in conduction-type heating of canned foods *J. Food Sci.* **44**, 1485-1490.
- ŠESTÁK, J. 1981. Transport and thermodynamic data., 3rd Ed. Textbook of ČVUT, Prague.
- SINGH, R.P. 1977. Energy consumption and conservation in food sterilization. *Food Technol.* **31**, 57-60.
- TEIXEIRA, A.A., STUMBO, C.R. and ZAHRADNIK, J.W. 1975. Experimental evaluation of mathematical and computer models for thermal process evaluation. *J. Food Sci.* **40**, 653-655.
- TEIXEIRA, A.A., ZINMEISTER, G.E. and ZAHRADNIK, J.W. 1975. Computer simulation of variable retort control and container geometry as a possible means of thiamine retention in thermally processed foods. *J. Food Sci.* **40**, 656-659.
- URBAN, J. 1989. Analysis of computer control of batch sterilization process. M.Sc. Thesis. Prague, VŠCHT, FPBT.

YIELD AND QUALITY OF ONION FLAVOR OIL OBTAINED BY SUPERCRITICAL FLUID EXTRACTION AND OTHER METHODS

ADITI DRON¹, DANIEL E. GUYER^{1,2}, DOUGLAS A. GAGE³ and CARL T. LIRA⁴

¹*Department of Agricultural Engineering*

³*Department of Biochemistry*

⁴*Department of Chemical Engineering*

Michigan State University

East Lansing, Michigan 48824

Accepted for Publication May 30, 1996

ABSTRACT

Methods of extraction of onion flavor oil were studied including supercritical fluid extraction using carbon dioxide (CO₂), liquid CO₂ extraction and steam distillation-solvent extraction. The effect of using entrainers with supercritical fluid extraction was also studied. The yield and the quality of onion extracts obtained from the different methods were compared. The maximum yield of 0.0324% was obtained by supercritical CO₂ extraction at 3600 psi (24.5 MPa), 37C at a CO₂ flow rate of 0.5 L/min. Ethyl alcohol used as entrainer enhanced the yield of onion oil over that obtained by supercritical CO₂ experiment without entrainer at the CO₂ flow rate of 1.0 L/min. Gas chromatography and combined gas chromatography-mass spectrometry of the extracts indicated that the flavor profiles were different for extracts obtained by different methods. Supercritical and liquid CO₂ extracts had fresh onion-like flavor as opposed to a cooked flavor of the extract obtained by steam distillation-solvent extraction.

INTRODUCTION

Onions possess strong, characteristic aromas and flavors which have made them important ingredients of food. Onion and onion flavors (onion oil) are important seasonings widely used in food processing. Currently the majority of onion oils are usually steam distilled, lack fresh onion flavor and their quality varies depending on the origin of production and are sometimes undesirable or inconsistent.

² Author to whom correspondence should be addressed: Daniel E. Guyer, 205 Farrall Hall, Agricultural Engineering Department, Michigan State University, East Lansing, MI 48824

The characteristic flavor of onions comes primarily from volatile organic sulfur compounds released enzymatically by the action of alliinase (alliin alkyl-sulfenate-lyase; EC 4.4.1.4) on several nonvolatile, odorless amino acid precursors, namely (+)-S-alkyl-cysteine sulfoxides, when the onion bulbs are chopped or crushed (Whitaker 1976). The primary reaction products of these amino acids are thiosulfates, which dissociate to produce thiosulfonates, sulfides containing methyl, propyl, and propenyl groups, thiophene derivatives, and other sulfur-containing heterocycles (Carson 1987). The alkyl thiosulfonates (methyl methane-, propyl methane-, and propyl propanethiosulfonates) have been associated with fresh onion-like flavors, while propyl- and propenyl-containing di- and trisulfides have been associated with cooked onions or steam distilled onion oils (Boelens *et al.* 1971).

Fenwick and Hanley (1985) have described onion oil as a brown-amber liquid obtained in 0.002 to 0.03% yield by the distillation of minced onions which were allowed to stand for some hours prior to distillation. The oil comprises a complex mixture of (mainly) sulfur containing volatiles. Sinha *et al.* (1992) have reported extraction of onion oil using supercritical carbon dioxide extraction. They have described the oil as having the characteristic fresh onion-like flavor. Several new components have been reported including diallyl thiosulfinate and propyl methanethiosulfonate.

Extraction using carbon dioxide (CO₂) as solvent is gaining attention because it is nontoxic, easily separated from the extract, nonflammable, inexpensive and available in high purity. The critical temperature and pressure of CO₂ are 31C and 1070.7 psi (7.4 MPa). Thus, supercritical CO₂ extractions can be carried out under relatively moderate conditions with minimal degradation of any thermally labile flavor components (Rizvi *et al.* 1986). This technique has the ability to change and "fine tune" its solubilizing power by controlling pressure and temperature. A reduction in solvent density with changes in temperature and/or pressure allows the separation and recovery of solute and solvent. Supercritical fluid extraction has been applied to a wide variety of flavor extraction applications: hops extraction, oleoresin and essential oil extraction from spices and herbs (Hubert and Vitzthum 1978), vanilla flavor extraction (Nguyen *et al.* 1991), onion flavor oil extraction (Sinha *et al.* 1992), citrus oil extraction from peels (Calame and Steiner 1982; Copella and Barton 1987).

While supercritical CO₂ has many desirable properties, its polarizability is very low. Therefore, small amounts of co-solvents, which are referred to as modifiers or entrainers, may be added to modify the polarity and solvent strength of supercritical CO₂ to increase the solute solubility (and/or selectivity). The entrainers used are commonly polar or nonpolar organic compounds which are miscible with supercritical CO₂ (Dobbs *et al.* 1986; Dobbs *et al.* 1987).

Liquid carbon dioxide has been found to be a very selective solvent for the extraction of flavor compounds such as terpenes, aldehydes and ketones, while other components of foods such as sugars, fruit acids, salts, amino acids, fats and water are practically insoluble (Schultz and Randall 1970). In general, the aromas and flavors of extracts obtained by liquid CO₂ extraction bear a closer resemblance to the original material than those obtained by organic solvent extraction. This is ascribed to the very mild conditions of the process and to the lack of oxygen in the extraction system (Grimmett 1981).

Steam distillation is widely used in the extraction of concentrates and essential oils of seasoning and aromatic herbs. It is usually followed by a liquid-liquid extraction with a solvent or simply is further concentrated (Teranishi *et al.* 1971). In steam distillation the starting material is subjected to a temperature of 100C. This can lead to artifacts of the flavor oil components which are often thermolabile. In addition, water can exert a hydrolytic influence, bringing about chemical changes in the oils (Stahl *et al.* 1988).

This study was undertaken to research various methods for extraction of onion flavor oil and to compare the yield and quality of the product obtained from each method with the goal of evaluating SFE-CO₂ (supercritical fluid extraction using CO₂) feasibility in extracting a unique fresh onion flavor. The specific objectives were: (1) to compare the yields of onion flavor oil obtained by Supercritical CO₂ Extraction, Liquid CO₂ Extraction, and Steam Distillation-Solvent Extraction under the conditions studied; (2) to investigate the effect of using entrainers with Supercritical Fluid Extraction on yield of onion flavor oil; and (3) to compare the quality of extracts obtained by various methods.

MATERIALS AND METHODS

Onions and Juice Preparation

Onions (*Allium cepa* L.) MSU experimental variety 3506 grown at Michigan State University (Muck Farm) were obtained in November 1993. They were stored at 2.8C. The onion bulbs were peeled, cut and immediately processed with an Acme Juicerator (Model: 11JE21) which uses filter paper to separate the pulp from the juice. The onion juice was stored in a covered container and held at ambient temperature (26-29C) for one hour to facilitate enzymatic action for flavor development. The pH of onion juice was 5.45 and the soluble solids content was 7.7 °Brix.

Supercritical CO₂ Extraction

Supercritical CO₂ extractions were conducted at 3600 psi (24.5 MPa) and 37C. The density of CO₂ under these conditions is 0.89 g/cm³ (Angus *et al.*

1976). The supercritical CO₂ extraction system is shown in Fig. 1. Industrial grade CO₂ (AGA gas, 99.5% purity) from a gas cylinder was compressed with a gas booster (Haskel, Inc.) and stored in a 2.0 L reservoir. A pressure regulator positioned between the reservoir and the extraction vessel controlled the extraction pressure. A two liter stirred autoclave (Model: Magnedrive II bolted closure autoclave, Autoclave Engineers) was used as the extraction vessel. The vessel was filled with 800 g onion juice prior to pressurization. CO₂ was monitored with a flow meter and a dry test meter. The extraction was commenced by slowly raising the pressure in the extraction vessel while the system outlet was closed. After reaching the extraction pressure, the heated micrometering outlet valve was opened to commence flow. The collection trap was weighed after passing 1100 L CO₂ (STP) through the system. Preliminary experiments had shown that passing larger volumes of CO₂ did not increase the yield by appreciable amounts after 1100 L. Hence, this amount was chosen for the experiments. For this study, CO₂ was vented and not recycled. To study the effect of CO₂ flow rate on the extraction process, similar experiments were done in triplicate at two different CO₂ flow rates, namely 1.0 L/min and 0.5 L/min. The collection trap was weighed periodically during these extractions.

Supercritical CO₂ Extraction with Entrainer

The entrainer was pumped into the supercritical CO₂ extraction system by a high pressure metering pump (Model: A-30-S, Eldex Laboratories Inc.). A static mixer, consisting of steel tubing filled lightly with glass beads, was installed between the extraction vessel and high pressure metering pump. Its purpose was to ensure that CO₂ and entrainer entering the extraction vessel were mixed properly (Fig. 1).

Ethanol (200 proof dehydrated alcohol) was used to evaluate the effect of a polar entrainer on the extraction of onion oil. Octane was used to evaluate the effect of a nonpolar entrainer. Extractions were conducted in triplicate at 3600 psi (24.5 MPa) and 37C. Two different amounts of each entrainer were used, 50 mL and 75 mL, to evaluate the effect of different concentrations of entrainer. These amounts were chosen on the basis of preliminary experiments. In each case, 10 mL entrainer was added initially to the juice before extraction and the remaining was added continuously during the time when the system was at the desired extraction pressure. In addition, an experiment was conducted at a lower pressure, i.e. 2600 psi (17.7 MPa), with 75 mL ethyl alcohol as entrainer to evaluate the effect of entrainer at a lower pressure (though still in the supercritical region). The temperature was kept the same at 37C.

Liquid CO₂ Extraction

Same equipment as for supercritical CO₂ extraction was used. Extraction

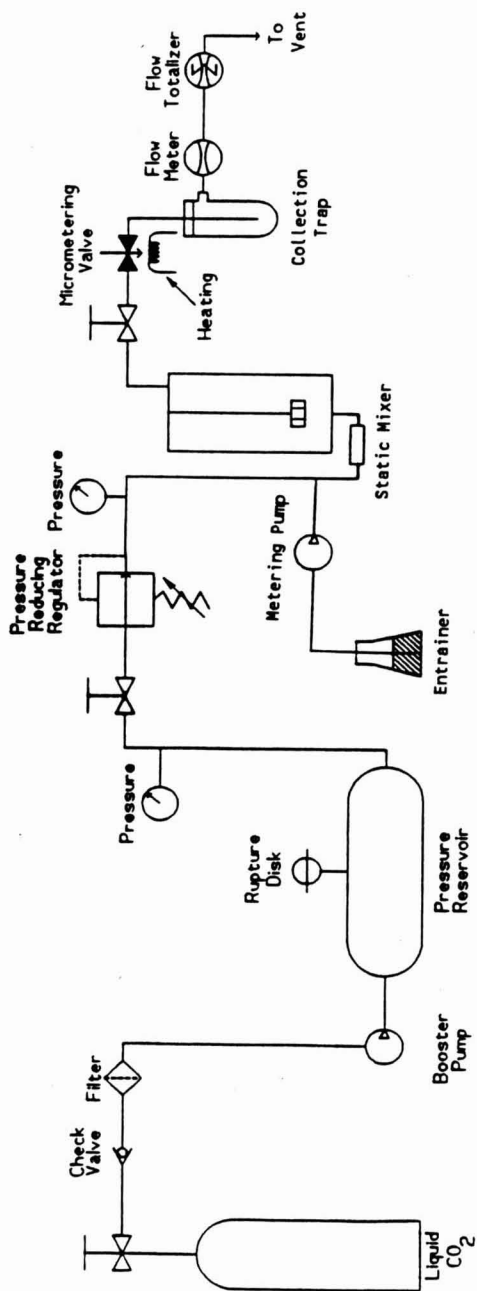


FIG. 1. SUPERCRITICAL CO₂ SYSTEM

was conducted at 2900 psi (19.7 MPa) and 27°C. The density of CO₂ is 0.90 g/cm³ under these conditions. The above conditions were chosen such that the density of CO₂ for the supercritical CO₂ and liquid CO₂ experiments was nearly equal so that a meaningful comparison of both methods could be made.

Steam Distillation-Solvent Extraction

Onion juice (200 mL) was mixed with 100 mL distilled water. The volatile components were extracted by 20 mL dichloromethane for 1 h in a modified Likens-Nickerson apparatus (Likens and Nickerson 1964; Schultz *et al.* 1977). Trace water in the extracted volatile solution was removed by anhydrous sodium sulfate and excess solvent was removed by nitrogen purging.

Onion Oil Yield by Gravimetric Method

Onion oil yield was estimated gravimetrically in the case of supercritical CO₂ extraction and liquid CO₂ extraction. The collection trap was weighed after passing 1100 L of CO₂ (STP) under desired conditions. However, in the case of (supercritical CO₂ + entrainer) and steam distillation-solvent extraction this was not possible because the extract contained some entrainer/solvent. The entrainer present in the extracts could have been removed by nitrogen purging and then the gravimetric yield determined. However, nitrogen purging could result in loss of some volatile flavor components. Hence, an alternative method, quantitative GC analysis, was used for estimating the yield of extracts containing entrainer/solvent.

Onion Oil Yield by Quantitative Gas Chromatography

Quantitative GC analysis was done to obtain information regarding the yield of onion oil obtained by all the methods studied on a relative basis. Gas chromatography was done in duplicate on all samples of extracts using GC (Model: Hewlett-Packard 5890 Series II). A 30 m HP-1 methyl silicone column of 0.53 mm inner diameter was used to separate the flavor components. A 1 µL dichloromethane dilution (containing 0.0045 g extract/mL dichloromethane) of each extract was injected for analysis. The operating conditions were as follows: injector temperature, 220°C; helium carrier gas flow rate, 6 mL/min; oven temperature, 35 to 200°C at a linear rate of 5°C/min and 15 min holding time at 200°C. A flame ionization detector at 240°C was used. HP 3365 Series II Chemstation Version A.03.21 by Hewlett Packard was used to control the GC and to record and integrate the data.

Abraham *et al.* (1976) and Sinha *et al.* (1992) reported that the characteristic flavor of onions is due to the volatile oil, which consists chiefly of sulfur compounds. Sulfur-compound peaks were identified using gas chromatography-

mass spectrometry (GC-MS). Summation of these peak areas was done for each sample. A known amount (0.005 g) of an internal standard, benzyl disulfide, was added to the juice before extraction. The amount of sulfur compounds present in each extract was evaluated as follows:

$$\text{Total Wt. of S Compounds} = \frac{[\sum \text{Peak Area of S Compounds}] \times \text{Wt. of IS}}{\text{Peak Area of IS}}$$

The following simplifying assumptions were made: (1) The internal standard and the onion flavor compounds have similar extraction properties and GC and MS responses. (2) Total weight of sulfur compounds present in the extracts was considered as an indicator of the yield of onion oil.

Estimation of Quality of Extracts by GC and GC-MS

Extracts obtained from all extraction methods were analyzed in duplicate by GC. The chromatograms were compared.

Extracts from different methods were analyzed by GC-MS to identify the sulfur compounds present. Analysis by GC-MS was carried out on a JEOL AX-505H double-focusing mass spectrometer coupled to a Hewlett-Packard 5890J gas chromatograph via a heated interface. GC separation employed a SPB-1 fused silica capillary column (30m length, 0.25mm i.d. with a 0.25 μ m film coating) available from Supelco, Inc. Direct (splitless) injection was used. 3 μ L methylene chloride solutions of different extracts were injected for analysis. Helium gas flow was approximately 1 mL/min. The GC temperature program was initiated at 35C, held at this temperature for 5 min then heated at 5C/min to 200C and held for 15 min at this temperature. MS conditions were as follows: interface temperature 280C, ion source temperature ca. 220C, scan rate of the mass spectrometer was 1 s/scan over the m/z range 35/500. The mass spectra were obtained by electron ionization at 70 eV.

Headspace Volatiles Analysis

The 30 mL onion juice was purged with purified nitrogen gas at the flow rate of 75 mL/min for 2.5 h. The headspace volatiles were adsorbed onto an activated coconut charcoal trap. For gas chromatography analysis, the onion headspace volatiles were eluted from the trap using 1 mL carbon disulfide. This analysis was done to evaluate the efficiency of the various extraction methods studied with regard to the quality of extract obtained. Headspace samples contain most of the volatile compounds responsible for fresh onion flavor. By comparing the profiles of extracts obtained from various methods with the headspace volatiles profile it can be determined if the specified method is capable of extracting the components found in the headspace of fresh onion juice.

Thiosulfinate Analysis

Thiosulfinate analysis was done by the method described by Thomas *et al.* (1992). The analysis was performed on onion oil obtained from SFE-CO₂ with ethyl alcohol as entrainer, onion oil obtained from SFE-CO₂ with octane as entrainer and steam distilled commercial onion oil. All the samples were purged with nitrogen to remove any traces of solvent/entrainer present. Isopropyl alcohol (5 mL) was added to equal amounts of these samples. One mL of 0.05 M N-ethylmaleimide in isopropyl alcohol, 1 mL of 0.25 M KOH in isopropyl alcohol, and 1.5 mL of 10 g L⁻¹ ascorbic acid in distilled water were added. After vortexing the solution for approximately 10 s, the absorbance at 515 nm was recorded using a LKB Biochrom spectrophotometer (Model: Ultrospec II). The purpose of doing this analysis was to get information about the quality of extract obtained from supercritical CO₂ extraction and compare it with commercial onion oil obtained from distillation. In addition, it is also a way of evaluating whether the extracts possess fresh-like or cooked flavor. The samples containing higher levels of thiosulfates tend to have fresh-like flavor.

RESULTS AND DISCUSSION

Gravimetric Yield of Onion Oil

Table 1 shows the yield for the three cases which could be gravimetrically measured. SFE-CO₂ extraction with CO₂ flow rate 0.5 L/min gave the maximum onion oil yield.

TABLE 1. GRAVIMETRIC YIELD OF ONION OIL

Method	Oil Yield ^a (g)	% Oil Yield ^b (wt. basis)
SFE-CO ₂ , CO ₂ flow: 1.0 l/min	0.2287 ^c	0.0286
SFE-CO ₂ , CO ₂ flow: 0.5 l/min	0.2592 ^d	0.0324
Liquid CO ₂ extraction	0.1719 ^e	0.0215

a. Mean of triplicate samples

b. On basis of weight of onion juice used

c, d, e. Indicate that the yields are significantly different at the 1% level.

Quantitative GC Analysis for Comparison of Onion Oil Yield from All Methods

Figure 2 shows the average of three replications of the total weight of detectable sulfur compounds present in the extracts from all the methods studied.

The total weight of sulfur compounds was assumed to be representative of the yield of onion oil. Extract obtained by SFE-CO₂ with CO₂ flow rate 0.5 L/min contained the maximum quantity of sulfur compounds thus indicating that the onion oil yield would be maximum in this case. Liquid CO₂ extract was found to contain the minimum quantity of sulfur compounds.

Effect of Volume and Flow Rate of CO₂ on Yield of Onion Oil

Figure 3 shows the yield of onion oil at different volumes of CO₂ passed through the extraction system under the conditions of SFE-CO₂ at 3600 psi and 37°C at CO₂ flow rates of 0.5 L/min and 1.0 L/min. The yield increases with increase in volume of CO₂ passed at a higher rate during the initial part of the extraction as indicated by the greater slope of the curves initially. This is followed by a region of lower extraction rate as indicated by the flattening of the curves during the latter part of the extraction. The lower extraction rate during the latter part of the extraction can be explained in terms of depletion of the solute (onion flavor oil) in the substrate (onion juice).

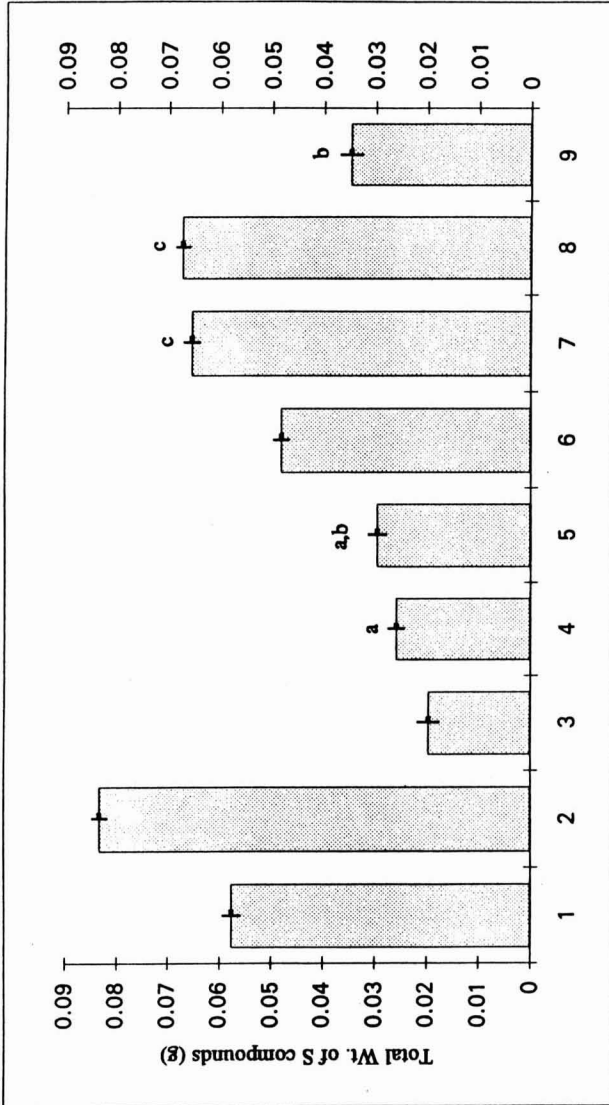
CO₂ flow rate was found to have an effect on the yield of onion oil (Fig. 3). The data points in the initial part of the curves indicate similar extraction rates. A possible reason for this could be the presence of headspace (more than 1 L) in the extraction vessel, which was the same during both the experiments. In the latter part of extraction, the 0.5 L/min CO₂ experiment resulted in a higher yield than the 1.0 L/min experiment. Higher yield in the case of the experiment with 0.5 L/min flow rate could be due to greater residence time of the solvent (CO₂) in the extraction system. The two curves also indicate that the process does not come to an equilibrium state under the conditions tested.

Effect of Entrainer

As indicated by Fig. 2, 26.4% greater yield was obtained in the case of 75 mL ethyl alcohol as compared with 50 mL ethyl alcohol. The 75 mL ethyl alcohol experiment enhanced the yield of onion oil over the experiment with no entrainer (at same CO₂ flow rate, i.e. 1.0 L/min) by 16.6%. In the case of the 50 mL ethyl alcohol experiment, the yield was lower than SFE-CO₂ without entrainer (Fig. 2).

The yield of onion oil obtained from experiments with 75 mL octane as entrainer with SFE-CO₂ extraction was higher than that obtained from 50 mL octane experiments. However, they were both less than the yield of SFE-CO₂ experiments without any entrainer. Thus, under the studied conditions, octane failed to enhance the yield of onion oil from SFE-CO₂.

The SFE-CO₂ system was found to behave almost identically in the case of 75 mL ethyl alcohol used as entrainer at 3600 psi (24.5 MPa) and at 2600 psi (17.7 MPa) in terms of the onion oil yield (Fig. 2). Experiments were not conducted at 2600 psi without entrainer. Although the solvent power of



- 1 SFE-CO₂ with CO₂ flow rate = 1.0 l/min
- 2 SFE-CO₂ with CO₂ flow rate = 0.5 l/min
- 3 Liquid CO₂ Extraction
- 4 SFE-CO₂ with 50 ml Octane as entrainer
- 5 SFE-CO₂ with 75 ml Octane as entrainer
- 6 SFE-CO₂ with 50 ml Ethanol as entrainer
- 7 SFE-CO₂ with 75 ml Ethanol as entrainer
- 8 SFE-CO₂ with 75 ml Ethanol as entrainer at a lower pressure (2600 psi)
- 9 Steam Distillation-Solvent Extraction

a,b,c: Results having same letter are not significantly different at $P < 0.05$ by Fisher's LSD.

┆ Indicates one standard deviation for three replications.

FIG. 2. TOTAL AMOUNT OF SULFUR COMPOUNDS IN THE ONION EXTRACTS OBTAINED BY QUANTITATIVE GC ANALYSIS

supercritical CO_2 is known to be higher at higher pressures, in these experiments the yield of onion oil was 2.7% higher at 2600 psi than that at 3600 psi. This is a very interesting result because it indicates the possibility of lowering the extraction pressure from 3600 psi to 2600 psi with no reduction in the yield of onion oil by using ethyl alcohol as entrainer in the above mentioned quantity. This could have positive effects on the economics of this process. This result supports the findings of Brunner and Peter (1982) that supercritical fluid extraction can be conducted at a lower pressure in the presence of an entrainer. The extract may contain the entrainer in small amounts. Since ethyl alcohol is a food-grade entrainer, it may not affect the extracts adversely. However, the presence of even trace amounts of organic solvents may be undesirable.

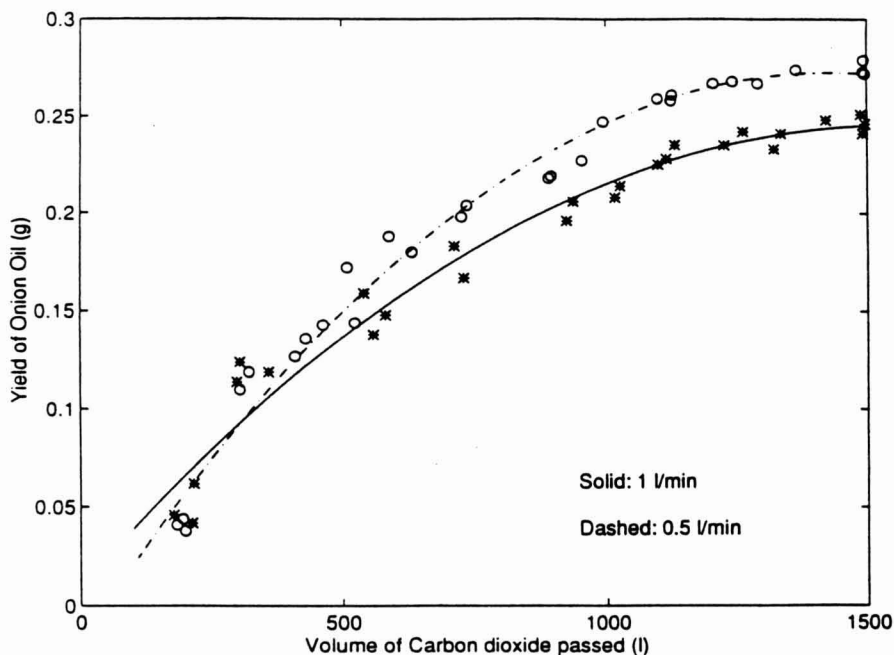


FIG. 3. YIELD OF ONION OIL AT DIFFERENT VOLUMES OF CO_2 PASSED AT DIFFERENT FLOW RATES OF CO_2

Quality of Extracts Obtained from Various Methods

The onion extracts produced through SFE- CO_2 (with or without entrainer) and liquid CO_2 extraction had characteristic fresh onion-like smell in contrast to the rather unpleasing cooked onion-like smell of steam distilled extracts. Gas chromatography-mass spectrometry was used to identify the chemical components of the various extracts and headspace volatiles of onion juice (Table 2).

TABLE 2.
ONION FLAVOR COMPOUNDS IDENTIFIED BY GC-MS IN ONION OIL

no.	Compound	Formula, Mass	SFE-CO ₂	SFE-CO ₂ + Ethanol	SFE-CO ₂ + Octane	Liq. CO ₂	Headspace
1	dimethyl disulfide	C ₂ H ₆ S ₂ , 94	✓	✓			
2	methyl ethyl disulfide	C ₃ H ₈ S ₂ , 108	✓	✓		✓	
3	2,5-dimethyl thiophene	C ₆ H ₈ S, 112	✓	✓		✓	
4	2,4-dimethyl thiophene	C ₆ H ₈ S, 112	✓	✓		✓	
5	3,4-dimethyl thiophene	C ₆ H ₈ S, 112	✓	✓	✓	✓	✓
6	diallyl sulfide	C ₆ H ₁₀ S, 114	✓	✓		✓	
7	methyl propyl disulfide	C ₄ H ₁₀ S ₂ , 122		✓	✓		
8	methyl cis-propenyl disulfide	C ₄ H ₈ S ₂ , 120	✓	✓	✓	✓	✓
9	methyl trans-propenyl disulfide	C ₄ H ₈ S ₂ , 120	✓	✓	✓	✓	✓
10	dimethyl trisulfide	C ₂ H ₆ S ₃ , 126	✓	✓		✓	✓
11	unknown compound	unknown, 130	✓	✓	✓		
12	dipropyl disulfide	C ₆ H ₁₄ S ₂ , 150	✓	✓			
13	1-propenyl propyl disulfide	C ₆ H ₁₂ S ₂ , 148	✓	✓	✓	✓	✓
14	propyl methane thiosulfonate	C ₄ H ₁₀ S ₂ O ₂ , 154		✓			
15	3-ethenyl-1,2-dithi-5-ene	C ₆ H ₁₀ S ₂ , 146	✓	✓	✓	✓	✓
16	methyl propyl trisulfide	C ₄ H ₁₀ S ₃ , 154	✓	✓	✓	✓	✓

17	methyl 1-propenyl trisulfide (<i>E/Z</i>)	C ₄ H ₆ S ₃ , 152	✓	✓	✓	✓	✓	✓	✓
18	methyl 1-propenyl trisulfide (<i>E/Z</i>)	C ₄ H ₆ S ₃ , 152	✓	✓	✓	✓	✓	✓	✓
19	3-ethenyl-1,2-dithi-4-ene	C ₆ H ₁₀ S ₂ , 146	✓	✓	✓	✓	✓	✓	✓
20	3,4-dihydro-3-vinyl-1,2-dithiin	C ₆ H ₈ S ₂ , 144	✓	✓	✓	✓	✓	✓	✓
21	methyl 5-methylfuryl sulfide	C ₆ H ₈ OS, 128		✓	✓	✓	✓	✓	
22	diallyl thiosulfinate	C ₆ H ₁₀ OS ₂ , 162	✓	✓	✓	✓	✓	✓	
23	1-propenyl propyl trisulfide (<i>E/Z</i>)	C ₆ H ₁₂ S ₃ , 180	✓	✓	✓	✓	✓	✓	✓
24	dipropyl trisulfide	C ₆ H ₁₄ S ₃ , 182		✓	✓	✓	✓	✓	✓
25	1-propenyl propyl trisulfide (<i>E/Z</i>)	C ₆ H ₁₂ S ₃ , 180		✓	✓	✓	✓	✓	✓
26	diallyl trisulfide	C ₆ H ₁₀ S ₃ , 178		✓	✓	✓	✓	✓	
27	dibenzothiophene	C ₁₂ H ₈ S, 184	✓	✓	✓	✓	✓	✓	
28	methyl 3,4-dimethyl-2-thienyl disulfide	C ₇ H ₁₀ S ₃ , 190	✓	✓	✓	✓	✓	✓	
29	4,6-dieethyl-1,2,3,5-tetrahiene	212		✓	✓	✓	✓	✓	
30	2,4-dimethyl-5,6-dithia-2,7-nonadienal 5-oxide	218		✓	✓	✓	✓	✓	
31	molecular sulfur	S ₈ , 256							✓
32	5,7-dieethyl-1,2,3,4,6-pentathiepane	264	✓	✓	✓	✓	✓	✓	

The emphasis was on sulfur compounds which are the main flavor components of onions (Abraham *et al.* 1976; Sinha *et al.* 1992). The identification of the flavor compounds was based on comparison of mass spectral data with published works, and in one case tentative identification was made by direct interpretation of mass spectral data. Where definitive characterization could not be made, the mass number is indicated.

The presence of most of the headspace flavor components in SFE-CO₂ + ethanol, SFE-CO₂ without entrainer and liquid CO₂ extracts indicates that these extracts had fresh onion like flavor.

The SFE-CO₂ without entrainer, SFE-CO₂ + ethanol and SFE-CO₂ + octane extracts contained diallyl thiosulfinate (22) or its isomer, di-1-propenyl thiosulfinate. Sinha *et al.* (1992) reported the presence of diallyl thiosulfinate or its isomer, di-1-propenyl thiosulfinate, in supercritical CO₂ onion extracts for the first time. However, they mentioned that the identification of diallyl thiosulfinate was tentative due to the absence of a synthesized reference compound or supporting NMR or IR spectra. Hence, the identification of diallyl thiosulfinate (22) is tentative.

In this study, diallyl thiosulfinate (or its isomer) (22), 3-ethenyl-1,2-dithi-4-ene (19), 3-ethenyl-1,2-dithi-5-ene (15), 3,4-dihydro-3-vinyl-1,2-dithiin (20) and diallyl trisulfide (26) have been found in each of the supercritical extracts (SFE-CO₂ without entrainer, SFE-CO₂ + ethanol, SFE-CO₂ + octane). The presence of above mentioned compounds in the extracts supports the identification of diallyl thiosulfinate since these compounds have been reported to be produced by decomposition of diallyl thiosulfinate (Brodnitz *et al.* 1971; Nishimura *et al.* 1988; Kallio and Salorinne 1990).

In this study propyl methanethiosulfonate (14) was identified and only in SFE-CO₂ + ethanol extracts (Table 2).

Molecular sulfur (31) is being reported in headspace of onion juice for the first time. The identification is based on spectral comparisons with data from Heller and Milne (1978). It is expected to be an artifact resulting from rearrangement of sulfur atoms during processing or GC-MS analysis due to heat. An unknown compound of molecular weight 130 was detected in SFE-CO₂, SFE-CO₂ + ethanol and SFE-CO₂ + octane extracts. The MS data for the unknown compound and for molecular sulfur is provided in Table 3.

GC and GC-MS techniques may preferably be replaced by high performance liquid chromatography (HPLC), cryogenic GC, SCF chromatography or other analytical techniques which employ lower temperatures. This is desirable because some onion flavor components are thermolabile and there is a possibility of their degradation or rearrangement under high temperatures which are usually employed in GC injectors and detectors (Block *et al.* 1992; Block 1993).

The SFE-CO₂ + ethanol sample contained maximum amount of thiosulfonates as indicated by the maximum absorbance recorded in this case (Table 4).

Its value was almost 5 times that of commercial onion oil. The absorbance for SFE-CO₂ + octane was also many times higher than that for commercial onion oil. By smelling the extracts it was found that SFE-CO₂ extracts (with and without entrainer) had similar, fresh-onion like, smell. On the other hand, steam distilled extracts had an aroma of cooked onions. Hence, on the basis of thiosulfinate analysis and subjective aroma analysis results it can be concluded that the SFE-CO₂ extracts (with or without entrainer) have a unique and pleasant aroma characteristics of fresh onions.

TABLE 3.
MASS SPECTRAL AND RETENTION DATA

Compound, Mass	I _k ^a	MS Data ^b
unknown, 130	1017	132(4.8), 131(10.3), 130(100) , 115(23.0), 114(2.3), 113(12.2), 101(83.1), 85(14.9), 69(26.8), 68(14.0), 67(39.6), 59(23.0), 53(13.9), 45(20.0), 41(31.1), 39(18.2)
molecular sulfur, 256	1878	257(41.2), 256(100) , 224(3.0), 194(7.4), 193(1.8), 192(31.3), 162(13.2), 161(3.8), 160(52.2), 130(11.0), 129(0.8), 128(56.4), 98(3.7), 97(0.7), 96(19.5), 66(8.2), 65(1.8), 64(64.2)

a. Kovats Retention Index

b. m/z(intensity)

TABLE 4.
RESULTS OF THIOSULFINATE ANALYSIS

Sample	Absorbance ^a
SFE-CO ₂ + Ethanol	1.673 ^b
SFE-CO ₂ + Octane	1.573 ^b
Steam distilled commercial oil	0.308 ^c

a. Measured at 515 nm in triplicate

b, c Numbers followed by different letters are significantly different at the 1% level.

CONCLUSIONS

In conclusion, this study shows that supercritical fluid extraction with CO₂ has the potential to produce higher yielding and better quality extracts than steam distillation-solvent extraction. The use of polar entrainer, ethyl alcohol, with SFE-CO₂ was found to enhance the yield over SFE-CO₂ without entrainer when compared under similar conditions. Results of thiosulfinate and subjective aroma analysis, and the presence of diallyl thiosulfinate and propyl methane thiosulfonate in SFE-CO₂ + ethanol extracts emphasize the fresh onion-like aroma of these extracts. Thus, onion flavor oil produced by SFE-CO₂ with ethyl alcohol as entrainer will result in a higher yielding, safe (free from organic solvent residues) and unique fresh onion-like flavor.

REFERENCES

- ABRAHAM, K.O., SHANKARANARAYANANA, M.L., RAGHAVAN, B. and NATARAJAN, C.P. 1976. *Alliums*-varieties, chemistry and analysis. *Lebensm. Wiss. Technol.* **9**, 193-200.
- ANGUS, S., ARMSTRONG, B. and DE REUCK, K.M. 1976. International thermodynamic tables of the fluid state: Carbon dioxide. IUPAC Project Centre, Imperial College, London.
- BLOCK, E. 1993. Flavor artifacts. *J. Agric. Food Chem.* **41**, 692.
- BLOCK, E., PUTMAN, D. and ZHAO, S.H. 1992. Allium chemistry: GC-MS analysis of thiosulfonates and related compounds from onion, leek, scallion, shallot, chive and chinese chive. *J. Agric. Food Chem.* **40**, 2431-2438.
- BOELEN, M., DE VALOIS, P., WOBLEN, H.J. and VAN DER GEN, A. 1971. Volatile flavor compounds from onion. *J. Agric. Food Chem.* **19**, 984-990.
- BRODNITZ, M.H., PASCALE, J.V. and DERSLICE, L.V. 1971. Flavor components of garlic extract. *J. Agric. Food Chem.* **19**, 273-275.
- BRUNNER, G. and PETER, S. 1982. On the solubility of glycerides and fatty acids in compressed gases in the presence of an entrainer. *Sep. Sci. and Tech.* **17**, 199-214.
- CALAME, J.P. and STEINER, R. 1982. Carbon dioxide extraction in the flavor and perfumery industries. *Chem. Ind. June*, 399-402.
- CARSON, J.F. 1987. Chemistry and biological properties of onions and garlic. *Food Rev. Int.* **3**(1,2), 71-107.
- COPELLA, S.J. and BARTON, P. 1987. Supercritical carbon dioxide extraction of lemon oil. In *Supercritical Fluids: Chemical Engineering Principles and Applications*. (T.G. Squires and M.E. Paulitis, eds.). ACS Symposium Series No. 329.

- DOBBS, J.M., WONG, J.M. and JOHNSTON, K.P. 1986. Nonpolar co-solvents for solubility enhancement in supercritical fluid carbon dioxide. *J. Chem. Eng. Data* 31, 303-308.
- DOBBS, J.M., WONG, J.M., LAHIERE, R.J. and JOHNSTON, K.P. 1987. Modification of supercritical fluid phase behavior using polar co-solvents. *Ind. Eng. Chem. Res.* 26, 56-65.
- FENWICK, G.R. and HANLEY, A.B. 1985. The genus *Allium*. *CRC Crit. Rev. Food Sci. Nutr.* 22, 199-271.
- GRIMMETT, C. 1981. The use of liquid carbon dioxide for extracting natural products. *Chem. Ind.* 16 (May), 359-362.
- HELLER, S.R. and MILNE, G.W.A. 1978. EPA/NIH Mass Spectral Data Base. U.S. Department of Commerce/National Bureau of Standards.
- HUBERT, P. and VITZTHUM, O.F. 1978. Extraction of hops, spices and tobacco with supercritical gases. *Agnew. Chem. Int. Ed. Engl.* 17, 710-754.
- KALLIO, H. and SALORINNE, L. 1990. Comparison of onion varieties by headspace gas chromatography-mass spectrometry. *J. Agric. Food Chem.* 38, 1560-1564.
- LIKENS, S.T. and NICKERSON, G.B. 1964. Detection of certain hop oil constituents in brewing products. *Proc Am. Soc. Brew. Chem.* 5-13.
- NGUYEN, K., BARTON, P. and SPENCER, J.S. 1991. Supercritical carbon dioxide extraction of vanilla. *J. Supercritical Fluids* 4, 40-46.
- NISHIMURA, H., WIJAYA, H. and JUNYA, M. 1988. Volatile flavor components and antithrombotic agents: vinylthiols (from *Allium victorialis*). *J. Agric. Food Chem.* 36, 563-566.
- RIZVI, S.S.H., BENADO, A.L., ZOLLWEG, J.A. and DANIELS, J.A. 1986. Supercritical fluid extraction: Fundamental principles and modeling methods. *Food Technol.* 40, 55-64.
- SCHULTZ, T.H., FLATH, R.A., MON, T.R., EGGLE, S.B. and TERANISHI, R. 1977. Isolation of volatile components from a model system. *J. Agric. Food Chem.* 25, 446-449.
- SCHULTZ, W.G. and RANDALL, J.M. 1970. Liquid carbon dioxide for selective aroma extraction. *Fd. Tech.* 24(11), 1282-1286.
- SINHA, N.K., GUYER, D.E., GAGE, D.A. and LIRA, C.T. 1992. Supercritical carbondioxide extraction of onion flavors and their analysis by gas chromatography-mass spectrometry. *J. Agric. Food Chem.* 40, 842-845.
- STAHL, E., QUIRIN, K.W. and GERARD, D. 1988. *Dense Gases for Extraction and Refining*. Springer-Verlag, New York.
- TERANISHI, R., FLATH, R.A. and SUGISAWA, H. 1971. In *Flavor Research: Principles and Techniques*. Marcel Dekker, New York.
- THOMAS, D.J., PARKIN, K.L. and SIMON, P.W. 1992. Development of a simple pungency indicator test for onions. *J. Sci. Food Agric.* 60, 499-504.

WHITAKER, J.R. 1976. Development of flavor, odor, and pungency in onion and garlic. *Adv. Food Res.* 22, 73–133.

CONCENTRATION OF ONION JUICE VOLATILES BY REVERSE OSMOSIS AND ITS EFFECTS ON SUPERCRITICAL CO₂ EXTRACTION

JEFFREY S. NUSS and DANIEL E. GUYER¹

*Department of Agricultural Engineering
Michigan State University
East Lansing, Michigan 48824*

AND

DOUGLAS A. GAGE

*Department of Biochemistry
Michigan State University
East Lansing, Michigan 48824*

Accepted for Publication May 30, 1996

ABSTRACT

Supercritical carbon dioxide extraction of onion oil at moderate temperatures produces a product which is characteristic of the fresh flavor of onions. It was attempted to improve extraction efficiency by concentrating the onion juice by reverse osmosis prior to supercritical CO₂ extraction. Reverse osmosis was carried out for all combinations of 600, 700, and 800 psi feed pressure and 25 and 35C. The juice was concentrated to 18 °Brix and then subjected to supercritical CO₂ extraction. The effect of concentration on the extraction process was evaluated by comparing the yields of extracts from concentrated juice with that of single strength juice. Concentration of onion juice by reverse osmosis improved the efficiency of supercritical CO₂ extraction of onion oil and did not alter its characteristic fresh aroma.

INTRODUCTION

The characteristic flavor of onions comes primarily from volatile organic sulfur compounds released enzymatically by the action of allinase on several naturally occurring amino acid precursors when the onion is crushed or

¹ Author to whom correspondence should be addressed: Daniel E. Guyer, 205 Farrall Hall, Agricultural Engineering Department, Michigan State University, East Lansing, MI 48824

macerated. The primary reaction products are thiosulfonates which have been associated with fresh onion flavor. Thiosulfonates are very unstable and readily dissociate upon heating to form di- and trisulfides and various other sulfur containing compounds which have been associated with cooked onion flavors (Block and O'Conner 1974; Boelens *et al.* 1971).

Onion oils are widely used as seasonings in food processing. The majority of onion oils used as food ingredients are steam distilled and lack fresh flavors. Sinha *et al.* (1992) investigated supercritical CO₂ extraction as a method for producing onion oil. They found the extraction at moderate temperatures produces a product which is characteristic of fresh onion flavor and lacks the cooked flavor present in steam distilled oils. Such an oil could be a unique product for the flavor industry if a feasible process is developed.

Another separation technique commonly used in liquid food processing is reverse osmosis. Reverse osmosis has received much attention as a method of concentrating fruit and vegetable juices (Merson and Morgan 1968; Matsuura *et al.* 1975; Sheu and Wiley 1983; Chua *et al.* 1987; Braddock *et al.* 1988; Chou *et al.* 1991; Koseoglu *et al.* 1991). Because heating is not necessary for separation, thermal damage to the flavor compounds is minimized. In addition to a sufficient water removal rate, the retention of flavor compounds during reverse osmosis ultimately determines the success of the process.

It was hypothesized that the yield of onion oil from supercritical CO₂ extraction could be improved by concentrating the onion juice by reverse osmosis prior to extraction. The goals of this research were (1) to investigate concentration of onion juice by reverse osmosis as a means of improving the yield of onion oil produced by supercritical CO₂ extraction, (2) to investigate the effect of reverse osmosis operating temperature and pressure on extraction yield, (3) to ascertain whether reverse osmosis prior to extraction affects the quality, or characteristic fresh flavor, of the onion oil, and (4) to examine the effects of reverse osmosis on the thiosulfonate content of the juice.

MATERIALS AND METHODS

Reverse Osmosis

Onions of the variety Spartan Banner were obtained from a Michigan onion producer. For reverse osmosis (RO) experiments, 4.5 L of juice was obtained with a juice extractor (Waring Model 6001 Juicerator). The onion juice was filtered prior to reverse osmosis to remove large pieces of pulp.

The RO feed pressures and temperatures examined were 600, 700, and 800 psi (4.14, 4.83, and 5.52 Mpa) and 25 and 35C, respectively. Experiments were performed in triplicate using all six combinations of the above pressures and

temperatures. A heat exchanger located between the membrane and feed tank maintained the juice at the desired temperature. The membrane used was an AFC99 polyamide, tubular membrane (PCI Membranes) with 0.024 m² of surface area.

During the concentration process, the permeate flux and °Brix of the retentate were measured and reported at thirty minute intervals. The permeate flux, recorded in L/m²/h, was measured by recording the time for the permeate to fill a 10 mL graduated cylinder. For °Brix measurements, a 2-3 mL sample of juice was taken with a needle and syringe through a silicon filled sampling port in the juice return line. A hand held, temperature compensated refractometer was used to measure °Brix. Samples of 10 mL each were taken at juice concentrations of 10, 12, 14, 16, and 18 °Brix and immediately stored at -21C for thiosulfinate analysis. The concentration process was terminated when the onion juice reached 18 °Brix.

Analytical

Relative amounts of aromas in the RO concentrate and permeate streams were estimated by comparing the integrated GLC peak areas of the volatiles collected using a dynamic headspace sampling technique. This technique consisted of stripping the volatile compounds from the liquid samples with a steady stream of nitrogen. The gaseous mixture was then passed through a collection tube packed with activated coconut charcoal (Supelco Orbo 32-small) onto which the volatiles are adsorbed. The adsorbed compounds were then eluted with 1 mL of carbon disulfide for GLC analysis. The volatiles of several single strength juices were also analyzed. Identification of volatiles was achieved using GC-MS.

The thiosulfinate content of concentrated juice samples was determined using the method of Nakata (1970). Thiosulfinate content was reported as the spectrophotometric absorbance at 515 nm (LKP Biochrom, Ultraspec II). Absorbances were the averages of four replicates from each juice sample.

Supercritical CO₂ Extraction

Figure 1 illustrates the supercritical CO₂ extraction system. Before beginning an extraction, the micrometering valve (11), shutoff valves (6,10), and CO₂ regulator (2) are turned to the open position. Industrial grade CO₂ is compressed with a gas compressor (3) and stored in a 2 L reservoir (4). A pressure regulator (7) located between the reservoir and the 500 mL extraction vessel (9) controls the extraction pressure. Pressure gauges (5,8) are used to monitor pressure in the reservoir and extraction vessel. Heating tape is used for heating of the extraction vessel. The vessel temperature is monitored and controlled by a thermocouple and temperature controller.

Separation of solutes from the supercritical CO₂ is achieved by passing the supercritical CO₂ through a micrometering valve (11) at which point the pressure is reduced to atmospheric. Cartridge heaters embedded in steel saddle blocks are mounted to the micrometering valve to keep the valve from freezing due to the instantaneous expansion of CO₂. A 1/8 in. i.d. stainless steel tube connects the micrometering valve with the collection trap (12) via a rubber stopper with a small hole. The collection trap is a 3.7 mL glass vial in the bottom of a glass side arm test tube. The tube extends through the rubber stopper to the bottom of the of the collection trap. The solute free CO₂ exits the collection trap and passes through a gas flow meter and is then vented.

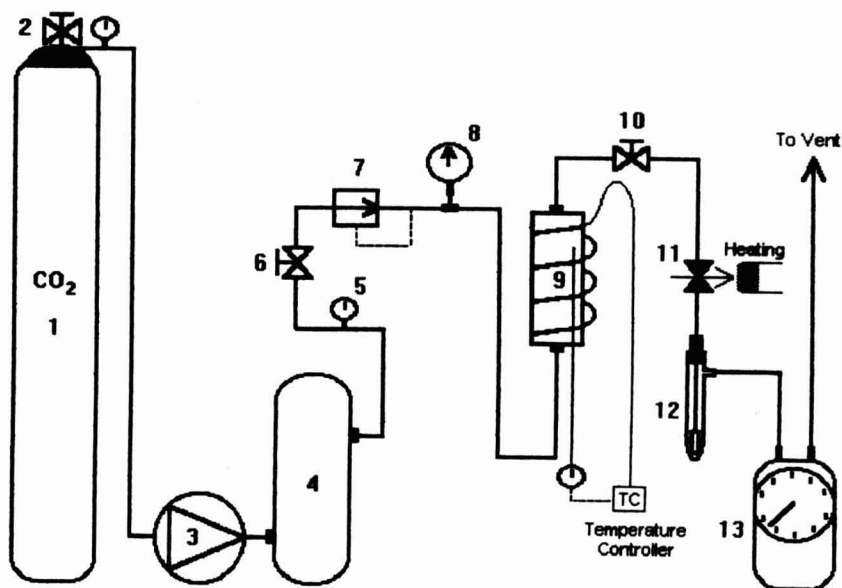


FIG. 1. SUPERCRITICAL CO₂ EXTRACTION APPARATUS

(1) CO₂ tank, (2) CO₂ regulator, (3) compressor, (4) 2 L reservoir pressure regulator, (5,8) pressure gauges, (6,10) shutoff valves, (7) pressure regulator, (9) 500 mL extraction vessel, (11) micrometering valve, (12) collection trap, (13) gas flow meter.

Immediately after reverse osmosis, the extraction vessel was filled with 475 mL of the concentrated onion juice. The extraction temperature and pressure were 37°C and 3500 psi (24.13 MPa). It was desired to operate at a constant CO₂ flow rate of 1.0 L/min. However, fluctuations in flow rate during the night resulted in variations (± 0.1 L/min) in flow rates among experiments. The extraction was terminated after 1000 L (STP) of CO₂ had passed through the extraction vessel.

Three extractions were also performed on unprocessed juice under the conditions described above to ascertain the effects of concentration by RO on extraction yield.

RESULTS AND DISCUSSION

Permeate Flux

In each experiment the permeate flux decreased nearly linearly with increase in °Brix of the juice (Fig. 2). The observed increase is primarily due to an increase in the osmotic pressure of the juice and hence a decrease in the driving force for water removal. Build-up of soluble solids at the solution-membrane interface may have also contributed to the decline in flux. This phenomenon is known as concentration polarization.

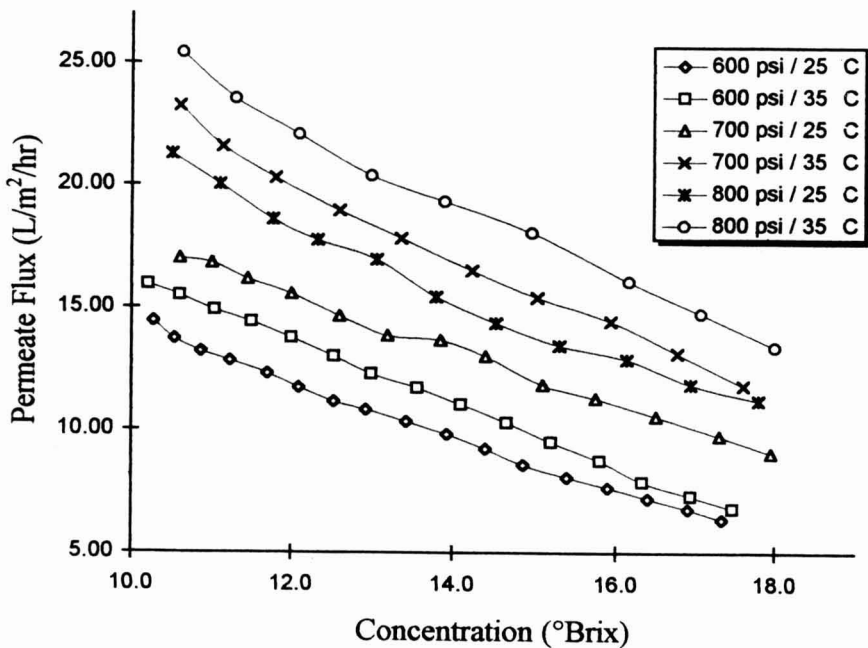


FIG. 2. PERMEATE FLUX AS A FUNCTION OF CONCENTRATION DURING REVERSE OSMOSIS OF ONION JUICE

Table 1 lists the average initial concentration and permeate fluxes of the three experiments at each temperature and pressure during concentration from the initial value to 18 °Brix. For a given temperature, the increase in flux with increase in pressure is a result of a greater driving force for water removal.

Significant differences existed in the rates of water removal among the experiments and hence in the processing times as illustrated by Fig. 3. The time required to concentrate the juice to 18 °Brix varied between 4.5 h for 800 psi and 35C to about 9 h for 600 psi and 25C.

TABLE 1.
AVERAGE INITIAL CONCENTRATION OF JUICE AND AVERAGE PERMEATE FLUX DURING REVERSE OSMOSIS CONCENTRATION OF ONION JUICE TO 18 °BRIX

Pressure (psi)	Temperature °C	Average Initial °Brix	Average Permeate Flux (L/m ² /h) [†]
600	25	10.0	9.90
600	35	10.0	11.14
700	25	10.2‡	13.18‡
700	35	10.0	16.91
800	25	10.0	15.61‡
800	35	10.1	19.25

[‡]Average of two replications. All other results are averages of three replications.

[†]Differences in fluxes were significant @ 1% level.

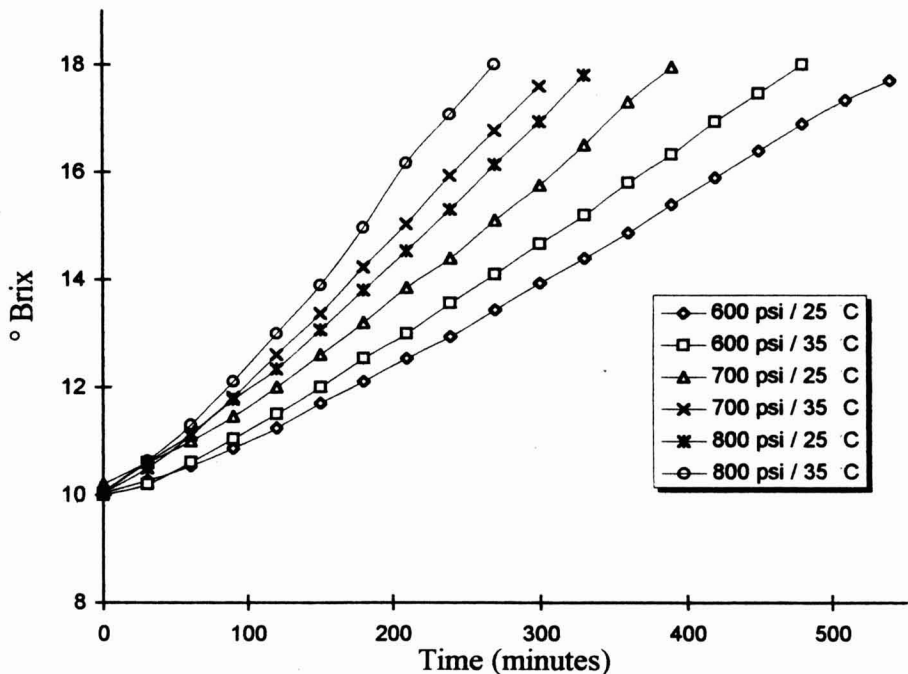


FIG. 3. CHANGE IN °BRIX OF ONION JUICE WITH TIME DURING REVERSE OSMOSIS

Volatile Flavor Compounds

The flavor compounds were identified by comparing the spectral data, retention times, and elution order with published GC and GC-MS data (Bernhard 1968; Brodnitz *et al.* 1969; Brodnitz and Pollock 1970; Boelens *et al.* 1971; Freeman and Whenham 1974; Mazza and LeMaguer 1979; Mazza *et al.* 1980; Kallio and Salorinne 1990; Kallio *et al.* 1990; Sinha *et al.* 1992; Martín-Lagos *et al.* 1992; Ohsumi *et al.* 1993).

Significant differences in GLC peak areas and their proportions existed among the juices. An organic oxygen compound, 2-methyl-2-pentenal, accounted for 84 to 94% of the total peak area in the RO concentrates. In single strength juices, it accounted for only 71 to 81% of the total peak area. Freeman and Whenham (1974) also found 2-methyl-2-pentenal to be the major compound in the headspace of onion juice. All other compounds detected were sulfur containing molecules, primarily di- and trisulfides.

There was no evidence of the presence of thiosulfinates in the headspace samples. The absence of thiosulfinates may be the result of thermal degradation during GC-MS analysis. Some researchers (Block *et al.* 1992; Calvey *et al.* 1994) have criticized GC-MS techniques that employ high injector and detection port, column, and GC-MS transfer line temperatures, alleging that many compounds identified in this manner are thermal artifacts. Block *et al.* identified a number of thiosulfinates in onion extracts using a cryogenic GC-MS procedure but found no evidence of di and trisulfides.

In addition to the effects of RO pressure and temperature, differences in the relative amounts of flavor compounds could be due to variability among onions or among the membranes' chemical nature and pore structure. Since all compounds detected were secondary reaction products resulting from the breakdown of thiosulfinates, the lengths of time between juicing, RO, and headspace sampling could have also affected the relative amounts of compounds detected.

Figure 4 shows a comparison of GC chromatograms of an RO concentrate and the permeate from the same experiment. Many compounds found in the concentrate were not detected in the permeate sample. The compounds which did appear in the permeate chromatogram were in very low concentration. Thus, it appears there were only minor losses of flavor compounds due to membrane permeation.

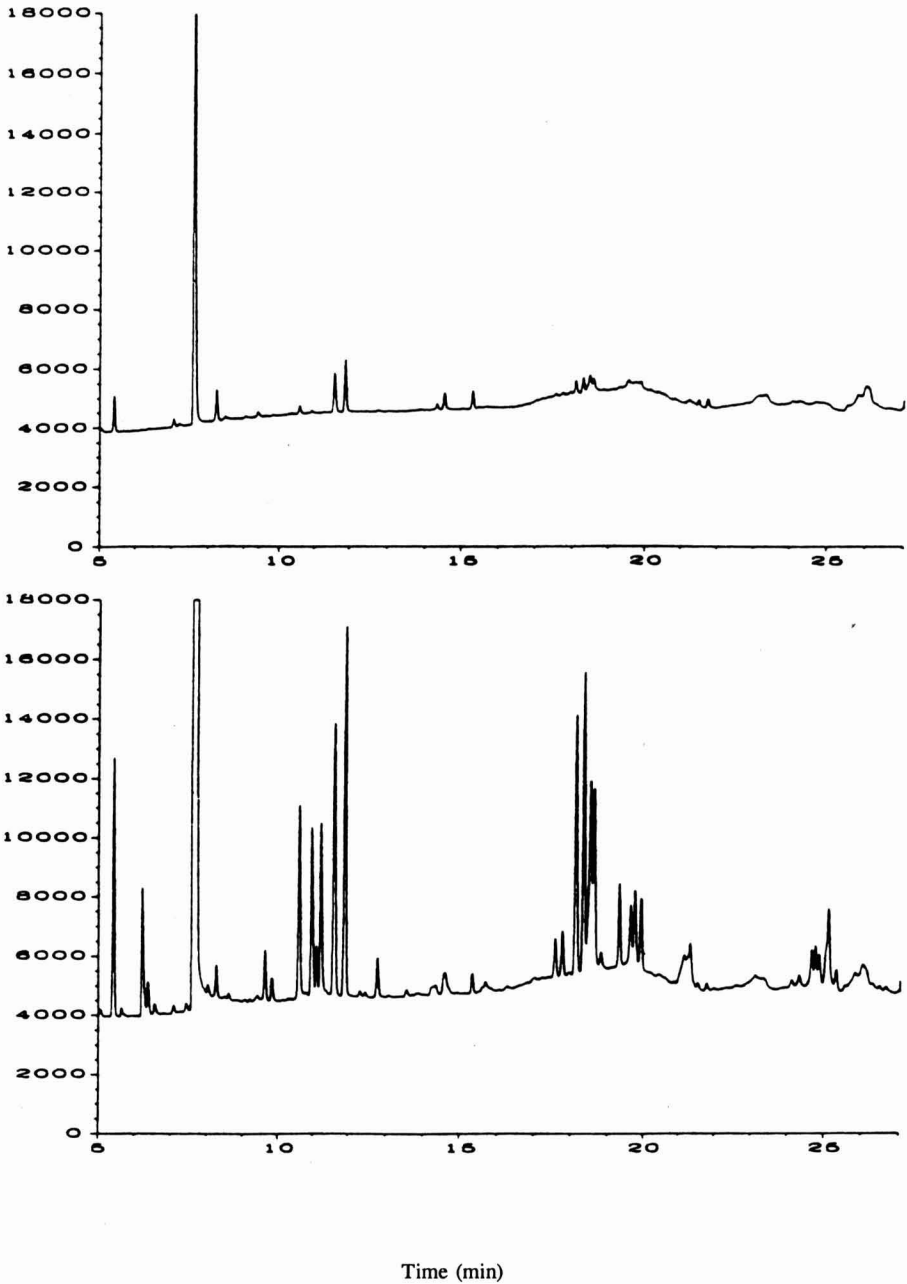


FIG. 4. GC CHROMATOGRAM OF VOLATILES COLLECTED FROM THE VAPOR IN EQUILIBRIUM WITH AN RO PERMEATE SAMPLE (TOP) AND RO CONCENTRATE (BOTTOM)

Thiosulfinates

The results of the thiosulfinate analysis of the concentrated juice samples are listed in Table 2. The percentage change in the spectrophotometric absorbance during reverse osmosis was calculated as follows:

$$\% \text{ change} = \frac{\text{absorbance at 18 } ^\circ\text{Brix} - \text{absorbance at initial concentration}}{\text{absorbance at initial concentration}} * 100$$

TABLE 2.
THIOSULFINATE CONTENT OF ONION JUICE SAMPLES TAKEN DURING REVERSE OSMOSIS AS MEASURED BY SPECTROPHOTOMETRIC ABSORBANCE AT 515NM

Pressure Temp. (psi)	RO °C	RO Date	Analysis Date	Spectrophotometric Absorbance @ the Given Juice °Brix					% Change in Abs.
				Initial	12	14	16	18	
600	25	6/1	6/2	0.699	0.685	0.722	0.844	0.849	21.46
600	25	6/15	7/14	0.581	0.665	0.702	0.744	0.750	29.09
600	35	5/5	5/5	0.755	0.741	0.759	0.761	0.740	-1.99
600	35	6/6	6/9	0.568	0.608	0.679	0.696	0.692	21.83
700	25	5/25	5/25	0.667	0.674	0.721	0.762	0.769	15.29
700	35	3/18	3/18	0.533	0.492	0.543	0.555	0.552	3.56
700	35	6/14	7/14	0.654	0.607	0.660	0.697	0.720	10.09
800	25	6/7	6/9	0.512	0.495	0.566	0.568	0.719	40.43
800	25	5/31	6/2	0.694	0.798	0.877	0.938	0.904	30.26
800	25	7/13	7/14	0.723	0.691	0.733	0.777	0.825	14.11
800	35	6/5	6/8	0.728	0.681	0.737	0.810	0.818	12.36

In all but one experiment, reverse osmosis resulted in an increase in absorbance and hence, an increase in the thiosulfinate content of the onion juice. The average increase in thiosulfinate content of the six 25C RO experiments which were investigated was 25.1% while that of the five 35C experiments was only 9.2%. A possible reason for this difference is that at 35C the thiosulfinates are more readily decomposed to disulfides than at 25C.

A notable feature of the results is the variation in the thiosulfinate content of the single strength juice. Though there were vast differences in initial thiosulfinate content, there was somewhat of a trend in thiosulfinate content throughout the concentration process (Fig. 5). The trend that was common to most of the RO processes was an initial decrease or increase in thiosulfinate content followed by a steady increase and then an eventual leveling off as the concentration of the juice approached 18 °Brix.

There are a couple possible explanations for the leveling out effect toward the end of the concentration process. It may be the result of a decrease in the percentage rejection of thiosulfinates as the juice becomes more concentrated.

The decrease in solute rejection with increasing solute concentration was explained by Matsuura and Sourirajan (1986). They associated this problem with decreasing water transport due to increasing viscosity and osmotic pressure in the feed stream. Braddock *et al.* (1991) observed similar results for the rejection of aroma compounds during reverse osmosis of citrus juice essence.

Another explanation may be that as the juice becomes more concentrated, the amount of viscous heating that occurs in the pump increases. Such an occurrence could accelerate the rate of conversion of thiosulfinates to secondary flavor compounds. The fact that the flow rate of cooling water in the heat exchanger had to be gradually increased throughout reverse osmosis supports this theory.

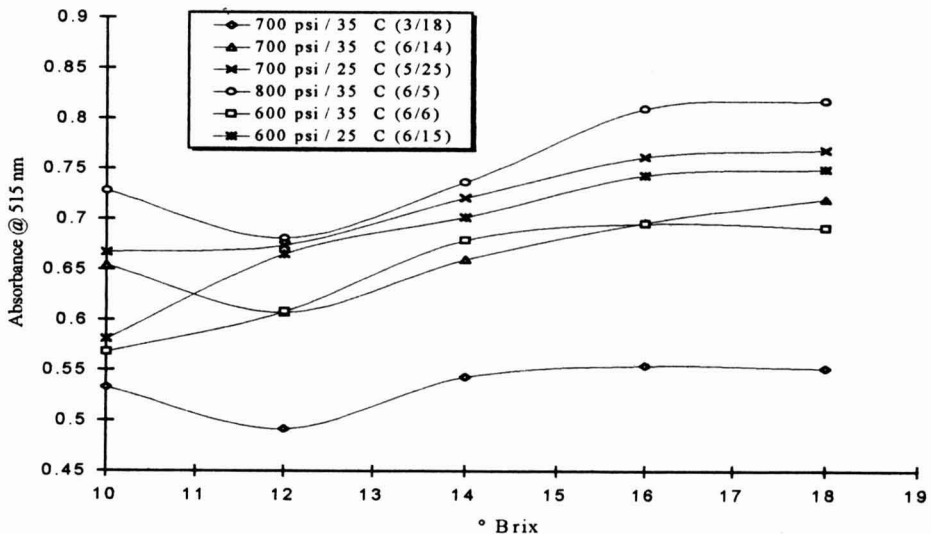


FIG. 5. THIOSULFINATE ANALYSIS: ABSORBANCE @ 515 NM OF SELECTED RO CONCENTRATES

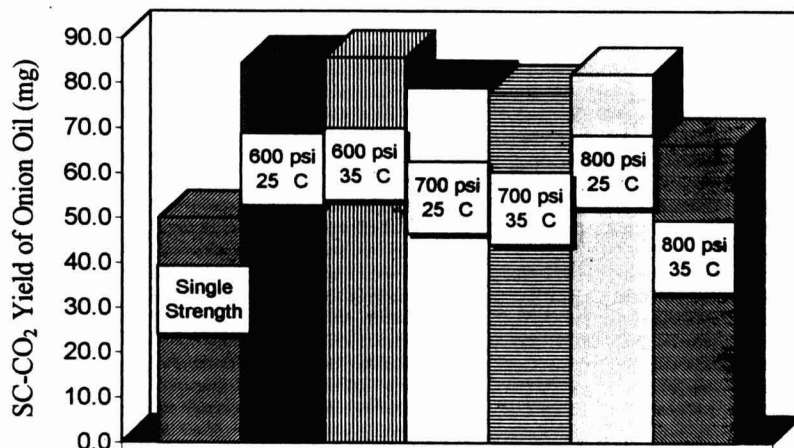
Supercritical CO₂ Extraction Yields

Figure 6 illustrates the effect of juice concentration by reverse osmosis on the yield of onion extract from supercritical CO₂ extraction. The average yields and the percentage increase in yield over the average single strength juice yield are listed in Table 3. Average yields from the 600 psi RO experiments were approximately 70% greater than the average yield from single strength juice and the 800 psi/25C RO treatment increased the yield by 64%. Juice concentrated by RO at 700 psi also improved the yield but to a lesser extent while juice

concentrated by RO at 800 psi and 35C resulted in an improvement of only about 33%.

Analysis of Variance for the 25C RO treatments using a completely randomized design showed that the yield from juices concentrated by RO at 25C were significantly different than the yield from single strength juice at the 5% confidence level. Concentration by RO at 25C, over all three pressures, improved the extraction yield by an average of 63.5%.

Analysis of Variance for the 35C RO treatments did not show a significant difference between yields from the RO concentrated juices and single strength juice though the 600 psi/35C treatment resulted in a 71.4% average increase over the single strength yield. One divergent data point in both the 600 psi/35C and 700 psi/35C experimental data sets produced substantial within-treatment variability which might have resulted in the inability of this test to detect a lack of statistical significance. Unfortunately, we were unable to verify the results of these with further experiments due to equipment failure. We believe that data from additional experiments would provide statistically conclusive evidence that RO concentration of the juice at 35C significantly increases SC-CO₂ extraction yield over the single strength juice.



F value for comparison of single strength with 25C experiments is significant at $p \leq 0.5$.

FIG. 6. AVERAGE YIELDS OF ONION OIL FROM SUPERCRITICAL CO₂ EXTRACTION OF SINGLE STRENGTH AND RO CONCENTRATED ONION JUICES

TABLE 3.
AVERAGE YIELDS OF ONION OIL FROM SC-CO₂ EXTRACTION AND % INCREASE IN
YIELD OVER THE AVERAGE YIELD FROM SINGLE STRENGTH JUICE

Reverse Osmosis Pressure (psi)	Average Yield (mg)		% Increase Over Single Strength Yield	
	25C	35C	25C	35C
600	84.3 [†] (19.7)	85.7 (35.2)	68.6	71.4
700	79.0 [†] (1.0)	78.0 (21.7)	58.0	56.0
800	82.0 [†] (7.9)	66.3 (6.1)	64.0	32.6
single strength	50.0 [†] (14.1)	50.0 (14.1)	---	---
Coeff. of Variance	18.5%	31.5%		

[†]Difference significant at $p \leq 0.05$.

Standard Deviations given in parentheses

A factorial approach was also employed to investigate interaction between reverse osmosis pressure and temperature. The interaction between temperature and pressure was not significant at the 1% level indicating that they act independently. In other words, the difference between extract yields for the different reverse osmosis pressures was not dependent on reverse osmosis temperature and visa versa.

If the juices concentrated by RO possess a higher concentration of flavor compounds than the single strength juice, then equations describing the equilibrium extraction of a material from one phase to another offers a generalized explanation for the observed increase in yield. Consider the equation for the distribution coefficient for a ternary system. For low concentrations of a solute in the two phases, the solute's distribution coefficient in a CO₂-solute-water system is given by

$$K_D = \frac{y_e}{x_e}$$

where K_D is the distribution coefficient, y_e is the concentration of solute dissolved in the carbon dioxide phase, and x_e is the concentration of solute dissolved in the water phase at equilibrium. The concentrations y_e and x_e are usually expressed as mole fractions or weight percents (McHugh and Krukonis 1994). At low concentrations the distribution coefficient is constant and thus an increase in solute concentration in the feed would result in an increase in concentration in the CO₂.

In our experience, we have found that onion oils produced by supercritical CO₂ extraction are remarkably different from steam distilled onion oils. The oils from supercritical CO₂ extraction have an aroma which is more natural or more characteristic of fresh onions while steam distilled onion oils possess a sharp,

synthetic-like aroma. These differences have been confirmed by an expert panel of flavorists. It was not our intent in this study to quantify these differences, for this would be a separate study in itself. Our intent here was to ascertain whether the SC-CO₂ extracts from onion juice concentrated by RO possess a characteristic fresh aroma when compared to steam distilled oils.

Despite differences in the proportions of the flavor compounds between the extracts from different experiments, all of the extracts had a characteristic fresh aroma when compared to a steam distilled onion oil obtained from a flavor manufacturer. Hence from a sensory perspective, concentration of onion juice by reverse osmosis prior to SC-CO₂ extraction does not alter the fresh-like quality of the SC-CO₂ extracts.

CONCLUSION

The following results were obtained from this investigation:

- (1) During concentration of onion juice to 18 °Brix by reverse osmosis, there was little loss of flavor compounds due to membrane permeation.
- (2) Reverse osmosis was effective in concentrating thiosulfinates. Reverse osmosis at 25C tends to be more effective than at 35C.
- (3) Concentration of onion juice to 18 °Brix by reverse osmosis prior to supercritical CO₂ extraction increased the extraction yield for all RO pressure-temperature combinations studied.
- (4) Quality aroma of the onion oils produced by SC-CO₂ was not effected by prior reverse osmosis at any pressure-temperature combination investigated when compared to extraction of onion oil using single strength juice.

Based on the results of this investigation, it is evident that concentration of onion juice by reverse osmosis can be employed as a means of improving the yield of onion oil from supercritical CO₂ extraction. Furthermore, reverse osmosis does not significantly alter the flavor quality of the onion oil. From a quality perspective, the combined process produces a unique product in comparison with steam distilled onion oil. An economic assessment is required to ascertain whether the proposed processing method can compete commercially with traditional processing methods.

REFERENCES

- BERNHARD, R.A. 1968. Comparative distribution of volatile aliphatic disulfides derived from fresh and dehydrated onion. *J. Food Sci.* 33, 298-304.

- BLOCK, E. and O'CONNOR, J. 1974. The chemistry of alkyl thiosulfinate esters. VI. Preparation and spectral studies. *J. Amer. Chem. Soc.* **96** (12), 3921-3929.
- BLOCK, E., PUTMAN, D. and ZHAO, S. 1992. *Allium* Chemistry: GC-MS analysis of thiosulfinates and related compounds from onion, leek, scallion, shallot, chive, and Chinese chive. *J. Agric. Food Chem.* **40**, 2431-2438.
- BOELEN, M., DE VALOIS, P.J., WOBLEN, H.J. and VAN DER GEN, A. 1971. Volatile flavor compounds from onion. *J. Agric. Food Chem.* **19**, 984-990.
- BRADDOCK, R.J., NIKDEL, S. and NAGY, S. 1988. Composition of some organic and inorganic compounds in reverse osmosis-concentrated citrus juices. *J. Food Sci.* **53** (2), 508-512.
- BRADDOCK, R.J., SADLER, G.D. and CHEN, C.S. 1991. Reverse osmosis concentration of aqueous-phase citrus juice essence. *J. Food Sci.* **56** (4), 1027-1029.
- BRODNITZ, M.H. and POLLACK, C.L. 1970. Gas chromatographic analysis of distilled onion oil. *Food Tech.* **24**, 78-80.
- BRODNITZ, M.H., POLLACK, C.L. and VALLON, P.P. 1969. Flavor components of onion oil. *J. Agric. Food Chem.* **17**, 760-763.
- CALVEY, E.M. *et al.* 1994. Off-line supercritical fluid extraction of thiosulfinates from garlic and onion. *J. Agric. Food Chem.* **42**, 1335-1341.
- CHOU, F., WILEY, R.C. and SCHLIMME, D.V. 1991. Reverse osmosis and flavor retention in apple juice concentration. *J. Food Sci.* **56** (2), 484-487.
- CHUA, H.T., RAO, M.A., ACREE, T.E. and CUNNINGHAM, D.G. 1987. Reverse osmosis concentration of apple juice: flux and flavor retention by cellulose acetate and polyamide membranes. *J. Food Process Engineering* **9**, 231-245.
- FREEMAN, G.C. and WHENHAM, R.J. 1974. Changes in onion (*Allium cepa* L.) flavour components resulting from some post-harvest processes. *J. Sci. Food Agric.* **25**, 499-515.
- KALLIO, H. and SALORINNE, L. 1990. Comparison of onion varieties by headspace gas chromatography-mass spectrometry. *J. Agric. Food Chem.* **38**, 1560-1564.
- KÖSEOĞLU, S.S., LAWHON, J.T. and LUSAS, E.W. 1991. Vegetable juices produced with membrane technology. *Food Tech.* **45** (1), 124-130.
- MARTÍN-LAGOS, R.F., OLEA SERRANO, M.F. and RUIZ-LÓPEZ, M.D. 1992. Comparative study by gas chromatography-mass spectrometry of methods for the extraction of sulfur compounds in *Allium cepa* L. *Food Chem.* **44**, 305-308.
- MATSUURA, T., BAXTER, A.G. and SOURIRAJAN, S. 1975. Reverse osmosis recovery of flavor components from apple juice waters. *J. Food Sci.* **40**, 1039-1046.

- MATSUURA, T. and SOURIRAJAN, S. 1986. Physicochemical and engineering properties of food in reverse osmosis and ultrafiltration. In *Engineering Properties of Food* (M.A. Rao and S.S.H. Rizvi, eds.) pp. 255-327, Marcel Dekker, New York.
- MAZZA, G. 1980. Relative volatilities of some onion flavour components. *J. Food Tech.* 15, 35-41.
- MAZZA, G. and LEMAGUER, M. 1979. Volatiles retention during dehydration of onion (*Allium cepa* L.). *Lebensm.-Wiss. u.-Technol.* 12, 333-337.
- MAZZA, G., LEMAGUER, M. and HADZIYEV, D. 1980. Headspace sampling procedures for onion (*Allium cepa* L.) aroma assessment. *Can. Inst. Food Sci. Technol. J.* 13, 87-96.
- MCHUGH, M.A. and KRUKONIS, V.J. 1994. *Supercritical Fluid Extraction*. (H. Brenner, ed.) Butterworth-Heinemann, Stoneham, Massachusetts.
- MERSON, R.L. and MORGAN, A.I. 1968. Juice concentration by reverse osmosis. *Food Tech.* 22, 97-100.
- NAKATA, C., NAKATA, T. and HISHIKAWA, A. 1970. An improved colorimetric determination of thiosulfates. *Anal. Biochem.* 37, 92-97.
- OSHUMI, C., HAYASHI, T., KUBOTA, K. and KOBAYASHI, A. 1993. Volatile flavor compounds formed in an interspecific hybrid between onion and garlic. *J. Agric. Food Chem.* 41, 1808-1810.
- SHEU, M.J. and WILEY, R.C. 1983. Concentration of apple juice by reverse osmosis. *J. Food Sci.* 48, 422-429.
- SINHA, N.K., GUYER, D.E., GAGE, D.A. and LIRA, C.T. 1992. Supercritical carbon dioxide extraction of onion flavors and their analysis by gas chromatography-mass spectrometry. *J. Agric. Food Chem.* 40, 842-845.

FLOW MODELING OF A POWER-LAW FLUID IN A FULLY-WIPED, CO-ROTATING TWIN-SCREW EXTRUDER¹

Y. LI, H.E. HUFF and F. HSIEH²

*Departments of Biological and Agricultural Engineering
and Food Science and Human Nutrition
University of Missouri
Columbia, MO 65211*

Accepted for Publication May 30, 1996

ABSTRACT

The two-dimensional flow theory of a power law fluid in a fully-wiped co-rotating twin-screw extruder was investigated under steady-state, isothermal conditions. The important distinction between this approach and previously published theories (Denson and Hwang 1980; Booy 1980; Wang and White 1989; Lai-Fook et al. 1989, 1991) is that actual boundary conditions were used instead of boundary conditions based on the parallel plate model developed for single screw extruders. The generalized screw curves constructed for both double-lead and single-lead screw elements were similar in shape to those published for single screw extruders with rectangular channels. Noticeable increases in the closed discharge pressure and the open discharge flow rate were observed, which are the result of the screw geometry. Experimental results with corn meal were in agreement with theoretical predictions for single-lead screw elements. Theoretical predictions for double-lead screw elements using the new solution also showed reasonable agreement with experimental data from published literature after the incorporation of the intermeshing effect.

INTRODUCTION

Food extrusion technology has played a very important role in today's food and feed processing industries of today, and will maintain its importance in new product development due to its versatility and multi-functional characteristics. While there are many different types of extruders, fully-wiped co-rotating twin-screw extruders have been of great interest for both polymer and food processing industries. The outstanding characteristics of this type of extruders

¹ Contribution from the Missouri Agricultural Experiment Station, Journal Series No. 12,386.

² To whom correspondence should be addressed. Tel: 573-882-2444, FAX: 573-882-1115.

are attributed to their unique screw geometry, allowing more positive pumping and self-cleaning. The latter particularly appeals to processing of heat and shear sensitive materials, such as foods.

The flow theory's importance to practical extrusion simulation and analysis cannot be overemphasized. Information that relates extruder parameters and operating conditions to flow rate, specific mechanical energy, power consumption, die pressure, etc. is readily provided by the flow theory. Unlike single-screw extruders, the flow theories of twin-screw extruders, particularly co-rotating twin-screw extruders, are less sophisticated. An isothermal flow of a Newtonian fluid in a fully-wiped co-rotating twin-screw extruder has been investigated by finite element and flow analysis network methods (Wyman 1975; Denson and Hwang 1980; Booy 1980; Szydlowski and White 1987; Szydlowski *et al.* 1987; Szydlowski and White 1988). Kalyon *et al.* (1988) and Wang and White (1989) also studied the isothermal flow of a power law fluid in fully-wiped, co-rotating twin-screw extruders. However, these studies provided very limited experimental data to confirm the theories developed. Using maize grits and low density polyethylene, Isherwood *et al.* (1988), Lai-Fook *et al.* (1989), and Lai-Fook *et al.* (1991) conducted a series of extrusion studies using maize grits and low density polyethylene. The agreement between their experimental results and established flow theories for twin-screw extruders was less than satisfactory.

It should be noted that the solutions published have one thing in common — boundary conditions were defined based on the parallel plate model developed for a single screw extruder. This simplified model assumed that the extruder screw is stationary and the barrel is rotating with a constant velocity ($V_b = R_b \cdot \omega$) across the channel. In reality, the barrel is stationary and the screws are rotating. Moreover, the velocities along the screw root and flight surfaces are not constant but a function of the angular position. Therefore, the screw tip velocity, V_b , is not a universal, representative velocity of an extruder system. Even for a single screw extruder system, results from many experimental data (Campbell *et al.* 1992; Choo *et al.* 1980; Middleman 1977) indicated the inaccuracy of the flow models based on conventional boundary conditions. Recently, Li and Hsieh (1994, 1995) have established new analytical solutions using actual boundary conditions of a single screw extruder. The problem associated with using the parallel plate model was elucidated.

Screw profiles usually consist of a combination of different screw elements, such as single-lead, double-lead or kneading discs in twin-screw extruders. Therefore, extrusion theories should be flexible enough to be readily adaptable to any selected screw profiles. Most studies in the literature emphasize the analyses of double-lead screw elements and kneading discs. Very limited information is available for the analysis of single-lead screw elements, which are commonly used in the metering section of twin-screw extruders.

The objectives of this research was to develop the flow theory of a power-law fluid in a co-rotating self-wiping twin-screw extruder using actual boundary conditions. The solution obtained would then be used to construct both double-lead and single-lead screw characteristics (flow rate versus pressure) and compare against experimental extrusion results with corn meal.

FORMULATION OF THE PROBLEM

Screw Geometry and Boundary Conditions

The geometry of a fully-wiped co-rotating twin-screw extruder has been derived by Booy (1978). A typical cross-sectional view of the screw elements with double leads is given in Fig. 1. For any given type of screw element with an inner radius of barrel R_b , clearance δ_c , and center distance C_L , the radius of the screw at any angular position is given by:

$$\begin{aligned} r(\theta) &= R_s \text{ for the screw roots where } 0 < \theta < \alpha; \\ r(\theta) &= R(\theta) = \sqrt{C_L^2 - (R_b - \delta_c)^2 \sin^2 \theta} - (R_b - \delta_c) \cos \theta \\ &\text{for the screw flanks where } 0 < \theta < 2\psi; \\ r(\theta) &= R_b - \delta_c \text{ for the screw tips where } 0 < \theta < \alpha \end{aligned} \quad (1)$$

where R_s is the radius of the screw root, α , the screw tip angle, and ψ , the flank angle. If the clearance δ_c is negligible, then the channel depth can be presented as:

$$\begin{aligned} h(\theta) &= R_b - R_x \text{ for the screw roots where } 0 < \theta < \alpha \text{ and } r(\theta) = R_s; \\ h(\theta) &= R_b (1 + \cos \theta) - \sqrt{C_L^2 - R_b^2 \sin^2 \theta} \text{ for the screw flanks} \\ &\text{where } 0 < \theta < 2\psi \text{ and } r(\theta) = R(\theta); \\ h(\theta) &= 0 \text{ for the screw tips where } 0 < \theta < \alpha \text{ and } r(\theta) = R_b \end{aligned}$$

Based on these equations, it is clear that $r(\theta)$ is not a constant with any given screw element. Since the screw element rotates with a constant angular velocity ω , the velocity along the boundaries of the screw surface including screw root, screw flank and screw tip is not a constant but a function of the angular position, or:

$$v_\theta = r(\theta) \omega \quad (3)$$

Therefore, the actual boundary conditions can be described as:

$$\begin{aligned} v_\theta &= 0, \text{ at the barrel where } r(\theta) = R_b; \\ v_\theta &= R_s \omega, \text{ at the screw roots where } r(\theta) = R_s; \\ v_\theta &= R_b \omega, \text{ at the screw tips where } r(\theta) = R_b; \\ v_\theta &= R(\theta) \omega, \text{ at the screw flanks where } r(\theta) = R(\theta) \end{aligned}$$

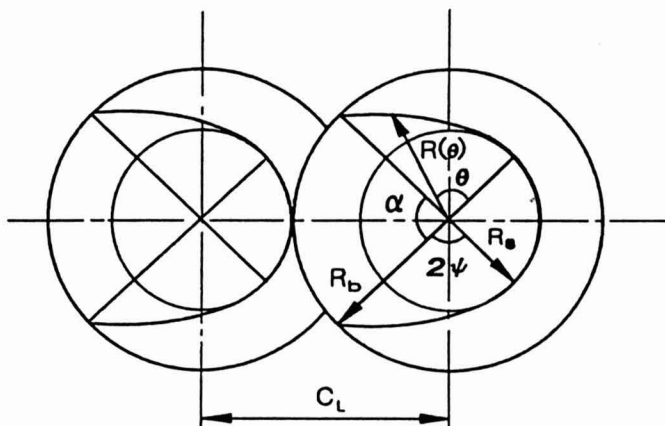


FIG. 1. THE CROSS-SECTIONAL GEOMETRY OF DOUBLE-LEAD SCREW ELEMENTS IN A CO-ROTATING SELF-WIPING TWIN-SCREW EXTRUDER

Equations (1), (2) and (3) can be used for both single- and double-lead screw elements. According to Booy (1978), two single-lead screw elements form one continuous channel while two double-lead screw elements form three continuous channels.

As mentioned before, published theories for fully-wiped co-rotating twin-screw extruders used boundary conditions based on the parallel plate model which was developed for single screw extruders with infinite channels. The barrel was assumed moving with the velocity of the screw tip: $v_{\theta} = V_b = R_b \omega$, at $r(\Theta) = R_b$ and $0 \leq \Theta \leq 2\pi$, and the screws were assumed stationary: $v_{\theta} = V_s = 0$, at $r(\Theta) = R(\Theta)$ and $0 \leq \Theta \leq 2\pi$. These boundary conditions are very different from the actual ones defined above.

As pointed out by Li and Hsieh (1994, 1996), the parallel plate model, strictly speaking, is only valid for single screw extruders with a stationary screw and rotating barrel and a very shallow channel. However, it is still acceptable for single screw extruders with a rotating screw and a stationary barrel but the following conditions have to be satisfied: (1) the channel is very shallow so that the screw flight effect is negligible and (2) the screw root velocity needs to be used instead of the screw tip velocity. In a co-rotating, self-wiping twin-screw extruder, the screw flight effect (or screw flank effect) is not negligible under any conditions because the screw roots and tips are usually a very small portion of the screw surface (Table 1 and Appendix I). In other words, the screw flanks or flights are always the major contributor to the drag flow in a twin-screw extruder. Therefore, the boundary conditions based on the parallel plate model are not applicable for twin-screw extruders.

TABLE 1.
BASIC SCREW GEOMETRY PARAMETERS FOR APV BAKER 50/25
TWIN-SCREW EXTRUDER

Screw Geometry	Double-lead	Single-lead
Tip diameter (D_b)	50.2mm	50.2mm
Root diameter (D_s)	29.6mm	29.6mm
Maximum channel depth (H)	10.3mm	10.3mm
Maximum channel width (W)	21.1mm	7.6mm
Tip width (e_t)	2.0mm	3.8mm
Root width (e_r)	1.2mm	2.3mm
Centerline distance (C_L)	39.9mm	39.9mm
Helix angle (ϕ_b)	17.67°	4.75°
Flank angle (ψ)	37.36°	37.36°
Tip angle (α)	15.30°	105.28°
Centerline ratio (ρ_c)	1.59	1.59
A_{tip}/A_{screw}^1	0.107	0.368
A_{root}/A_{screw}^2	0.063	0.217

¹Screw tip to screw surface ratio

²Screw root to screw surface ratio

Governing Equations and Assumptions

With an incompressible power-law fluid, it is assumed that the flow in a screw channel is isothermal, laminar, and fully developed in the down-channel direction, the inertia is negligible, and the channel is completely filled with the fluid. One can further assume that the curvature of the channel is relatively small ($H \ll R$). The channel can then be imaginarily peeled off and laid on a flat surface (Fig. 2) so that rectangular coordinates can be applied. A similar approach has been used by Kalyon *et al.* (1988), Wang and White (1989), and others. The experimental results of Kalyon *et al.* (1988) qualitatively supported the assumptions used in this approach.

With these above assumptions, the equations governing the flow in the screw channel are reduced to:

$$\frac{\partial P}{\partial x} = m \frac{\partial}{\partial y} \left[\dot{\gamma}^{n-1} \frac{\partial v_x}{\partial y} \right] \quad (4)$$

$$\frac{\partial P}{\partial z} = m \frac{\partial}{\partial y} \left[\dot{\gamma}^{n-1} \frac{\partial v_z}{\partial y} \right] \quad (5)$$

with the following boundary conditions:

$$v_x = v_z = 0, \quad \text{at } y = 0$$

$$v_x = R(x) \omega \sin \phi_b, \quad v_z = R(x) \omega \cos \phi_b, \quad \text{at } y = h(x)$$

where:

$$\begin{aligned}
 h(x) &= R_b \left[1 + \cos \left(\frac{x - e_r/2}{R_b \sin \phi_b} \right) \right] - \sqrt{C_L^2 - R_b^2 \sin^2 \left(\frac{x - e_r/2}{R_b \sin \phi_b} \right)} & \frac{e_r}{2} \leq x \leq \frac{W}{2} \\
 h(x) &= H & 0 \leq x < \frac{e_r}{2} \\
 R(x) &= R_b - h(x)
 \end{aligned}$$

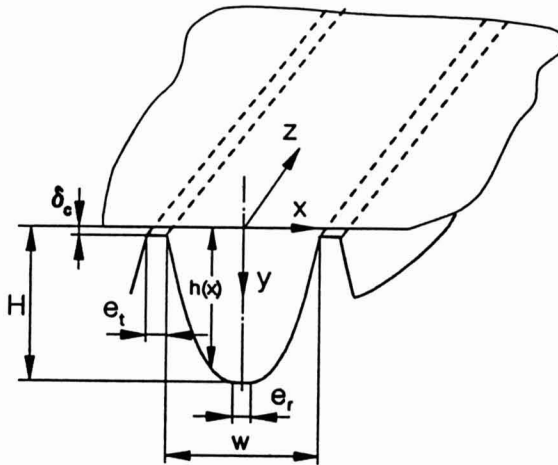


FIG. 2. THE CROSS-SECTIONAL VIEW OF THE SCREW CHANNEL

To further simplify calculations, the following dimensionless parameters are applied:

$$\begin{aligned}
 v^* &= \frac{V}{R_s \omega \cos \phi_b}, \xi = \frac{y}{H}, \dot{\gamma}^* = \left[\frac{H}{R_s \omega \cos \phi_b} \right] \dot{\gamma} \\
 P_z &= \frac{\partial P}{\partial z} \cdot \frac{H^{n+1}}{m(R_s \omega \cos \phi_b)^n}, P_x = \frac{\partial P}{\partial x} \cdot \frac{H^{n+1}}{m(R_s \omega \cos \phi_b)}
 \end{aligned} \tag{6}$$

The problem then becomes solving the following coupled equations:

$$P_x = \frac{\partial}{\partial \xi} \left[\dot{\gamma}^{*n-1} \frac{\partial v_x^*}{\partial \xi} \right] \quad (7)$$

$$P_z = \frac{\partial}{\partial \xi} \left[\dot{\gamma}^{*n-1} \frac{\partial v_z^*}{\partial \xi} \right] \quad (8)$$

where the dimensionless shear rate is in the following form:

$$\dot{\gamma}^* = \sqrt{\left(\frac{\partial v_z^*}{\partial \xi} \right)^2 + \left(\frac{\partial v_x^*}{\partial \xi} \right)^2}$$

with the following boundary conditions:

$$v_x^* = v_z^* = 0, \text{ at } \xi = 0$$

Since the variation in the hydrostatic pressure with ξ is negligible for very shallow channels (Griffith 1962; Booy 1964; Zamodits and Pearson 1969; Wang and White 1989), Eqs. (7) and (8) may be integrated once to give:

$$\dot{\gamma}^{*n-1} \frac{\partial v_z^*}{\partial \xi} = P_z \cdot \xi - c_1(x) \quad (9)$$

$$\dot{\gamma}^{*n-1} \frac{\partial v_x^*}{\partial \xi} = P_x \cdot \xi - c_2(x) \quad (10)$$

From these two equations the relationship between the partial shear rates can be found:

$$\frac{\partial v_z^*}{\partial \xi} = \left(\frac{P_z \cdot \xi - c_1(x)}{P_x \cdot \xi - c_2(x)} \right) \frac{\partial v_x^*}{\partial \xi} \quad (11)$$

From this relationship, the partial shear rates are found to be:

$$\frac{\partial v_z^*}{\partial \xi} = (P_z \cdot \xi - c_1(x)) [(P_z \cdot \xi - c_1(x))^2 + (P_x \cdot \xi - c_2(x))^2]^{-\frac{1-n}{2n}} \quad (12)$$

$$\frac{\partial v_x^*}{\partial \xi} = (P_x \cdot \xi - c_2(x)) [(P_z \cdot \xi - c_1(x))^2 + (P_x \cdot \xi - c_2(x))^2]^{-\frac{1-n}{2n}} \quad (13)$$

Integrating Eqs. (12) and (13) again with $v_z^* = v_x^* = 0$ (at $\xi = 0$) gives the velocity distributions:

$$v_z^* = \int_0^\xi (P_z \cdot \xi - c_1(x)) [(P_z \cdot \xi - c_1(x))^2 + (P_x \cdot \xi - c_2(x))^2]^{-\frac{1-n}{2n}} d\xi \quad (14)$$

$$v_x^* = \int_0^\xi (P_x \cdot \xi - c_2(x)) [(P_z \cdot \xi - c_1(x))^2 + (P_x \cdot \xi - c_2(x))^2]^{\frac{1-n}{2n}} d\xi \tag{15}$$

If P_z is chosen to be the independent variable, P_x , v_z^* and v_x^* are solved with the remaining boundary conditions:

$$\frac{R(x)}{R_s} = \int_0^{\frac{h(x)}{H}} (P_z \cdot \xi - c_1) [(P_z \cdot \xi - c_1)^2 + (P_x \cdot \xi - c_2)^2]^{\frac{1-n}{2n}} d\xi$$

$$\frac{R(x)\tan\phi_b}{R_s} = \int_0^{\frac{h(x)}{H}} (P_x \cdot \xi - c_2) [(P_z \cdot \xi - c_1)^2 + (P_x \cdot \xi - c_2)^2]^{\frac{1-n}{2n}} d\xi$$

and the third constraint, assuming that the flow rate over the flights is zero:

$$Q_x^* = \frac{Q_x}{R_s \omega \cos\phi_b HW} = 2 \int_0^1 \int_0^{\frac{h(x)}{H}} v_x^* d\xi d\zeta = 0$$

For every given P_z , the down channel flow rate can then be calculated using the resulting parameters:

$$Q_z^* = \frac{Q_z}{R_s \omega \cos\phi_b HW} = 2 \int_0^1 \int_0^{\frac{h(x)}{H}} v_z^* d\xi d\zeta \tag{16}$$

The assumption made in the third constraint is valid for zero clearance, an ideal case, but is still reasonable for very small clearance. Values other than zero may be assigned to Qx^* to investigate the clearance effect, which is out of the scope of this research.

THE ANALYTICAL SOLUTION OF A NEWTONIAN FLUID

When the fluid is Newtonian (a special case of power-law fluids with $n = 1$), an analytical solution is possible, which is useful for checking the more general numerical solution of the power-law fluids. Integration of Eqs. (14) and (15) with $n = 1$ gives:

$$v_z^* = \int_0^\xi (P_z \cdot \xi - c_1(x)) d\xi = \frac{1}{2} P_z \cdot \xi^2 - c_1(x) \cdot \xi \tag{17}$$

$$v_x^* = \int_0^{\xi} (P_x \cdot \xi - c_2(x)) d\xi = \frac{1}{2} P_x \cdot \xi^2 - c_2(x) \cdot \xi \quad (18)$$

Substituting the boundary condition at $\xi = h(x)/H$ into Eqs. (17) and (18) and using the constraints for the cross channel flow rate.

$$\frac{R(x)}{R_s} = \frac{1}{2} P_z \left(\frac{h(x)}{H} \right)^2 - c_1(x) \cdot \frac{h(x)}{H}$$

$$\frac{R(x) \tan \phi_b}{R_s} = \frac{1}{2} P_x \left(\frac{h(x)}{H} \right)^2 - c_2(x) \cdot \frac{h(x)}{H}$$

$$Q_x^* = \int_0^1 \int_0^{\frac{h(x)}{H}} v_x^* d\xi d\zeta = \frac{1}{6} P_x \left(\frac{h(x)}{H} \right)^3 - \frac{1}{2} c_2(x) \left(\frac{h(x)}{H} \right)^2 = 0$$

Solving the above system of equations results in $c_1(x)$, the cross channel pressure gradient, P_x , and $c_2(x)$:

$$c_1(x) = \frac{P_z \cdot h(x)}{2H} - \frac{H \cdot R(x)}{R_s \cdot h(x)}$$

$$P_x = \frac{6R(x) \tan \phi_b}{R_s} \left(\frac{H}{h(x)} \right)^2$$

$$c_2(x) = \frac{2R(x) \tan \phi_b}{R_s} \left(\frac{H}{h(x)} \right)$$

Finally, the down-channel flow rate can be written as:

$$Q_z^* = \frac{2}{W} \int_0^{\frac{w}{2}} \left[\frac{1}{2} \frac{R(x) \cdot h(x)}{R_s \cdot H} - \frac{P_z}{12} \left(\frac{h(x)}{H} \right)^3 \right] dx \quad (19)$$

or

$$Q_z^* = \frac{1}{2} F_b - \frac{P_z}{12} F_p \quad (20)$$

The shape factors, F_d and F_p , are given by:

$$F_d = \frac{2}{WR_s H} \int_0^{\frac{w}{2}} R(x) \cdot h(x) dx$$

$$F_p = \frac{2}{WH^3} \int_0^{\frac{w}{2}} [h(x)]^3 dx$$

This analytical solution is found to be in the same form as given by Levine (1992).

SCREW CHARACTERISTICS

The dimensionless flow curves for the double-lead and single-lead screw elements are presented in Figs. 3 and 4. These curves are obtained using the geometrical parameters shown in Table 1. Q_z^* in Fig. 3 and 4 is the dimensionless flow rate for one channel. Since two double-lead screws form three screw channels (Booy 1978), the total dimensionless flow rate is actually $3Q_z^*$. When compared to the results published for single screw extruders with rectangular channels (Middleman 1977; Rauwendaal 1986), the shape of these curves is

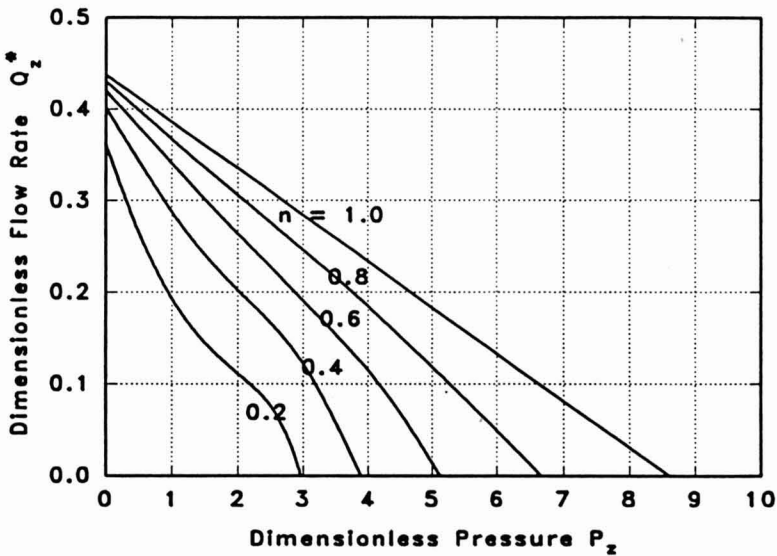


FIG. 3. GENERALIZED SCREW CHARACTERISTICS OF DOUBLE-LEAD SCREW ELEMENTS

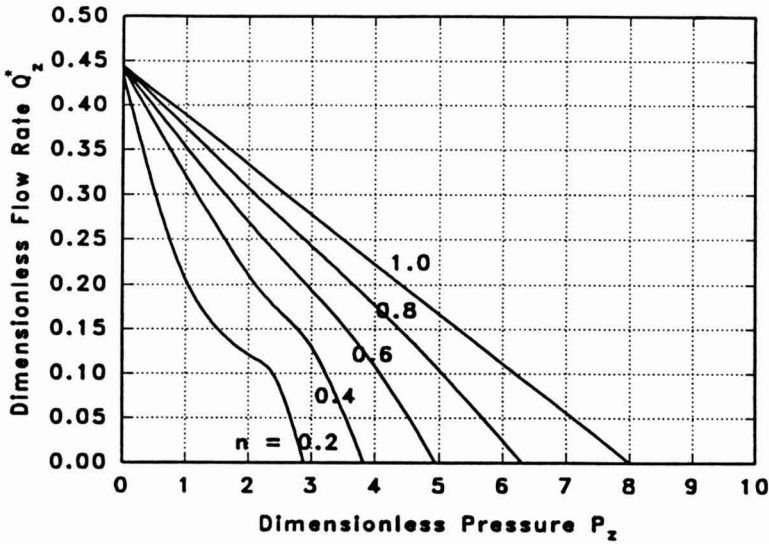


FIG. 4. GENERALIZED SCREW CHARACTERISTICS OF SINGLE-LED SCREW ELEMENTS

similar, particularly for highly non-Newtonian fluids (e.g., at $n = 0.2$). This was not observed in published twin-screw extrusion studies (Wang and White 1989; Lai-Fook *et al.* 1989).

It is interesting to compare double-lead and single-lead screw elements at open (Q_z^* at $P_z = 0$) and closed (P_z at $Q_z^* = 0$) discharge conditions. If the partial pressure gradient in the z -direction from Eq. (6) is written in the following form:

$$\frac{\partial P}{\partial z} = P_z \cdot \left(\frac{R_s \cdot \cos \phi_b}{H} \right)^n \cdot \frac{m \omega^n}{H} = f_p \frac{m \omega^n}{H} \tag{21}$$

where

$$f_p = P_z \cdot \left(\frac{R_s \cdot \cos \phi_b}{H} \right)^n$$

and then f_p is plotted as a function of dimensionless pressure P_z and flow behavior index for both screw geometries, the results are shown in Fig. 5. In addition, Table 2 shows the values of P_z , Q_z^* , f_p and Q_z at two flow behavior indices (0.2 and 1) and at open and closed discharge conditions for both single-

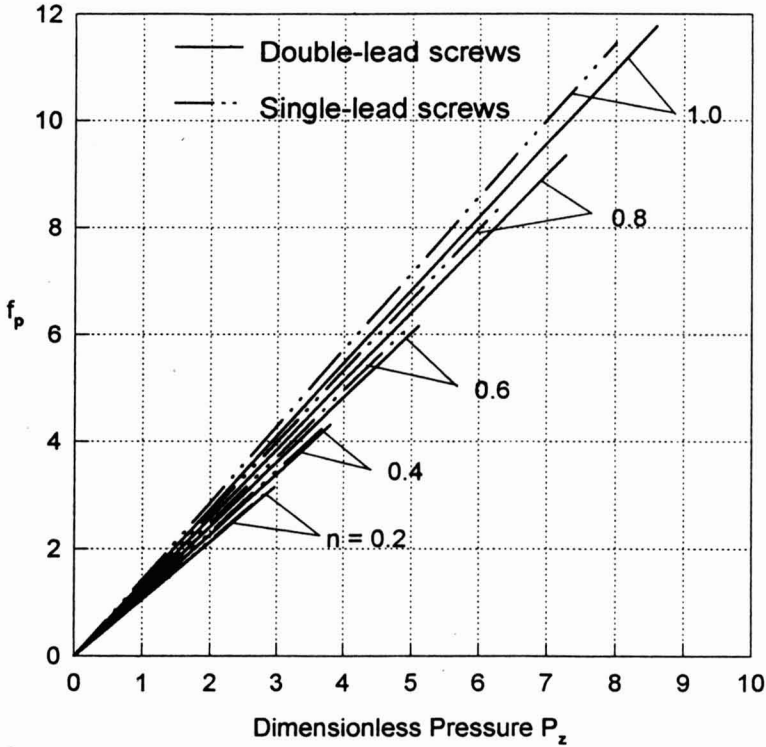


FIG. 5. COMPARISON OF PRESSURE FACTOR (f_p) FOR DOUBLE-LEAD AND SINGLE-LEAD SCREW ELEMENTS

TABLE 2.
COMPARISON OF DOUBLE-LEAD AND SINGLE-LEAD SCREW ELEMENTS AT OPEN AND CLOSED DISCHARGE CONDITIONS

Flow Behavior Index	Double-Lead Screw Elements				Single-Lead Screw Elements			
	P_z	Q_z^*	f_p	Q_z^1	P_z	Q_z^*	f_p	Q_z (cm ³ /s)
Open discharge $n=1.0$	0	0.437	0	1.339ω	0	0.444	0	0.513ω
Closed discharge $n=1.0$	8.601	0	11.776	0	8.000	0	11.456	0
Open discharge $n = 0.2$	0	0.362	0	1.109ω	0	0.434	0	0.501ω
Closed discharge $n = 0.2$	2.960	0	4.053	0	2.870	0	4.110	0

¹ Q_z is calculated from Eq. (16) using screw geometry parameters listed in Table 1.

double-lead and single-lead screw elements are very small. Thus, for the same screw speed and same material properties, m and n , the pressure drops of these two types of screw element over the same length are about the same [Eq. (21)], especially for highly non-Newtonian fluids (e.g., $n = 0.2$). However, the volumetric flow rate of the single-lead screw elements is much smaller than that of the double-lead screws (Table 2). The volumetric flow rate Q_z or pumping capacity of single-lead screw elements is less than that of double-lead ones can be explained by their smaller channel width (7.6 mm for single-lead screw elements versus 21.1 mm for double-lead screw elements, Table 1). However, their operational stability is improved since the flow rate is less sensitive to the pressure change. This could explain why single-lead screw elements are commonly used immediately behind the die of extruders.

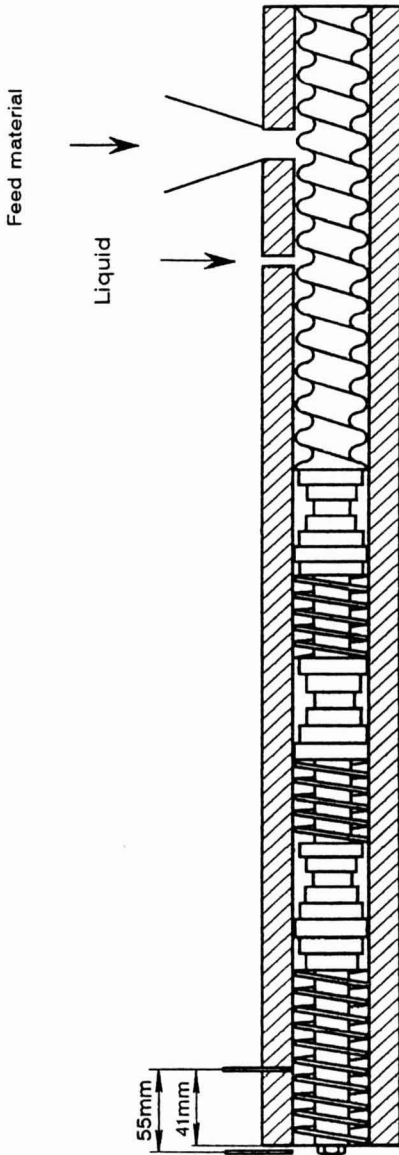
EXPERIMENTAL WORK

Corn meal (CCM 250) was used in this study because of its importance in food processing applications. It was supplied by Lauhoff Grain Company (Danville, IL.), with a moisture content of 12% wet basis and the final feed moisture content during the extrusion was adjusted to 20% wet basis.

Extrusion experiments were conducted on an MPF 50/25 fully-wiped co-rotating twin-screw extruder (APV Baker, Grand Rapids, MI). The basic geometry parameters are listed in Table 1 and the screw profiles and the temperature settings used are given in Fig. 6. Two extruder dies with a diameter of 3.18 mm were used. Two pressure transducers were used to record the pressure drops. One was located at 14 mm upstream from the die entrance and the other was located in the extruder barrel. The axial distance between these two pressure transducers was 55 mm. It was determined that the axial distance of the single-lead screw between those two pressure transducer was 41 mm (55 mm - 14 mm, see Fig. 7 and Appendix II), which gave a helical distance of 495 mm ($41 \text{ mm}/\sin 4.75^\circ$) or a channel length to maximum channel depth (10.3 mm) ratio of 48.1.

The feed rate was controlled by a K-Tron type T-35 twin-screw volumetric feeder (K-tron Corp., Pitman, NJ). In order to cover a broad range of feed rates, the experiments were run at eleven specific feeding loads. The specific feeding load is defined as:

$$\text{SFL (g/rev)} = \frac{\text{Feed Rate (g/s)}}{\text{Screw Speed (rev/s)}}$$



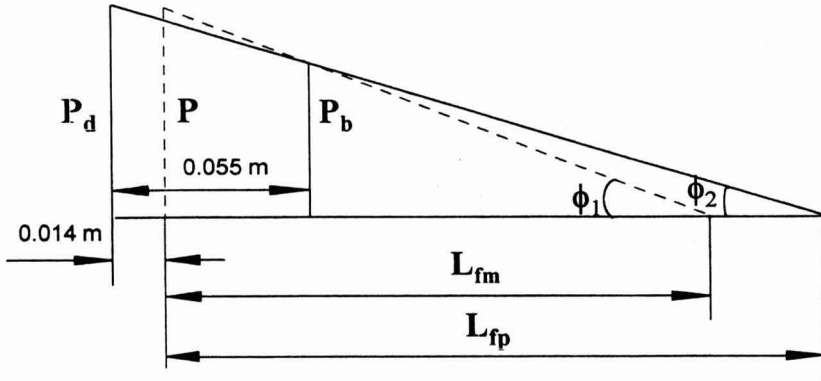
Zones	6	5	4	3	2	1
T (°C)	121.1	121.1	93.3	51.7	23.9	Ambient

Length (mm)	125	50	87.5	50	37.5	37.5	50	87.5	225
Screws	SLS	RP	FP	SLS	RP	FP	SLS	FP	DLS

Degrees	-30	30	-60	60	30
---------	-----	----	-----	----	----

DLS = Double-Lead Screw; FP = Forward Kneading Paddles
 RP = Reverse Kneading Paddles; SLS = Single-Lead Screw

FIG. 6. THE COMPOSITE SCREW PROFILE OF APV BAKER TWIN-SCREW EXTRUDER



$$\text{Axial pressure gradient} = \tan \phi_1 = \frac{P - P_b}{0.041 \text{ m}} = \frac{P_d - P_b}{0.055 \text{ m}} \cdot \frac{L_{fp} - 0.041 \text{ m}}{L_{fm} - 0.041 \text{ m}}$$

$$\tan \phi_2 = \frac{P_d - P_b}{0.055 \text{ m}}, L_{fp} = \frac{P_b}{\tan \phi_2} + 0.041 \text{ m}, L_{fm} = \frac{P_b}{\tan \phi_1} + 0.041 \text{ m}$$

FIG. 7. CORRECTION OF PRESSURE GRADIENT USING THE MEASURED FILLED LENGTH

The SFLs and the corresponding feed rates used are listed in Table 3.

Dead-stop runs with SFL = 2.0, 3.0, and 4.0 g/rev were carried out to measure filled lengths. The measured lengths were compared with those predicted by measured pressure gradients (Table 3). The fill length predicted was calculated based on the following equation (Appendix II):

$$L_{fp} = \frac{0.055 \text{ m}}{\frac{P_d}{P_b} - 1} + 0.041 \text{ m} \quad (22)$$

where \$P_b\$ is the pressure recorded by the transducer mounted in the barrel and \$P_d\$ the pressure recorded by the transducer upstream of the die entrance. The density of the melted corn meal was obtained using the dead-stop run with SFL = 3.0 g/rev. For completely melted corn meal at 121C and 20% moisture, the density was found to be 1215 kg/m³. The data for predicting rheological properties was obtained in a separate set of experiments using the torque-screw speed method, which was developed and tested by Li *et al.* (1996). The rheological properties of corn meal used are listed in Table 3.

TABLE 3.
SPECIFIC FEEDING LOADS, FEED RATES, AND RHEOLOGICAL PROPERTIES
OF CORN MEAL

Run	SFL (g/rev)	Feed Rate (kg/h)	n	m (Pa·s ⁿ)	L _{fm} (mm)	L _{fp} ^a (mm)
1	1.00	21.0	0.235	(8105)	-	65.25
2	1.33	28.0	0.235	(13710)	-	62.23
3	1.67	35.0	0.235	(15260)	-	57.97
4	2.00	42.0	0.235	17314	50.0	55.91
5	2.33	49.0	0.235	(19972)	-	54.51
6	2.67	56.0	0.235	(24532)	-	52.57
7	3.00	63.0	0.235	31188	51.0	52.27
8	3.33	70.0	0.235	(40092)	-	58.55
9	3.67	77.0	0.235	(51801)	-	67.77
10	4.00	84.0	0.168	66222	79.0	77.23
11	4.33	91.0	0.168	(83566)	-	84.62

^a Values of L_{fp} were predicted using Eq.(22) with experimental P_b and P_d data. They were the average of two replications with a total of 44 points

^b Values in parenthesis were obtained using interpolation or extrapolation from the nonlinear regression of the measured values

COMPARISON WITH THE EXPERIMENTAL RESULTS

Figure 8 is the comparison of the theoretical screw curves of double-lead screw elements and experimental results obtained by Isherwood *et al.* (1988) and Lai-Fook *et al.* (1989 and 1991). Similar to the screw curve obtained by Lai-Fook *et al.* (1991), the flow rate (n = 0.22) based on our model was significantly underestimated over the entire experimental range. However, if the original predictions were corrected by adding the flow rate caused by the intermeshing effect, predicted by Lai-Fook *et al.* (1991), the results showed reasonable agreement with the experimental results (Fig. 8). This indicates that the volumetric flow rate resulting from the intermeshing effect of double-lead screw elements might be very important.

Figure 9 is the comparison between the theoretical screw curves of single-lead screw elements and the experimental data obtained in this study. The feed rates and the screw speeds were selected to generate dimensionless flow rates that would cover most of the curve tested. For SFL = 1.0 g/rev, the experiments were only possible at a screw speed higher than 350 rpm without blocking the dies. For SFL < 1.0 g/rev and SFL > 4.0 g/rev the experiments were not possible due to the extruder's overload. Therefore, the experimental range used in this study was about the maximum range for testing the theoretical curves using the APV Baker twin-screw extruder.

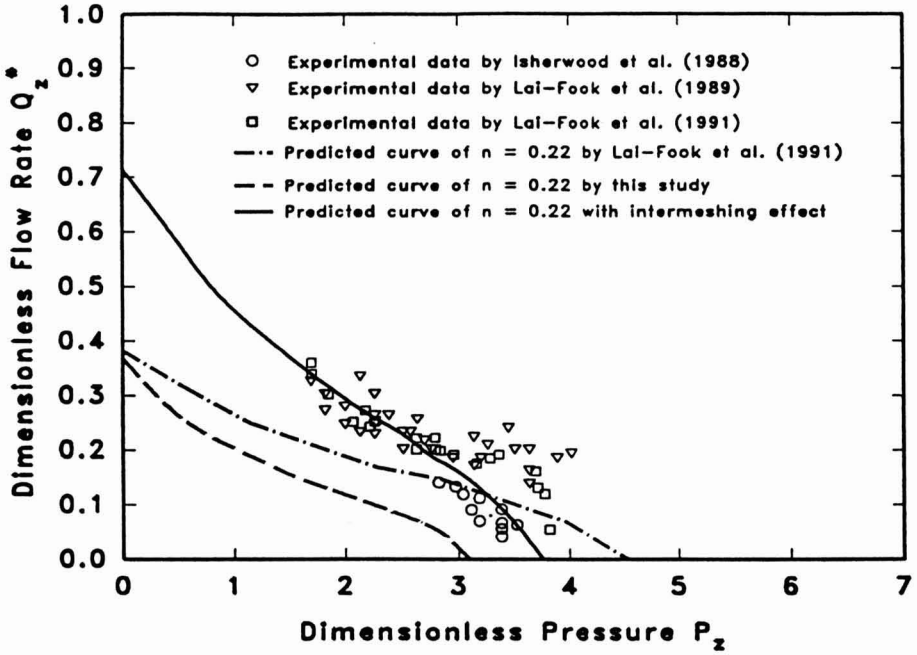


FIG. 8. COMPARISON BETWEEN THE THEORETICAL PREDICTIONS (WITH AND WITHOUT INTERMESHING EFFECT) AND THE EXPERIMENTAL DATA BY ISHERWOOD *ET AL.* (1988), LAI-FOOK *ET AL.* (1989, 1991) FOR DOUBLE-LEAD SCREW ELEMENTS

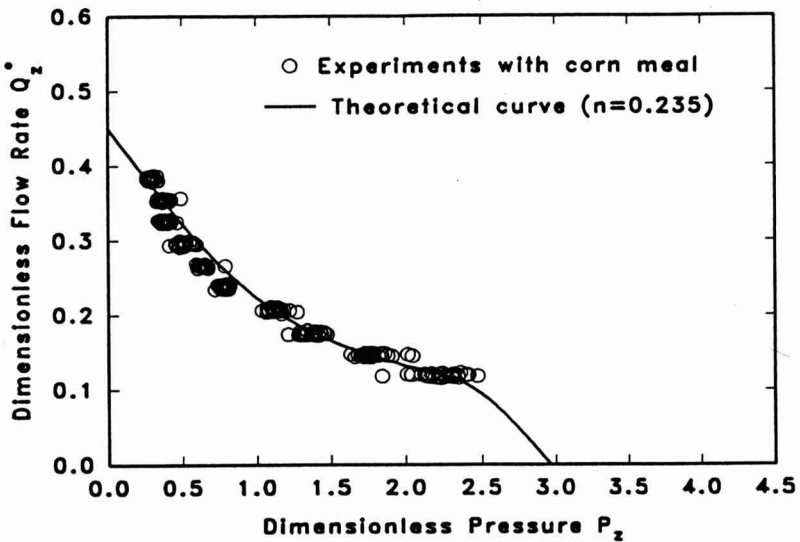


FIG. 9. COMPARISON BETWEEN THE THEORETICAL PREDICTIONS AND EXPERIMENTAL RESULTS USING CORN MEAL FOR SINGLE-LEAD SCREW ELEMENTS

As shown in Table 3, for SFLs = 3.0 and 4.0 g/rev, the differences between the measured lengths and the predicted ones were within 5%, indicating that the pressure measurements were reasonably accurate. From Fig. 7, it can be seen that if $L_{fp} = L_{fm}$, then $\phi_1 = \phi_2$. Therefore, for SFLs from 2.33 to 4.33 g/rev, the axial pressure gradients were directly determined using $\tan\phi_2 = (P_d - P_b)/0.055\text{m}$ without further correction. For SFL = 2.0 g/rev, the predicted length was about 12% higher than the measured one, indicating that the errors of the pressure measurements were slightly higher. Therefore, the calculation of the pressure gradient for SFL ≤ 2.0 g/rev was corrected using the measured length (Fig. 7) and the axial pressure gradient was determined using $\tan\phi_1 = P_b/(L_{fm} - 0.041\text{ m})$. Since no dead-stop runs were carried out for SFL < 2.0 g/rev, the errors for SFL < 2.0 g/rev were estimated by using the extrapolation method and assumed that the error for L_{fp} remained to be 12% higher than L_{fm} . Therefore, the pressure gradients were determined using $\tan\phi_2 = P_b/[L_{fp} \cdot (1 - 0.12) - 0.041\text{ m}]$. Note that these pressure corrections were only used for the experimental data but not for the theoretical curves. Figure 9 shows that the theoretical results agrees with the experimental data obtained for SFL = 1.67 - 4.0 g/rev. Thus, the intermeshing effect caused by single-lead screw elements with the given geometry seemed negligible. Further studies are needed to check the range of SFL = 1.0-2.0 g/rev.

One of the reasons for double-lead screws having a much higher intermeshing effect than single-lead screws is probably due to the geometrical difference between these two types of screws. According to Booy (1980), the intermeshing effect introduces an additional volumetric flow rate which depends on the geometry of the intermeshing region and the screw geometrical parameters:

$$Q_i = \frac{1}{2} \cdot k_i \cdot \tan\phi_b \cdot R_s^3 \cdot \omega$$

where: Q_i is the volumetric flow rate due to the intermeshing effect and k_i is the nip flow coefficient. For the screws used in this study, $k_i = 0.16$ for the single-lead screws and 0.25 for the double-lead screws. Based on this Booy's equation, the volumetric flow rate due to the intermeshing effect of the double-lead screws ($\phi_b = 17.67^\circ$) is thus at least four times higher than that of the single-lead screws ($\phi_b = 4.75^\circ$). Booy's equation is a simple estimation and does not include the effect of other factors such as pressure and the flow behavior index. From Lai-Fook *et al.* (1991), the volumetric flow rate due to intermeshing effect decreased as the dimensionless pressure increased. The effect of flow behavior index on the volumetric rate due to the intermeshing effect, however, has not been well studied. The flow in the intermeshing region of the screws is three-dimensional and is much more complicated than that of the

nonintermeshing region. Further investigation is needed to study the intermeshing effect for different types of screw elements.

CONCLUSIONS

A new solution of the flow of a power-law fluid in a fully-wiped co-rotating twin-screw extruder is established. This solution uses the actual boundary conditions encountered in such an extruder. Dimensionless screw characteristics for both double-lead and single-lead screw elements are generated and tested experimentally and also using experimental data from published literature. The new solution predicts the volumetric flow rate well for single-lead screw elements, but underestimates the flow rate of double-lead screw elements. After correcting for the intermeshing effect, however, the predictions for double-lead screw elements also show reasonable agreement with the experimental data reported in the literature.

NOMENCLATURE

c_1, c_2	constant
C_L	centerline distance = $R_b + R_s$
f_p	pressure factor [Eq. (21)]
F_d	shape factor of drag flow
F_p	shape factor of pressure flow
H	maximum channel depth in the y direction (m)
$h(\Theta), h(x)$	channel depth as a function of Θ or x, respectively (m)
L_{fm}	filled length measured by dead-stop runs (m)
L_{fp}	filled length predicted (m)
m	consistency index ($\text{Pa}\cdot\text{s}^n$)
n	flow behavior index
P_x, P_z	dimensionless pressure gradients in x and z directions, respectively
Q_x, Q_z	flow rate in x and z directions, respectively (m^3/s)
Q_x^*, Q_z^*	dimensionless flow rate in x and z directions, respectively
R_b, R_s	radius of screw tip and screw root, respectively (m)
$R(\Theta), R(x)$	radius of screw flank as a function of Θ or x, respectively (m)
$r(\Theta)$	radius (m)
v, v^*	velocity and dimensionless velocity, respectively (m/s)
V_s	velocity of screw (m/s)
v_x, v_z	velocity components (m/s)

v_x^* , v_z^*	dimensionless velocity components
v_θ	tangential velocity (m/s)
W	maximum channel width in the x direction (m)
x, y, z	rectangular coordinates
α	tip angle
$\dot{\gamma}$, $\dot{\gamma}^*$	shear rate and dimensionless shear rate, respectively (1/s)
δ_c	clearance between barrel and screw tips (m)
Θ	angular coordinate
ξ, ζ	dimensionless coordinate
ρ_c	centerline ratio
ϕ_b	helix angle
ψ	flank angle
ω	angular velocity (1/s)

APPENDIX I

Ratios of Screw Tip and Screw Root to Screw Surface

The following equations from Booy (1978) were used to calculate ratios of screw tip and screw root to surface:

- (1) The surface generated by one tip

$$A_{\text{tip}} = \alpha R_b L$$

- (2) The surface area generated by one root

$$A_{\text{root}} = \alpha R_s L$$

- (3) The surface area generated by one flank

$$A_{\text{flank}} = \psi (R_b + R_s) L$$

- (4) The surface area generated by one screw

$$A_{\text{screw}} = n_t (A_{\text{tip}} + A_{\text{root}}) + 2n_t A_{\text{flank}}$$

For tip to screw surface ratio:

$$\frac{A_{\text{tip}}}{A_{\text{screw}}} = \frac{\alpha}{\alpha + 2\psi} \frac{1}{\rho_c}$$

For root to screw surface ratio:

$$\frac{A_{\text{root}}}{A_{\text{screw}}} = \frac{\alpha}{\alpha + 2\psi} \frac{1}{\rho_c} \frac{R_s}{R_b}$$

APPENDIX II

Correction of Pressure Gradient Using the Measured Filled Length

The pressure gradient defined in Fig. 7 is the axial pressure gradient dP/dl . The assumption made in the derivation of the equations in Fig. 7 was that the pressure development in the z direction is linear. The relationship between the down channel pressure gradient and the axial gradient is:

$$\frac{dP}{dz} = \frac{dP}{dl} \cdot \sin\phi_b = \frac{P}{L_{fm}} \cdot \sin\phi_b = \tan\phi_1 \cdot \sin\phi_b \quad (A1)$$

From Fig. 7, $\tan\phi_1$ can be determined by:

$$\tan\phi_1 = \frac{P}{L_{fm}} = \frac{P_b}{L_{fm} - 0.041m} = \frac{P - P_b}{0.041m} \quad (A2)$$

From Eq. (A2), L_{fm} can be determined as:

$$L_{fm} = \frac{P_b}{\tan\phi_1} + 0.041m \quad (A3)$$

Similarly, $\tan\phi_2$ can be expressed as:

$$\tan\phi_2 = \frac{P_d}{L_{fp} + 0.014m} = \frac{P_b}{L_{fp} - 0.041m} = \frac{P_d - P_1}{0.055m} \quad (A4)$$

From Eq. (A4), L_{fp} can be expressed as:

$$L_{fp} = \frac{P_b}{\tan\phi_2} + 0.041m \quad (A5)$$

Substituting $\tan\phi_2$ from Eq. (A4) into Eq. (A5), L_{fp} becomes:

$$L_{fp} = \frac{0.055m}{\frac{P_d}{P_b} - 1} + 0.041m \quad (22)$$

Also from Eqs. (A2) and (A4), the ratio of $\tan\phi_1$ to $\tan\phi_2$ can be found to be:

$$\frac{\tan\phi_1}{\tan\phi_2} = \frac{L_{fp} - 0.041m}{L_{fm} - 0.041m} \quad (A6)$$

From Eqs. (A6) and (A4), the following relationship is obtained:

$$\tan\phi_1 = \frac{P_d - P_b}{0.055m} \cdot \frac{L_{fp} - 0.041m}{L_{fm} - 0.041m} \quad (A7)$$

REFERENCES

- BOOY, M.L. 1978. Geometry of fully wiped twin-screw equipment. *Polymer Eng. Sci.* 18, 973-984.
- BOOY, M.L. 1980. Isothermal flow of viscous liquids in corotating twin screw devices. *Polymer Eng. Sci.* 20, 1220-1228.
- CAMPBELL, G.A., SWEENEY, P.A. and FELTON, J.N. 1992. Experimental investigation of the drag flow assumption in extruder analysis. *Polymer Eng. Sci.* 32, 1765-1770.
- CHOO, K.P., NEELAKANTAN, N.R. and PITTMAN, J.F.T. 1980. Experimental deep-channel velocity profiles and operating characteristics for a single-screw extruder. *Polymer Eng. Sci.* 20, 349-356.
- DENSON, C.D. and HWANG, B.K. 1980. The influence of the axial pressure gradient on flow rate for Newtonian liquids in a self wiping, co-rotating twin screw extruder. *Polymer Eng. Sci.* 20, 965-971.
- GRIFFITH, R.M. 1962. Fully developed flow in screw extruders. *Indust. Eng. Chem. Fundamentals* 1, 180-187.
- ISHERWOOD, D.P., LAI-FOOK, R.A., SENOUCI, A. and SMITH, A.C. 1988. Some studies on the conveying of foods stuffs in the metering section of self-wiping co-rotating twin-screw extruders. *Prog. Trends Rheology II*, p. 437 (H. Giesekus and M.F. Hibberd, eds.) Steinkopff Verlag.
- KALYON, D., M., GOTSIS, A.D., IMAZER, U.Y., GOGOS, C.G., SANGANI, H., ARAL, B. and TSENOGLOU, C. 1988. Development of experimental techniques and simulation methods to analyze mixing in co-rotating twin screw extrusion. *Adv. Polymer Technol.* 8, 337-353.
- LAI-FOOK, R.A., LI, Y. and SMITH, A.C. 1991. A 2-D numerical study of intermeshing self-wiping screws in biopolymer extrusion. *Polymer Eng. Sci.* 31, 1157-1163.
- LAI-FOOK, R.A., SENOUCI, A., SMITH, A.C. and ISHERWOOD, D.P. 1989. Pumping characteristics of self-wiping twin-screw extruders-A theoretical and experimental study on biopolymer extrusion. *Polymer Eng. Sci.* 29, 433-440.
- LEVINE, L. 1992. Extrusion process. In *Handbook of Food Engineering*. (D.R. Heldman and D.B. Lund, eds.) Marcel Dekker, New York.
- LI, Y. and HSIEH, F. 1994. New melt conveying models for a single screw extruder. *J. Food Process Engineering* 17, 299-324.
- LI, Y. and HSIEH, F. 1996. Modeling of flow in a single screw extruder. *J. Food Eng.* 27, 353-375.
- LI, Y., LU, Q., HUFF, H.E. and HSIEH, F. 1996. On-line measurements of rheological properties of corn meal using a co-rotating self-wiping twin-screw extruder. *Trans. Inst. Chem. Eng.: Part C - Food and Bioprod. Proc.* 74, 149-158.

- MIDDLEMAN, S. 1977. *Fundamentals of Polymer Processing*. McGraw-Hill, New York.
- RAUWENDAAL, C. 1986. *Polymer Extrusion*. Hanser Publishers, New York.
- SZYDLOWSKI, W., BRZOSKOWSKI, R. and WHITE, J.L. 1987. Modeling flow in an intermeshing corotating twin screw extruder: Flow in kneading discs. *Intern. Polymer Proc.* 1, 207-214.
- SZYDLOWSKI, W. and WHITE, J.L. 1987. An improved theory of metering in an intermeshing corotating twin-screw extruder. *Adv. Polymer Technol.* 7, 177-183.
- SZYDLOWSKI, W. and WHITE, J.L. 1988. A non-Newtonian model of flow in a kneading disc region of a modular intermeshing corotating twin screw extruder. *J. Non-Newtonian Fluid Mech.* 28, 29-46.
- WANG, Y. and WHITE, J.L. 1989. Non-Newtonian flow modeling in the screw regions of an intermeshing corotating twin screw extruder. *J. Non-Newtonian Fluid Mech.* 32, 19-38.
- WYMAN, C. 1975. Theoretical model for intermeshing twin screw extruders: axial velocity profile for shallow channels. *Polymer Eng. Sci.* 15, 606-611.
- ZAMODITS, H.J. and PEARSON, J.R. 1969. Flow of polymer melts in extruders. Part I. The effect of transverse flow and of a superposed steady temperature profile. *Trans. Soc. Rheology* 13, 357-385.

VELOCITY PROFILES OF FLUID/PARTICULATE MIXTURES IN PIPE FLOW USING MRI

KATHRYN L. McCARTHY¹, WILLIAM L. KERR, ROBERT J. KAUTEN
and JEFFREY H. WALTON²

Department of Food Science and Technology
²*UCD NMR Facility*
University of California
Davis, CA USA 95616

Accepted for Publication August 15, 1996

ABSTRACT

Magnetic resonance imaging (MRI) techniques have been utilized to experimentally measure velocity profiles and apparent rheological properties of fluid/particulate mixtures as functions of flow rate, particle loading, and particle size. The experimental velocity profiles were described by a power law model for these systems. A 3% aqueous sodium alginate solution was used to form two particle sizes of 2.5 mm and 5.0 mm in diameter. The spheres were suspended in a 0.5% carboxymethyl cellulose solution at loadings of 0, 10, 20, and 30% by weight. The average fluid velocity ranged from 2-35 cm/s. The flow behavior index decreased as flow rate, particle loading or particles size increase. Cumulative residence time curves were evaluated based on this modeling procedure. Results of this research have direct application to aseptic processing of fluid/particulate mixtures.

INTRODUCTION

Aseptic processing and filling consists of presterilizing a food product before filling a sterile package. The atmosphere and mechanical means of closing the package must also be sterile. This type of processing has several advantages, primarily in the quality of the treated foods and ease or cost of storage and distribution. However, limitations to aseptic processing still exist in the area of presterilization of difficult products, such as liquids with large particles (Buchner 1993). The heat sterilization of fluid/particulate mixtures requires that the products are heated to an appropriately high temperature and maintained at that temperature for a given period in order to achieve the desired

¹ To whom correspondence should be addressed. Tel: 916-752-1487, FAX: 916-752-4759

degree of sterility. The time/temperature process must ensure that the fastest moving particles in the continuous system receive adequate heat treatment. In many cases, the heat treatment of these fluid/particulate mixtures incorporates tube-type heat exchangers and holding tubes. However, the lack of fundamental information on particle and fluid flow in holding tubes has to date limited the application of this technology (Sastry 1989). This lack of fundamental knowledge results in over processing and substantial product degradation.

The objectives of this study were to measure velocity profiles and apparent rheological properties of fluid/particulate mixtures under conditions relevant to aseptic processing. Current techniques include dye tracer (Singh and Lee 1992), timed collection (Hong *et al.* 1991), Hall effect (Tucker and Withers 1994), photo sensor (Yang and Swartzel 1992), video image analysis (Simunovic *et al.* 1995), hot wire anemometry, and Doppler ultrasonic methods (Fregert and Tragardh 1995). Developments in nuclear magnetic resonance (NMR) and imaging capabilities have allowed magnetic resonance imaging (MRI) techniques to be used for flow measurements. One advantage to MRI is that it is noninvasive and does not require the addition of special particles to the flow medium. In addition, any given slice of fluid can be sampled and velocity profiles developed for that slice. MRI velocity phase encode techniques are well covered in the literature (Stepisnik 1985; Caprihan and Fukushima 1990; Callaghan 1991; Pope and Yao 1993). The velocity phase encode technique utilized in this work is a spin echo method (Hahn 1950; Carr and Purcell 1954) using pulsed magnetic field gradients (Stejskal 1965) which measures the displacement probability of an ensemble of nuclei localized within a voxel of the sample flowing through a pipe.

THEORY

In order to characterize the rheological behavior or apparent rheological behavior, a power law model was used to model the velocity profiles of the fluid and fluid/particulate mixtures. For this approach, the relationship between the velocity, v , at the radial position r and the volumetric average velocity, $\langle v \rangle$, is

$$\frac{v}{\langle v \rangle} = \left[\frac{3n+1}{n+1} \right] \left[1 - \left(\frac{r}{R} \right)^{(n+1)/n} \right] \quad (1)$$

where R is the inner radius of the pipe (Steffe 1992). This expression arises from integration of the force balance for pipe flow with the incorporation of

$$\sigma = K\dot{\gamma}^n \quad (2)$$

to describe the relationship between shear stress, σ , and shear rate, $\dot{\gamma}$, where K is the consistency coefficient and n is the flow behavior index. $\dot{\gamma}$ is the derivative of v with respect to radial position. In this study, n is a true rheological parameter for only the homogeneous CMC solutions (no particles) in steady laminar flow. However, the flow behavior index allows us to describe the apparent rheological behavior of the fluid/particulate mixtures under the specified flow condition. In other words, n characterizes the degree of "bluntness" of the velocity profile. This approach to modeling allows a straightforward comparison of velocity profiles and residence time distributions (RTD) as a function of flow rate, particle loading, and particle size.

The residence time distribution, which is a standard technique to describe the uniformity of the history of the material in the system, is a function of the flow behavior index. Middleman (1977) outlined the procedure to evaluate the residence time of a Newtonian fluid in laminar flow in a pipe from the velocity profile. The following analysis is for power law fluids and incorporates the velocity profile for these fluids given in Eq. (1). Consider an element of fluid at radial position r . The element moves at velocity $v(r)$ through an axial distance L in the time given by

$$t = \frac{L}{v(r)} \quad (3)$$

Fluid elements which all enter the pipe at the same time will leave at different times as a function of their radial position. For a quantitative interpretation of residence time, the function $f(t)$ is defined such that $f(t) dt$ is the fraction of the output of the flow which had been in the pipe for a time in the range t to $t+dt$.

$$f(t)dt = \frac{d\dot{V}}{\dot{V}} = \frac{2\pi r v(r) dr}{\pi R^2 \langle v \rangle} = \frac{2r}{R^2} \frac{v(r)}{\langle v \rangle} dr \quad (4)$$

where $d\dot{V}$ is the incremental change in volumetric flow rate, \dot{V} . The cumulative residence time distribution function, or F function, is an integration of Eq. (4),

$$F(t) = \int_{t_0}^t f(t) dt \quad (5)$$

where the lower limit is the first appearance time and corresponds to the fluid moving along the pipe axis ($r = 0$) where the velocity is the greatest. Therefore in terms of velocity, the cumulative residence time distribution for a power law fluid is

$$F(t) = \int_0^t \frac{d\dot{V}}{\dot{V}} = \int_{r=0}^r \frac{2r}{R^2} \left[\frac{3n+1}{n+1} \right] \left[1 - \left(\frac{r}{R} \right)^{(n+1)/n} \right] dr \quad (6)$$

The ideal residence time is a unit step function, which would correspond to plug flow. This condition is "ideal" since all fluid elements have exactly the same residence time in the pipe. Because of no-slip condition at the pipe wall, the plug flow condition can only be approached.

MATERIALS AND METHODS

The flow loop was constructed of 26.2 mm i.d. clear PVC pipe. A straight length of pipe with a length of 175 pipe diameters preceded the section centered in the horizontal bore of the 2 T Oxford magnet. The magnet was connected to a General Electric CSI-II NMR imaging spectrometer operating at a proton frequency of 85.5 MHz. The receiver/transmitter for the radio frequency signal was a 100 mm bird-cage coil. A positive displacement pump (SPS-20, Sine Pump, Orange, MA) circulated the fluid and fluid/particulate mixtures through the flow loop.

The model particulates were 2.5 and 5.0 mm diameter gel spheres. These spheres were formed with an aqueous 3 wt. % sodium alginic acid (Sigma Chemical, St. Louis, MO). The alginic acid solution was prepared and agitated for 8 h. The aqueous solution was then pumped via a syringe pump into a 0.08 M (minimum) calcium chloride solution for gelation, with calcium acting as a crosslinking agent. Two different syringes were used to form the spheres; the syringe size determined the relative contribution of gravity and surface tension and therefore, the drop size. Once formed, the alginate drops were allowed to gel completely in the calcium chloride solution over an 8 h period. The solution was stirred to prevent deformation of the spheres upon settling.

The suspending fluid was a 0.5 wt % carboxymethyl cellulose (CMC) (Methocel, Dow Chemical Co., Midland, MI) solution. The fluid had a density of 1.01 g/mL and consisted of 66 g of CMC, 500 mL of methanol (0.79 sp gr), and 13 L of deionized water. The purpose of the methanol was to solubilize the CMC prior to hydration. The CMC solution was best characterized as a power law fluid; the flow behavior index, n , was determined by the best power law fit of the velocity profile (Eq. 1) with regression coefficients greater than or equal to 0.998 in all cases. These flow behavior indices were a function of flow rate and varied slightly between batches of CMC solution. The three batches of CMC solution used in this study have been characterized in Table 1. The shear rate ranges were determined by differentiation of the fits to Eq. 1.

TABLE 1.
CHARACTERIZATION OF THREE BATCHES OF CMC SOLUTION USED AS
SUSPENDING FLUID

Batch	n	Ave. Velocity (cm/s)	Shear Rate Range (s ⁻¹)	R
1	0.72	34.6	0 - 60	0.999
	0.85	15.3	0 - 35	0.999
	0.83	7.4	0 - 15	0.999
	0.94	2.2	0 - 6	0.999
2	0.88	16.1	0 - 40	0.999
3	0.95	17.2	0 - 50	0.998

For the fluid/particulate suspensions, the gel spheres were suspended in the CMC solution at loadings of 10, 20, and 30% by weight. Imaging experiments were performed in the flow rate range from 12 to 186 cm³/s.

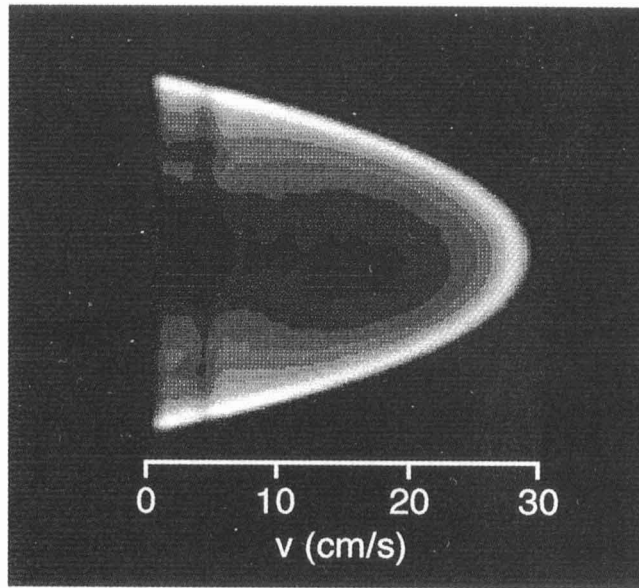
NMR Method

The NMR flow imaging technique yields a joint spatial-velocity ¹H spin density distribution. The NMR pulse sequence consists of three basic parts — slice selection, velocity encoding, and frequency encoding — to provide the axial velocity versus radial position within the pipe. Since, the flow was along the magnet axis in the z direction, the slice selection was done with the z gradient. The resulting slice was a 2 mm thick disk across the pipe. Velocity encoding with the z gradient then tags the z component of the velocity. Finally, frequency encoding in the x direction reads out the radial position of the volume elements. There were 128 phase encode steps and 128 points were used to digitize each echo. The resulting matrix was zero filled to 256 × 256 and a 2D fourier transform performed. The plot of velocity versus radial position was determined by the maximum signal intensity in each row of the matrix. The velocity profile was fit to power law model using commercially available nonlinear least squares fitting routine (KaleidaGraph, Abelbeck Software).

RESULTS AND DISCUSSION

Figure 1 illustrates an example of a joint spatial-velocity ¹H spin density distribution images for the pure suspending fluid and a fluid/particulate mixture. The signal intensity portrays the axial velocity as a function of radial position, with the maximum velocity at the centerline and a no-slip condition at the pipe wall. In Fig. 1(a) the signal intensity of the pure fluid is uniform and has the characteristic blunting of a pseudoplastic (i.e., shear thinning) fluid. The average

(a)



(b)

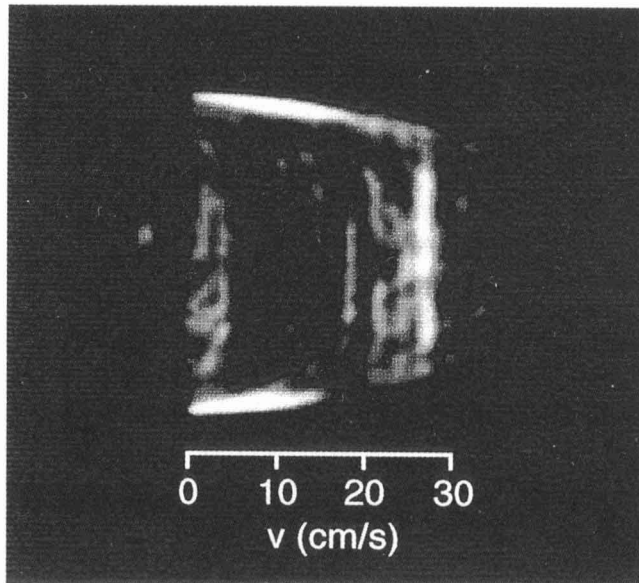


FIG. 1. REPRESENTATIVE MR FLOW IMAGES FOR THE (a) PURE SUSPENDING FLUID AND (b) A FLUID/PARTICULATE MIXTURE AT A 20% LOADING OF 2.5 MM DIAMETER GEL SPHERES

velocity of the fluid was 15.3 cm/s with a maximum velocity of 29.4 cm/s; the flow behavior index of the fluid under these conditions was 0.85. Figure 1(b) illustrates the image obtained at 20% particle loading of the 2.5 mm diameter spheres at an average velocity of 18.1 cm/s. This image illustrates a greater degree of blunting as compared to the pure suspending fluid and has been characterized by an n of 0.41.

Flow Profiles as a Function of Flow Rate

Velocity profiles of the pure suspending fluid were obtained at several flow rates from 12 to 186 cm³/s, which correspond to average velocities of 2.2 to 34.6 cm/s, respectively. As shown in Table 1, the flow behavior index of Batch 1 of 0.5% CMC solution is a function of shear rate range, i.e., flow rate. As expected for a power law fluid, the profiles become more blunt as the flow rate increases. As the flow rate increased the flow behavior index decreases from 0.94 to 0.72. This blunting results in a maximum velocity that is closer to the average velocity and more uniform treatment of the fluid. This change in rheological parameter would not occur if the suspending fluid had been a Newtonian fluid. Therefore, when evaluating the profiles of fluid/particulate mixtures, there is a contribution to the blunting from both the pure fluid as well as the suspended particles. To illustrate this concept, Fig. 2 plots the velocity

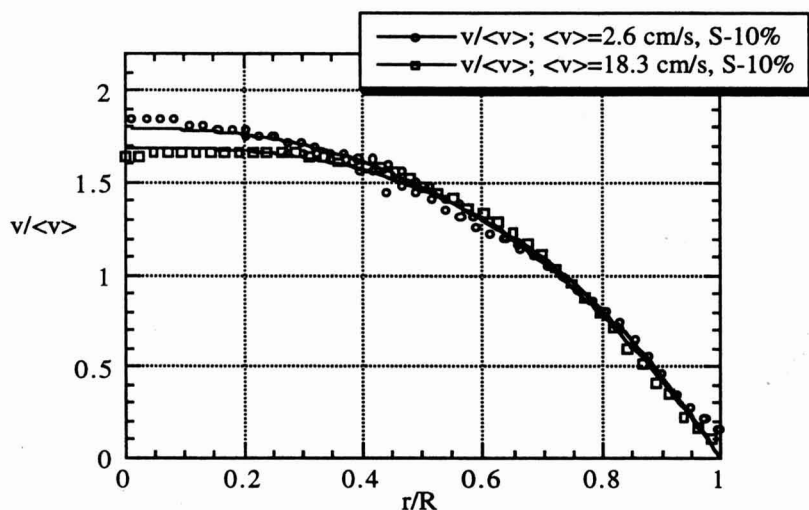


FIG. 2. AS WITH PURE FLUID, FLOW PROFILES FOR THE FLUID/PARTICULATE MIXTURES ARE A FUNCTION OF FLOW RATE

Here, a mixture of 10% loading of small spheres are shown at a fluid/particulate velocity of 2.6 cm/s and 18.3 cm/s shown with the power law fit of the experimental data. The suspending fluid is the same batch of CMC solution.

profiles for a fluid/particulate mixture at 10% loading of 2.5 mm diameter gelspheres. The velocity profiles are dimensionless by the average velocity of the flowing fluid, $\langle v \rangle$ and the pipe radius, R . The average velocity of the upper curve is 2.6 cm/s and that of the lower curve is 18.3 cm/s. Not only are the flow indices considerably lower than that of pure fluid (Table 2), but the change in n is greater than that of pure fluid for comparable flow rates. In other words, the ratio of n values of the lower flow rate to higher flow rate is 1.25 for the fluid/particulate mixture and 1.11 for the pure suspending fluid.

TABLE 2.
CHARACTERIZATION OF FLUID/PARTICULATE MIXTURES

Particle Loading	Suspend- ing Fluid Batch	n	Ave. Velocity (cm/s)	R
<u>Small</u>	1	0.52	18.3	0.998
10	1	0.65	2.6	0.996
20	1	0.41	18.1	0.999
30	2	0.33	21.1	0.996
<u>Large</u>				
20	3	0.20	17.5	0.988

Flow Profiles as a Function of Particle Loading

Figure 3 illustrates the change in the shape of the velocity profiles for fluid/particulate mixtures as a function of particle loading. The 2.5 mm diameter particles are shown at loadings of 0, 10, 20% in Fig. 3(a) and 0% and 30% loading in Fig. 3(b); the suspending fluid (i.e., 0% loading) in these two figures is different (see Table 2). These profiles are obtained at an average velocity in the range of 18 ± 3 cm/s, thereby minimizing the contribution of the flow rate differences in the comparisons. The addition of particles is a significant contribution to the change in the flow behavior index. The value of n drops from 0.85 to 0.65 with a 10% loading of 2.5 mm diameter particles. As the particle loading increases to 30%, the flow index drops to 0.33. This decrease in flow behavior index from 0.85 to 0.33 changes the ratio of maximum velocity to average velocity from 1.92 to 1.50. The practical implication is that holding tubes designed assuming a maximum velocity that is twice the average velocity (i.e., Newtonian fluid) over processes fluid/particulate mixtures.

Flow Profiles as a Function of Particle Size

Velocity profiles of the fluid/particulate mixtures are also a function of particle size. Figure 4 illustrates the extent of blunting at 20% loading for small

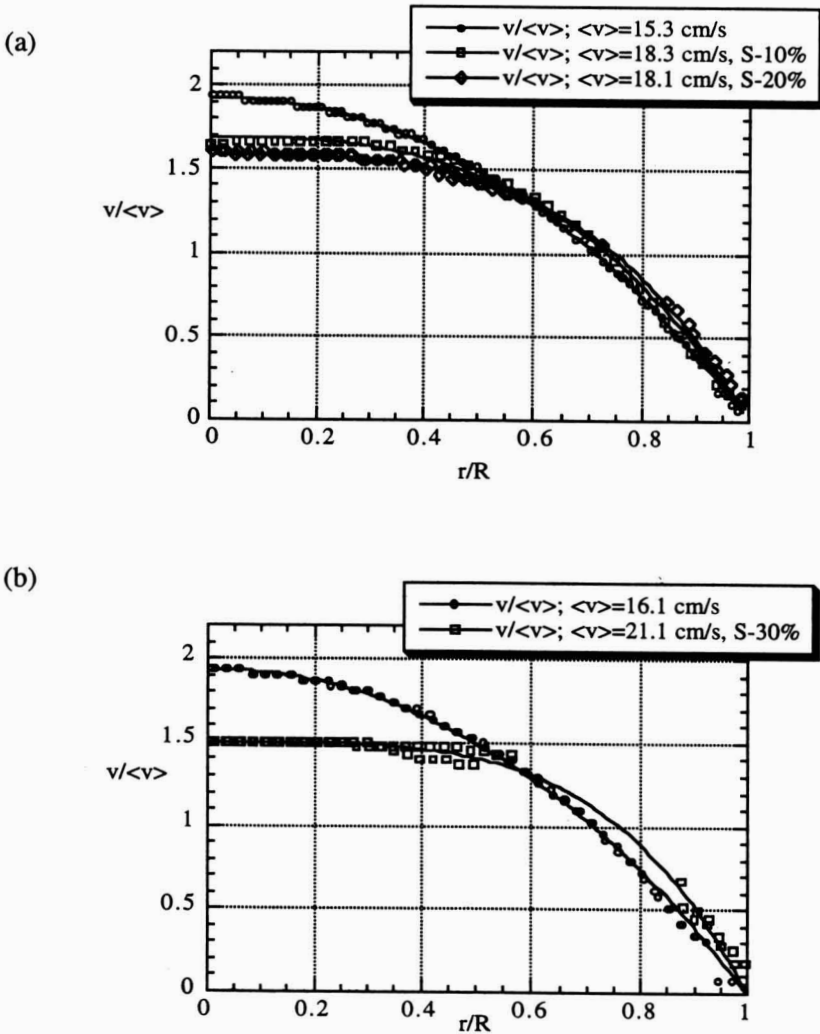


FIG. 3. VELOCITY PROFILES FOR FLUID/PARTICULATE MIXTURES AT PARTICLE LOADINGS OF (a) 10% AND 20%, AND (b) 30%

For each fluid/particulate mixture, the velocity profile for the pure suspending fluid is also shown at approximately the same volumetric flow rate with its power law fit.

particles (2.5 mm diameter) and large particles (5.0 mm diameter). The fluid/particulate mixtures shown in Fig.4 (a) and 4(b) are compared to their own suspending fluid at average velocities in the range of 16.7 ± 1.4 cm/s. Under these conditions, the ratio of $n/n_{suspending}$ is 0.48 and 0.21 for small and large particles, respectively.

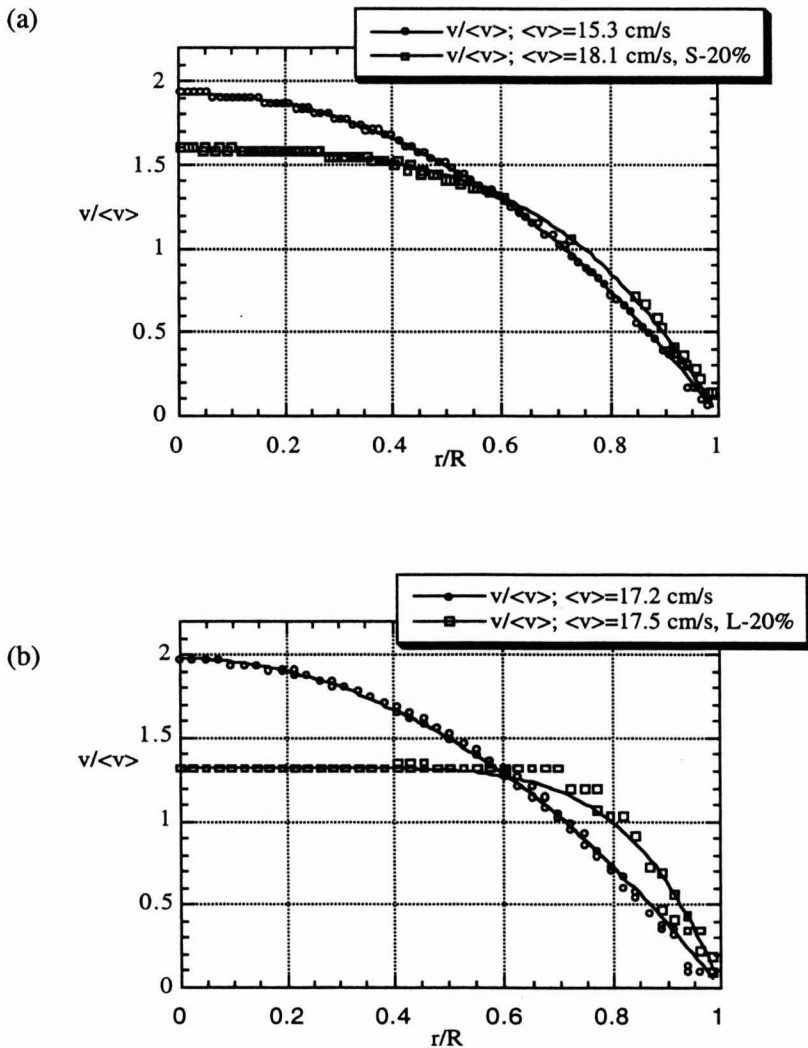


FIG. 4. THE EXTENT OF BLUNTING OF THE VELOCITY PROFILE IS ALSO A FUNCTION OF PARTICLE SIZE AS SHOWN AT 20% LOADING WITH SMALL PARTICLES IN (a) AND LARGE PARTICLES IN (b)

Each of the fluid/particulate mixtures is referenced to its own suspending fluid; the curves are the power law fit of the experimental data.

Residence Time Distribution Curves

The residence time distribution curve is altered considerably as the velocity profile becomes blunter. Figure 5 illustrates the $F(t)$ curve for the flow behavior

indices that characterize the velocity profiles given in Fig. 4. The vertical line at $t/\langle t \rangle = 1.0$ is the curve for plug flow, where $\langle t \rangle$ is the average time; all fluid has traveled through the pipe with the same uniform history. The other limiting case is the curve for a Newtonian fluid ($n = 1$) which yields the greatest deviation of the cases shown with respect to the history of the fluid elements. The first appearance time, which is the shortest time fluid resides in the pipe is $t/\langle t \rangle = 0.5$. Under these flow conditions, at $5\langle t \rangle$, 1% of the fluid still resides in the pipe. By contrast, as n decreases, the first appearance time approaches $t/\langle t \rangle = 1.0$.

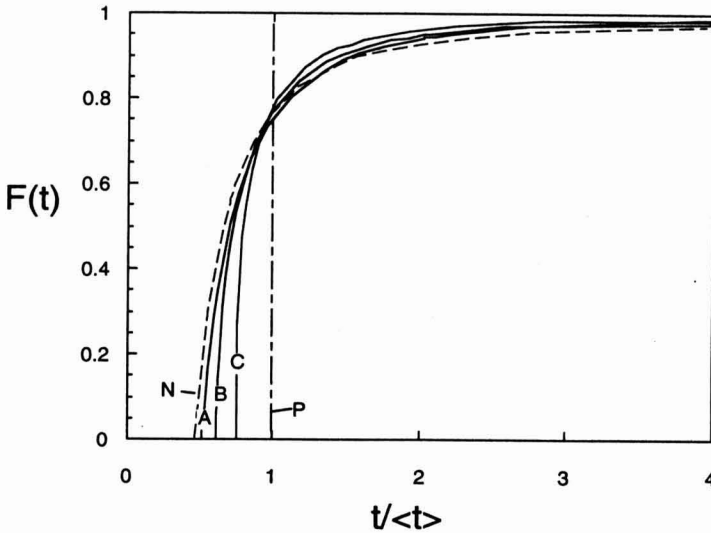


FIG. 5. RTD FOR PLUG (P) FLOW, AND FOR FLUIDS WITH FLOW BEHAVIOR INDICES OF 1.0 (N), 0.85 (A), 0.41 (B), AND 0.20 (C)

Also shown are RTD curves for the following systems: 0.5% CMC, $\langle v \rangle = 15.3$ cm/s, $n=0.85$; 20% particles (2.5 mm), $\langle v \rangle = 18.1$ cm/s, $n=0.41$; and 20% particles (5.0 mm), $\langle v \rangle = 17.5$ cm/s, $n=0.20$. These represent a range of flow index values determined in these experiments. The curves show behavior intermittent between the limiting cases of Newtonian and plug flow. At $n=0.85$, the first appearance time (0.55) is closest to that of a Newtonian fluid, while at $n=0.21$ the first appearance time (0.68) is closest to plug flow. In addition, the time $t/\langle t \rangle$ at which $F=0.99$ decreases as n decreases. In other words, the increasing pseudoplastic nature improves the uniformity of the history during pipe flow.

CONCLUSIONS

In summary, the information obtained by MRI for these systems is useful for understanding the flow of fluid/particulate mixtures at particle loadings that are relevant to aseptic processing. Furthermore, due to the opaque nature of these fluids, MRI is the only way to get this information. In these fluids, velocity profiles are increasingly blunted as (a) flow rate increases, (b) particle loading increases, and (c) particle size increases. The RTD is a function of the flow behavior index n that characterizes the rheological behavior in pipe flow. As the velocity profile becomes more blunt, n decreases and the fluid/particulate mixture is subjected to a more uniform flow history.

Strictly speaking, n is a true rheological parameter for only homogeneous fluids (no particles) in steady laminar flow. However, the flow behavior index allows us to describe the apparent rheological behavior of the fluid/particulate mixtures under the specified flow condition. This approach to modeling allows a straight-forward comparison of velocity profiles and residence time distributions (RTD) as a function of flow rate, particle loading, and particle size.

ACKNOWLEDGMENTS

This research was funded by the Center for Aseptic Processing and Packaging Studies (CAPPS).

REFERENCES

- BUCHNER, N. 1993. Aseptic processing and packaging of food particulates. In *Aseptic Processing and Packaging of Particulate Foods*. (E.M.A. Willhoft, ed.) pp. 1-22, Blackie Academic and Professional, London.
- CALLAGHAN, P.T. 1991. *Principles of Nuclear Magnetic Resonance Microscopy*. Oxford University Press, New York.
- CAPRIHAN, A. and FUKUSHIMA, E. 1990. Flow measurements by NMR. *Physics Reports*. 198 (4), 195-235.
- CARR, H.Y. and PURCELL, E.M. 1954. Effects of diffusion on free precession in nuclear magnetic resonance experiments. *Physical Review* 94(3), 630-638.
- FREGERT, J. and TRAGARDH, C. 1995. Solid-liquid flow in a horizontal pipe. *Proceedings of the International Symposium on Advances in Aseptic Processing and Packaging Technologies*, Copenhagen, Denmark.
- HAHN, E.L. 1950. Spin echoes. *Physical Review* 80(4), 580-594.

- HONG, C.W., PAN, B.S., TOLEDO, R.T. and CHIOU, K.M. 1991. Measurement of residence time distribution of fluid and particles in turbulent flow. *J. Food Science* 56(1), 255-259.
- MIDDLEMAN, S. 1977. *Fundamentals of Polymer Processing*. pp. 301-303, McGraw-Hill Book Co., New York.
- POPE, J.M. and YAO, S. 1993. Quantitative NMR imaging of flow. *Conc. Mag. Res.* 5, 281-302.
- SASTRY, S.K. 1989. Theoretical calculations for ensuring safe aseptic process design. *Activities Report of the R&D Associates*. Fall 1988 Meeting. U.S. Army Natick Research, Development & Engineering Center, Natick, MA.
- SIMUNOVIC, J., SWARTZEL, K., FARKAS, B. and ADAMS, J. 1995. Particle residence time measurement of single and multiple solid phase particulate products in clear aseptic holding tube segments. *Proceedings of the International Symposium on Advances in Aseptic Processing and Packaging Technologies*, Copenhagen, Denmark.
- SINGH, R.K. and LEE, J.H. 1992. Residence time distributions of foods with/without particulates in aseptic processing systems. In *Advances in Aseptic Processing Technologies* (R.K. Singh and P.E. Nelson, eds.) pp. 7-62, Elsevier Applied Science, London.
- STEFFE, J.F. 1992. *Rheological Methods in Food Process Engineering*. p. 58, Freeman Press, East Lansing, MI.
- STEJSKAL, E.O. 1965. Use of spin echoes in a pulsed magnetic field gradient to study anisotropic, restricted diffusion and flow. *J. Chem. Phys.* 43, 3597-3603.
- STEPISNIK, J. 1985. Measuring and imaging of flow by NMR. *Prog. NMR Spect.* 17, 187-209.
- TUCKER, G.S. and WITHERS, P.M. 1994. Determination of residence time distribution of nonsettling food particles in viscous food carrier fluids using Hall effect sensors. *J. Food Process Engineering* 17, 401-422.
- YANG, B.B. and SWARTZEL, K.R. 1992. Particle residence time distributions in two-phase flow in straight round conduit. *J. Food Science* 57(2), 497-502.

F N P PUBLICATIONS IN FOOD SCIENCE AND NUTRITION

Journals

JOURNAL OF FOOD LIPIDS, F. Shahidi
JOURNAL OF RAPID METHODS AND AUTOMATION IN MICROBIOLOGY,
D.Y.C. Fung and M.C. Goldschmidt
JOURNAL OF MUSCLE FOODS, N.G. Marriott, G.J. Flick, Jr. and J.R. Claus
JOURNAL OF SENSORY STUDIES, M.C. Gacula, Jr.
JOURNAL OF FOODSERVICE SYSTEMS, C.A. Sawyer
JOURNAL OF FOOD BIOCHEMISTRY, N.F. Haard, H. Swaisgood and B. Wasserman
JOURNAL OF FOOD PROCESS ENGINEERING, D.R. Heldman and R.P. Singh
JOURNAL OF FOOD PROCESSING AND PRESERVATION, D.B. Lund
JOURNAL OF FOOD QUALITY, J.J. Powers
JOURNAL OF FOOD SAFETY, T.J. Montville and D.G. Hoover
JOURNAL OF TEXTURE STUDIES, M.C. Bourne and M.A. Rao

Books

APPETITE FOR LIFE: AN AUTOBIOGRAPHY, S.A. Goldblith
HACCP: MICROBIOLOGICAL SAFETY OF MEAT AND POULTRY, J.J. Sheridan,
R.L. Buchanan and T.J. Montville
OF MICROBES AND MOLECULES: FOOD TECHNOLOGY AT M.I.T., S.A. Goldblith
MEAT PRESERVATION: PREVENTING LOSSES AND ASSURING SAFETY,
R.G. Cassens
S.G. PRESCOTT, M.I.T. DEAN AND PIONEER FOOD TECHNOLOGIST,
S.A. Goldblith
FOOD CONCEPTS AND PRODUCTS: JUST-IN-TIME DEVELOPMENT, H.R. Moskowitz
MICROWAVE FOODS: NEW PRODUCT DEVELOPMENT, R.V. Decareau
DESIGN AND ANALYSIS OF SENSORY OPTIMIZATION, M.C. Gacula, Jr.
NUTRIENT ADDITIONS TO FOOD, J.C. Bauernfeind and P.A. Lachance
NITRITE-CURED MEAT, R.G. Cassens
POTENTIAL FOR NUTRITIONAL MODULATION OF AGING, D.K. Ingram *et al.*
CONTROLLED/MODIFIED ATMOSPHERE/VACUUM PACKAGING OF
FOODS, A.L. Brody
NUTRITIONAL STATUS ASSESSMENT OF THE INDIVIDUAL, G.E. Livingston
QUALITY ASSURANCE OF FOODS, J.E. Stauffer
THE SCIENCE OF MEAT AND MEAT PRODUCTS, 3RD ED., J.F. Price and
B.S. Schweigert
HANDBOOK OF FOOD COLORANT PATENTS, F.J. Francis
ROLE OF CHEMISTRY IN PROCESSED FOODS, O.R. Fennema *et al.*
NEW DIRECTIONS FOR PRODUCT TESTING OF FOODS, H.R. Moskowitz
ENVIRONMENTAL ASPECTS OF CANCER: ROLE OF FOODS, E.L. Wynder *et al.*
FOOD PRODUCT DEVELOPMENT AND DIETARY GUIDELINES, G.E. Livingston,
R.J. Moshy and C.M. Chang
SHELF-LIFE DATING OF FOODS, T.P. Labuza
ANTINUTRIENTS AND NATURAL TOXICANTS IN FOOD, R.L. Ory
UTILIZATION OF PROTEIN RESOURCES, D.W. Stanley *et al.*
POSTHARVEST BIOLOGY AND BIOTECHNOLOGY, H.O. Hultin and M. Milner

Newsletters

MICROWAVES AND FOOD, R.V. Decareau
FOOD INDUSTRY REPORT, G.C. Melson
FOOD, NUTRITION AND HEALTH, P.A. Lachance and M.C. Fisher

GUIDE FOR AUTHORS

If the manuscript has been produced by a word processor, a disk containing the manuscript would be greatly appreciated. Word Perfect 5.1 is the preferred word processing program. The original and THREE copies of the manuscript should be sent along with the disk to the editorial office. The typing should be double-spaced throughout with one-inch margins on all sides.

Page one should contain: the title, which should be concise and informative; the complete name(s) of the author(s); affiliation of the author(s); a running title of 40 characters or less; and the name and mail address to whom correspondence should be sent.

Page two should contain an abstract of not more than 150 words. This abstract should be intelligible by itself.

The main text should begin on page three and will ordinarily have the following arrangement:

Introduction: This should be brief and state the reason for the work in relation to the field. It should indicate what new contribution is made by the work described.

Materials and Methods: Enough information should be provided to allow other investigators to repeat the work. Avoid repeating the details of procedures that have already been published elsewhere.

Results: The results should be presented as concisely as possible. Do not use tables *and* figures for presentation of the same data.

Discussion: The discussion section should be used for the interpretation of results. The results should not be repeated.

In some cases it might be desirable to combine results and discussion sections.

References: References should be given in the text by the surname of the authors and the year. *Et al.* should be used in the text when there are more than two authors. All authors should be given in the Reference section. In the Reference section the references should be listed alphabetically. See below for style to be used.

RIZVI, S.S.H. 1986. Thermodynamic properties of foods in dehydration. In *Engineering Properties of Foods*, (M.A. Rao and S.S.H. Rizvi, eds.) pp. 133-214, Marcel Dekker, New York.

MICHAELS, S.L. 1989. Crossflow microfilters ins and outs. *Chem. Eng.* 96, 84-91.

LABUZA, T.P. 1982. *Shelf-Life Dating of Foods*, pp. 66-120, Food & Nutrition Press, Trumbull, CT.

Journal abbreviations should follow those used in Chemical Abstracts. Responsibility for the accuracy of citations rests entirely with the author(s). References to papers in press should indicate the name of the journal and should only be used for papers that have been accepted for publication. Submitted papers should be referred to by such terms as "unpublished observations" or "private communication." However, these last should be used only when absolutely necessary.

Tables should be numbered consecutively with Arabic numerals. The title of the table should appear as below:

TABLE 1.

ACTIVITY OF POTATO ACYL-HYDROLASES ON NEUTRAL LIPIDS, GALACTOLIPIDS AND PHOSPHOLIPIDS

Description of experimental work or explanation of symbols should go below the table proper. Type tables neatly and correctly as tables are considered art and are not typeset. Single-space tables.

Figures should be listed in order in the text using Arabic numbers. Figure legends should be typed on a separate page. Figures and tables should be intelligible without reference to the text. Authors should indicate where the tables and figures should be placed in the text. Photographs must be supplied as glossy black and white prints. Line diagrams should be drawn with black waterproof ink on white paper or board. The lettering should be of such a size that it is easily legible after reduction. Each diagram and photograph should be clearly labeled on the reverse side with the name(s) of author(s), and title of paper. When not obvious, each photograph and diagram should be labeled on the back to show the top of the photograph or diagram.

Acknowledgments: Acknowledgments should be listed on a separate page.

Short notes will be published where the information is deemed sufficiently important to warrant rapid publication. The format for short papers may be similar to that for regular papers but more concisely written. Short notes may be of a less general nature and written principally for specialists in the particular area with which the manuscript is dealing. Manuscripts that do not meet the requirement of importance and necessity for rapid publication will, after notification of the author(s), be treated as regular papers. Regular papers may be very short.

Standard nomenclature as used in the engineering literature should be followed. Avoid laboratory jargon. If abbreviations or trade names are used, define the material or compound the first time that it is mentioned.

EDITORIAL OFFICE: DR. D.R. HELDMAN, COEDITOR, *Journal of Food Process Engineering*, University of Missouri-Columbia, 214 Agricultural Engineering Bldg., Columbia, MO 65211 USA; or DR. R.P. SINGH, COEDITOR, *Journal of Food Process Engineering*, University of California, Davis, Department of Agricultural Engineering, Davis, CA 95616 USA.

CONTENTS

Simulation of Dynamic Properties of Batch Sterilizer with External Heating
M. LOUČKA 91

Yield and Quality of Onion Flavor Oil Obtained by Supercritical Fluid
Extraction and Other Methods
A. DRON, D.E. GUYER, D.A. GAGE and C.T. LIRA 107

Concentration of Onion Juice Volatiles by Reverse Osmosis and Its Effects
on Supercritical CO₂ Extraction
J.S. NUSS, D.E. GUYER and D.A. GAGE 125

Flow Modeling of a Power-Law Fluid in a Fully-Wiped, Co-Rotating
Twin-Screw Extruder
Y. LI, H.E. HUFF and F. HSIEH 141

Velocity Profiles of Fluid/Particulate Mixtures in Pipe Flow Using MRI
**K.L. McCARTHY, W.L. KERR, R.J. KAUTEN and
J.H. WALTON** 165